The Analyst

The Analytical Journal
of The Chemical Society

A monthly international publication dealing
with all branches of analytical chemistry

Volume 104 No 1236 Pages 177–272 March 1979

THE ANALYST

THE ANALYTICAL JOURNAL OF THE CHEMICAL SOCIETY

Published by The Chemical Society

Editorial: The Director of Publications, The Chemical Society, Burlington House, London, W1V 0BN. Telephone 01-734 9864. Telex No. 268001

Advertisements: Advertisement Department, The Chemical Society, Burlington House, Piccadilly, London, W1V 0BN. Telephone 01-734 9864

Subscriptions (non-members): The Chemical Society, Distribution Centre, Blackhorse Road, Letchworth, Herts., SG6 1HN

Volume 104 No 1236 March 1979

MARCH 1979 Vol. 104 No. 1236

The Analyst

Energy-dispersive X-ray Emission Analysis

A Review

W. C. Campbell

Imperial Chemical Industries Limited, Petrochemicals Division, Research and Development Department, P.O. Box 90, Wilton, Middlesbrough, Cleveland TS6 8JE

Summary of Contents

Keywords: Review; energy-dispersive X-ray emission analysis

Introduction

In their review of X-ray fluorescence analysis in 1970 Carr-Brion and Payne[1] stated that resolutions of the order of 190 eV, at 6 keV, had been reported for semiconductor detectors and that better values were to be expected with improvement in detectors and associated electronics. Today, detectors are routinely produced with resolutions in the 150–160-eV range and values as low as 140 eV can be attained.

Energy dispersion, using a lithium-drifted silicon, Si(Li), detector, was first introduced as a practical tool for X-ray spectrometry in the mid-1960s.[2–5] Initially, the major impact of the new technology was as an accessory on electron beam microprobes and scanning electron microscopes.[6] It was not long, however, before dedicated X-ray spectrometers were being built around the new detectors.[7–12] Today, energy-dispersive attachments are almost standard on electron microscopes and a number of manufacturers offer dedicated X-ray fluorescence equipment for qualitative and quantitative analysis.

It is intended to limit this review to those techniques which utilise the energy-dispersive properties of semiconductor detectors, specifically the Si(Li) detector. There is some confusion over the terminology applied to this field of analytical chemistry. Detectors, such as the scintillation and flow proportional counters, used in wavelength-dispersive X-ray fluorescence analysis, are capable of limited energy resolution. It is, therefore, possible to consider these as energy-dispersive detectors, and indeed use is made of this property in the application of "pulse-height analysis." However, the inability of these detectors to provide sufficient spectral resolution leads to their use in combination with diffraction crystals. Terms such as semiconductor, solid-state, non-dispersive and energy-dispersive have appeared associated with the Si(Li) detector. It is intended here to follow the guidelines given in the *IUPAC Information Bulletin* on X-ray emission spectroscopy,[13] for terminology and symbols. It has become the convention to express X-ray wavelengths in Ångstroms when considering wavelength-dispersive systems and X-ray energy in kiloelectronvolts when considering energy-dispersive systems. The principal difference between energy-dispersive electron microscope attachments and energy-dispersive X-ray fluorescence analysers is in the mode of excitation used. The techniques share much of the data collection and data processing technology. It is, therefore, difficult to differentiate between the two systems in an absolute manner and some reference will be made to electron-excitation systems.

For those new to the technique, a number of books and descriptive articles are available with respect to both X-ray fluorescence analysis in general[1,14–20] and energy-dispersive X-ray fluorescence analysis in particular.[7,12,21–30]

Instrumentation

Fig. 1 shows the components of a typical energy-dispersive X-ray fluorescence analyser. The source of excitation shown is the X-ray tube, but of course excitation of secondary X-rays can be achieved by using a variety of sources including electrons, protons and other charged particles. The building blocks of the system are a source of excitation, the sample compartment, the solid-state Si(Li) detector, the electronic package including pre-amplifier, amplifier and multi-channel analyser (M.C.A.) and the data processing package, generally including computer with relevant software to convert the raw data into meaningful results. The over-all system efficiency of an energy-dispersive X-ray fluorescence instrument is a

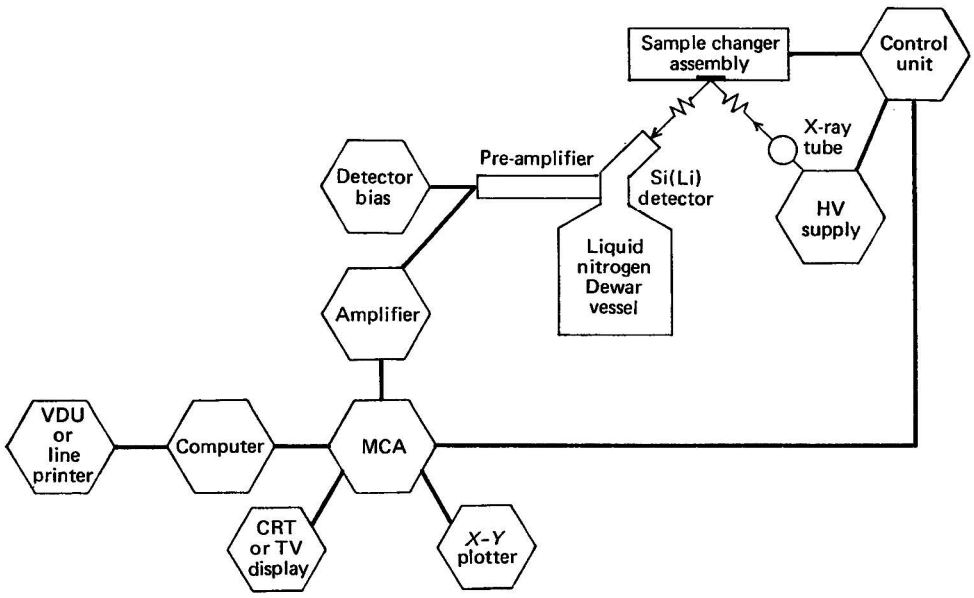

Fig. 1. Typical energy-dispersive X-ray fluorescence spectrometer.

function of a number of parameters including geometry, mode of excitation, excitation cross-section, fluorescence yield and detector efficiency. Cothern *et al.*[31] investigated the system efficiency for the situation where the source of excitation was broad-band X-rays.

Excitation

As in conventional wavelength-dispersive X-ray fluorescence analysis it is necessary to remove core electrons from the atoms of interest in order to produce the secondary fluorescent X-rays, which are characteristic of the elements present in the sample. Normally X-rays, from an X-ray tube, are used to fulfil this function and this is still true of most commercial energy-dispersive X-ray fluorescence spectrometers. The alternatives to the X-ray tube are electrons, protons and radioisotopes, all of which are capable of ejecting core electrons and all of which have various advantages and limitations. Jaklevic[32] has compared the use of electrons, charged particles (protons or alpha particles) and X-rays (continuous or mono-energetic) as excitation sources for energy-dispersive X-ray analysis. Electron excitation was shown to have much poorer limits of detection. The high continuous background found in electron-induced spectra increases the difficulty of determining low concentrations. Middleman and Geller[33] have demonstrated the improved peak to background ratios that can be achieved in the X-ray spectra from an electron microscope, using X-ray excitation instead of the usual electron beam.

Reldy *et al.*[34] have used muons to excite secondary X-rays. This produces a muonic X-ray spectrum in which the characteristic X-rays are raised in energy, hence allowing the light elements to be determined more easily.

X-ray Tube

X-ray tubes on conventional wavelength-dispersive spectrometers use up to 3 kW of power and produce a high characteristic X-ray flux from the sample. In energy-dispersive X-ray fluorescence systems all X-rays are incident simultaneously on the detector, and because there is a finite counting capacity, it is necessary to modify the X-ray tube output to reduce the secondary X-ray flux. There are basically two approaches to this problem. One is to reduce the power of the X-ray tube to around 10 W and the other to use a secondary target system. Fig. 2 shows the configurations typical for primary or direct excitation and secondary excitation.

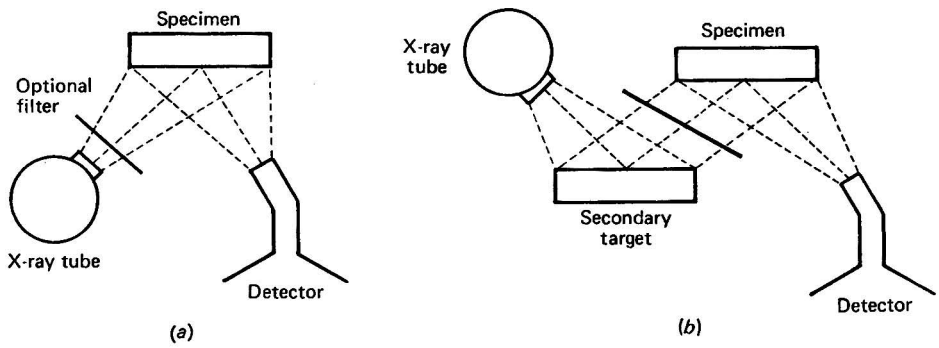

Fig. 2. X-ray excitation: (*a*), primary or direct; (*b*), secondary.

The low-power tube used for primary excitation emits a broad band of X-ray energies from just below the tube potential. Used directly, this has the advantage of exciting a wide range of elements but unfortunately produces a high spectral background due to scattering of the radiation by the sample. The use of a filter placed between the tube and the sample attenuates the X-rays and can be used to moderate the primary broad-band radiation to approximate to a mono-energetic source. A proper choice of filter will increase the sensitivity for particular elements while reducing the spectral background over a given region.

In the secondary-excitation geometry, X-rays from a high-power tube impinge on a chosen target material. The target material itself is induced to emit characteristic and mainly monochromatic X-rays, which are made to fall upon the sample. This produces a well monochromated beam that gives rise to a lower spectral background contribution. Gedcke *et al.*[35] compared the detection limits that could be obtained with the two geometries for a variety of elements and concluded that over the 5–30-keV range there was little to choose between the two techniques. However, in a similar study Artz and Short[36] found that the best sensitivity was achieved in the atomic number range 35–60 with direct radiation from a tungsten X-ray tube, but that secondary excitation with properly chosen targets produced a higher sensitivity for other elements. In a study of the detection limits for light elements in a "synthetic rock mixture" and NBS orchard leaves, Anselmo[37] found that secondary excitation was generally superior. Investigations of this nature are complicated by a dependence on system geometry.

Both primary- and secondary-excitation systems are available on commercial spectrometers. The primary-excitation system with the optional filter appears to offer a more flexible approach in terms of exciting a large number of elements simultaneously, or efficiently exciting just a few. The secondary target geometry probably gives somewhat better sensitivity over narrow ranges, necessitating the use of a variety of targets to cover the X-ray spectrum of interest. Counting times on energy-dispersive X-ray fluorescence instruments are, typically, 100–1000 s owing to the low count-rate capability of the detection and amplification system. This places a high stability requirement, both long and short term, on the output from the X-ray tube. Low-power generators are more stable than high-power generators and this favours the use of primary excitation. Van Espen and Adams[38] have described a technique to compensate for the fluctuating X-ray intensity from a high-power system by making use of a reference signal from a thin metal wire. Detection limits are a function of counting time, excitation conditions, spectrometer geometry, matrix and atomic number. For X-ray excitation they are, typically, less than 1 p.p.m. for the transition elements and about 0.1% for sodium.

The use of pulsed X-ray beams is advocated as a means of increasing the counting-rate capacity of energy-dispersive systems.[39,40] Basically, the system operates by turning off the X-ray tube as soon as an event is detected by the spectrometer. Pulse pile-up events are virtually eliminated and counting rates are considerably increased.

Polarised X-rays can be obtained by scattering from a suitable material, such as boron carbide, or from a synchrotron source. Polarised radiation is not scattered isotropically. Therefore, if a detector is placed in the plane of polarisation and at right-angles to the incident beam, the scatter signal reaching the detector is considerably reduced. This results in a lowering of the spectral background and, therefore, an improvement in detection limits.[41–46] When using the X-ray tube and polariser it is necessary to use high power to compensate for energy loss on polarisation. Ryon[45] found improvements in detection limits of up to 4.5 times for the elements from potassium to strontium in NBS orchard leaves when compared with direct excitation.

Radioisotopes

Most radioisotopes decay with the emission of X-rays, γ-rays or α-particles or a combination of these and they are, therefore, suitable for use as excitation sources. Typical radioisotope sources used in energy-dispersive X-ray fluorescence work include iron-55, cadmium-109, americium-241, cobalt-57 and gadolinium-153 for photon excitation and polonium-210 for α-particle excitation. It is possible to produce broad-band excitation sources utilising radioisotopes. β-Emitters, such as promethium-147 or tritium, when mixed with a suitable target material, produce an X-ray continuum. However, as the conversion efficiency is low, high activity levels must be employed to obtain good counting rates. A description of the available photon-emitting radioisotopes and a discussion on the design and construction of new sources were given by Leonowich *et al.*[47]

A major constraint on the use of radioisotopes is that the emission should be as simple as possible. Where a large number of photon energies are emitted, elastic and inelastic scatter from the sample will give rise to a complicated X-ray spectrum. Where high-energy γ-rays are emitted high backgrounds can occur owing to detector Compton escape. Hence, to cover the spectral region of interest several simple emitters are preferable.

The use of an α-emitter, such as polonium-210, together with a windowless detector has been shown to allow the detection of oxygen and fluorine by energy-dispersive X-ray fluorescence.[48] Curium-244, a photon and particle source, has been used for the excitation of the light elements in rocks by Franzgrote.[49] In a study of the limits of detection that can be attained using radioisotope excitation Spatz and Lieser[50] found that, given the correct choice of isotope, values were almost as good as those found using X-ray tube excitation.

Electrons and Protons

The use of electrons to excite characteristic sample X-rays is the basis of electron-microprobe analysis and it was in this field that energy-dispersive X-ray emission first found application.[51] The topic has been extensively dealt with by a number of workers.[52–56] The major disadvantage in the use of electron excitation is the high spectral background produced by electron deceleration.

The use of protons to excite characteristic X-rays is attractive from a number of viewpoints. The ionisation cross-section shows a marked increase with decreasing atomic number, thus increasing the sensitivity in this region. Protons (and other charged particles) do not produce the intense continuum found with electrons and the X-ray spectral background is, therefore, small. However, proton-induced X-ray emission, or PIXE, when applied to conventional "thick" samples can, in fact, exhibit a high spectral background. This is caused by the production of energetic photoelectrons in the sample that give rise to an X-ray continuum and for this reason PIXE has found most application in "thin" sample analysis. The need to obtain the use of a charged-particle accelerator is an obvious drawback, limiting the production of standard equipment. The principles of the technique have been described[57,58] and two review papers have appeared[59,60] along with application studies in water analysis,[57,61] biological material[57,62] and airborne particulates.[63] A description of the design requirements of the experimental apparatus and a thorough evaluation of the qualitative and quantitative nature of the technique have been given by Johansson *et al.*[64] Reuter and Lurlo[65] investigated the application of proton excitation to "thick" samples and compared it with the use of electron excitation. Proton excitation produced sensitivities higher by factors of 2 or 3 when applied to low-alloy steels. It has been demonstrated[66] that the sample depth probed by protons is smaller and more consistent across the elemental range than it is with X-ray excitation. Ahlberg and Adams[67] compared the use of proton with X-ray excitation in the analysis of air particulate matter. PIXE was shown to be more sensitive for most elements. However, the inhomogeneities found on air particulate filters caused problems due to the small sampling area in the PIXE technique.

Detectors

Most X-ray detectors have some capacity to resolve photons in terms of their energy but none perform this task so well as the solid-state detectors. It was chiefly the advent of the solid-state detector, with its associated pulse-processing electronics, which gave rise to the technique of energy-dispersive X-ray fluorescence. Fig. 3 shows a diagrammatic representation of a solid-state Si(Li) detector. The detector is a diode consisting of a cylindrical piece of p-type silicon, doped with lithium to increase the electrical resistivity. A Schottky barrier contact at the front of the detector produces the p - i - n diode, and the application of a reverse bias voltage, typically 1000 V, depletes the diode of free charge carriers. The dimensions of the detector vary with the application but are typically 4–16 mm in diameter and 3–5 mm thick. An X-ray photon entering the diode causes ionisation of the silicon and produces a number of "electron-hole pairs," the number of which is proportional to the energy of the incident X-ray photon. The applied voltage sweeps the charge from the diode and it is collected at a charge sensitive pre-amplifier. The use of lithium-drifted silicon arises from two factors. The ionisation energy or band gap is small enough at 1.1 eV to produce sufficient charge carriers for good statistical definition of the pulse size, but is high enough to prevent thermal-electron excitation being significant. The detector is normally contained in a vacuum behind a thin beryllium window. Both the detector and pre-amplifier are held at liquid-nitrogen temperature to reduce lithium migration and minimise electronic noise. A useful review of the design of solid-state detectors and their

application to X-ray spectrometry has been given by Heath,[68] while Keith and Loomis[69] have critically examined the use of the detector with respect to energy calibration, detector efficiency and detector phenomena, such as escape and sum peaks.

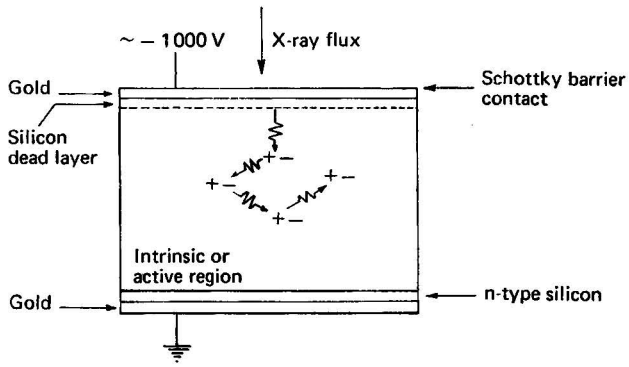

Fig. 3. Silicon(lithium) detector.

The efficiency of a solid-state detector in recording an event is a function of such parameters as area and thickness of the active region, dead layer and contact material and thickness of the entrance window. At low X-ray energies (low atomic number) much of the intensity is attenuated by the beryllium window. At high X-ray energies the efficiency is dependent on the detector thickness. Between 4 and 20 keV the detector efficiency exceeds 90% but falls off above and below this energy range.[69]

The fundamental limitation to the resolving power of the Si(Li) detector lies in the statistical fluctuation in the number of electron-hole pairs produced by a given X-ray energy. It is customary to express the resolution of an energy-dispersive X-ray system as the full width at half maximum (FWHM) of a peak in the energy spectrum, normally that of manganese Kα. The FWHM contains contributions from noise sources other than the detector and in particular from the pre-amplifier. At low energies, electronic noise is greater than that associated with statistical fluctuations. The detector resolution is normally expressed as FWHM (eV) $= 2.355\sqrt{FE\epsilon}$, where E is the energy of the X-ray, F the Fano factor and ϵ the average energy to create an electron-hole pair. The Fano factor is related to the fractional amount of total energy absorbed resulting in the production of electron-hole pairs and is normally assumed to be about 0.15.[68]

The total system resolution, including the contribution from electronic noise, is expressed as

$$\text{FWHM (eV)} = \sqrt{(\text{FWHM})^2_{\text{noise}} + (2.355\sqrt{FE\epsilon})^2}$$

Typically, the values of FWHM at 5.9 keV (manganese Kα) are in the range 150–180 eV.

The Si(Li) solid-state detector finds application in other fields including X-ray diffraction[70,71] and astronomical spectroscopy.[72] At photon energies above about 50 keV it is usual to employ another solid-state detector, namely the lithium-drifted germanium diode.

Electronics

The electronic package used to process the output from the detector consists of the pre-amplifier, amplifier, pile-up rejector and multi-channel analyser. It is beyond the scope of this review to describe these components in detail but they will be discussed briefly, for completeness. A more detailed explanation of the design and operation of these components can be found elsewhere.[12,21]

Pre-amplifier

The function of the pre-amplifier is to convert the charge pulse from the detector into a voltage signal, while still retaining the proportionality to the incident X-ray photon energy and adding as little electronic noise as possible. The operation generally involves a form of current integration, utilising a cooled field-effect transistor (FET) and electronic band-pass filters controlled by electronic shaping time constants. There are a number of pre-amplifier types, each using a different technique to minimise the noise contribution. These include continuous optical feedback,[73] drain feedback,[74,75] modified-resistive feedback,[76] pulsed-optical feedback[77] and dynamic-charge restoration.[78]

Amplifier

The function of the amplifier[8,75] is to convert and amplify the signals from the pre-amplifier in such a manner as to make them suitable for presentation to the multi-channel analyser. This function is achieved by "pulse shaping" techniques to attempt to obtain the optimum in energy resolution and counting-rate performance. A large shaping time constant produces optimum energy resolution at the expense of counting-rate performance and a small constant produces the reverse effect. Clearly, these must be weighed against each other. The important characteristics of a good amplifier are sophisticated pulse shaping, good correlation between pulse height and energy, and stability of gain and base line to changes in temperature and counting rate.

The use of long shaping time constants to obtain optimum energy resolution increases the probability of pulse overlap or "pulse pile-up." This gives rise to two undesirable spectral features. Pulses are lost from the full energy peaks and a pulse pile-up continuum extends from just above the full energy peak, for all peaks in the spectrum, giving rise to complicated spectra. A further complication is that the overlap increases with counting rate and the pile-up loss is non-linear with counting rate. These problems can be almost completely overcome by the use of a "pulse pile-up rejector" system.[79] This operates by inspecting the time interval between successive pulses from the pre-amplifier and denies entry to those signals where overlap is detected, so that the system has a dead time associated with it. The pile-up rejector eliminates all but those sum peaks that are within the pulse width of the pre-amplifier and the intrinsic charge collection time of the detector. The use of a pulsed-excitation source will markedly reduce the problems of pulse overlap.[39]

Multi-channel Analyser

The MCA performs the function of sorting the pulses from the amplifier in terms of pulse amplitude and placing these in a "memory" composed of voltage windows or channels. The first stage of the MCA, the analogue to digital converter (ADC), allows the incoming pulse to charge a capacitor, which is then discharged at a constant current. The time of discharge is proportional to the pulse amplitude and this is used to gate on a constant frequency oscillator to produce a number of pulses. This "number" can then be related to a specific address or channel number. During this process the system will exhibit a dead time, during which pulses cannot be accepted, and this must be accounted for. There must be sufficient channels available in the MCA memory to span the energy range of interest with good coverage. Normally 1024 channels are used, each with the capacity to store 10^6 counts. This is important in order to allow good statistical precision when analysing trace amounts in the presence of major components. The information stored in the MCA memory is, therefore, a histogram of number of counts *versus* channel number or, after proper calibration, energy. The important features of the MCA[12] are channel number varying linearly with energy, uniform channel widths, low dead time, live-time clock adequately compensating for dead time and sufficient channels to cover the required energy range.

Dead Time

It is imperative to employ adequate dead-time compensation for quantitative analysis.[78,80] Normally the correction procedure employs the concept of "live time." A clock measures the actual data accumulation time and ignores those intervals when the system is dead. This generally gives adequate compensation of up to about 10^4 counts s^{-1} and above this level pulse pile-up effects can cause problems.

From the foregoing discussion it is obvious that each parameter must be considered in the light of the requirements and limitations of the others. Typically, counting rates of about 10^4 counts s^{-1} can be achieved with amplifier shaping constants of between 4 and 10 μs, giving rise to little peak shift or resolution degradation.

Data Processing

The raw data accumulated by the MCA must be processed to obtain useful information. For simple qualitative analysis the spectral peaks must be identified. More important, to make use of a spectral feature for quantitative analysis, the peak area, spectral background, overlap effects and inter-element absorption and enhancement effects must be considered. It has become customary to interface the MCA to a mini-computer or micro-processor. Data stored by the MCA are passed to the computer, processed according to the user's program and the final data printed out. An obvious progression from this situation is the use of the computer to control spectrometer parameters such as X-ray tube current and voltage, filter or secondary target material and sample changer. The coupling of a computer to an energy-dispersive X-ray fluorescence system, and the design of suitable software, has been discussed by Keenan.[81] Most commercial manufacturers offer systems with either partial or full computer control.

Making use of a computer to help identify the elements giving rise to an energy-dispersive X-ray spectrum is a relatively simple matter. By storing data, such as spectral line energies and relative intensities of lines from the same element, the computer can be used to produce K, L and M line markers with which spectral identification can be made. Positive identification is made by the presence of two X-ray lines in the correct intensity ratio for a particular element.

In quantitative analysis there are certain features in the energy-dispersive spectra that complicate quantitative analysis when compared with wavelength-dispersive X-ray analysis. The poorer energy resolution increases the number of spectral overlaps, and the peak to background ratio is normally poorer, making the operation of background subtraction much more important. Fortunately, the phenomena of higher order reflections from the diffraction crystal can be ignored. The need to correct for inter-element effects, both absorption and enhancement, exists with all X-ray fluorescence systems.

The problems of background subtraction and peak overlap effects are inter-related and a number of papers have dealt with these topics.[56,82–87] There are principally four methods used to calculate the background under a peak of interest: shape fitting, interpolation, blank subtraction and the regressed constant method. Peak stripping, utilising library spectra, overlap factors, generated peak shapes or a combination of these, is generally used to overcome overlap effects. Russ[86] gives an excellent review of the methods applicable to background subtraction and peak overlaps and lists a number of typical computer programs in BASIC that can be applied to the interpretation of energy-dispersive X-ray spectra. The high backgrounds encountered in electron-excited spectra make it imperative to use effective background calculation techniques.[88,89] In an attempt to remove the dependence on efficient background subtraction Nielson[87] has described a method of direct peak analysis based on a method proposed originally by Covell.[90] No background subtraction is attempted and only a partial peak area is used. The precision is claimed to be acceptable for many routine applications. Statham[91,92] has proposed a procedure for deconvolution and background subtraction, by suppressing the background using a digital filter and then proceeding to a conventional least-squares fit.

The procedures developed for conventional X-ray analysis are equally applicable to energy-dispersive X-ray spectra for the correction of inter-element effects. There are basically two approaches, the empirical and the theoretical. The empirical approach, proposed by Lucas-Tooth and co-workers,[93,94–97] employs a number of standards to determine influence coefficients. The theoretical approach or "fundamental-parameters" method[98–100] utilises known values of absorption coefficients and fluorescence yields, as well as instrumental parameters.

The specific application of these correction procedures, after modification, to energy-dispersive X-ray fluorescence analysis has been discussed by a number of workers.[101,102] Neilson[103] has described a matrix correction program based on the measurement of the scatter

of the characteristic primary radiation. Shen and Russ[104] have produced a modified version of Stephenson's[99] fundamental-parameter model for application to energy-dispersive X-ray spectra. The results obtained indicate that, when used carefully, this approach can produce acceptable results for many applications without resort to conventional standardisation, but that the method should not be used for work where high accuracy and precision are required.

Spectral Features and Interpretation

In the X-ray spectra obtained with the energy-dispersive X-ray fluorescence spectrometer, the major features are the characteristic X-ray lines from the elements present in the sample being analysed. Unfortunately, these are not the only spectral features encountered. A number of other phenomena can give rise to features that must be recognised so as to avoid confusion with the characteristic X-ray lines, or "full-energy" peaks as they are known.

Sum Peaks

Pulse pile-up effects were discussed above and it is inevitable with conventional systems that a certain amount of pulse pile-up will occur. Pulse pile-up increases with increasing counting rate and its effect is to produce sum peaks in the spectra, which are essentially the sum of two X-rays being detected simultaneously. Normally, sum peaks will appear only for the most intense features of a spectrum. For example, in the X-ray spectrum of a steel sample it is probable that sum peaks will occur for the intense iron Kα and Kβ lines. These will appear in the spectrum at energies corresponding to 2Kα, 2Kβ and Kα + Kβ. Elimination of sum peaks can be accomplished by either reducing the counting rate or using a filter between the sample and detector to remove a portion of the spectrum.

Escape Peaks

The escape peak phenomenon is caused by the escape of a silicon Kα X-ray from the intrinsic region of the detector. Generally, an X-ray entering the detector transfers all of its energy to ionisation in this region. This results in the production of silicon Kα X-rays, which are normally contained within the active region, producing further ionisation. However, where the probability of silicon Kα X-ray production is high, less than 10 keV incoming X-ray energy, a significant number of these photons can escape from the intrinsic region. The energy deposited in the detector will, therefore, be the energy of the incoming photon less the energy of the escaping X-ray, 1.74 keV. This will give rise to a spectral feature at full energy minus 1.74 keV. The ratio of the escape peak to the full energy peak decreases with increasing atomic number and is normally about 1:200 for chlorine and 1:1000 for iron. This feature is characteristic of the detector, independent of the sample and cannot be eliminated from the spectrum.

Diffraction Peaks

A sample of a highly ordered or crystalline nature can give rise to a peak in the spectrum by diffraction of the primary X-ray beam. A diffraction peak will appear when the incident X-ray energy and the spectrometer geometry are such that Bragg's law is satisfied. The diffraction peak can be identified by altering the sample to detector or X-ray tube distance, thus changing the angle and causing the peak to appear at a different energy. This phenomenon is normally seen where a continuum source of X-rays is used. The probability of satisfying the Bragg condition with mono-energetic excitation is small. The diffraction peak is generally broad and irregular in shape.

Anomalous Silicon, Gold and Argon Peaks

The anomalous silicon and gold X-ray peaks are produced by the interaction of secondary X-rays with the detector dead layer and the gold Schottky barrier. X-rays interacting in these regions produce silicon and gold X-rays, which have a probability of reaching the intrinsic region of the detector and being recorded as discrete pulses. Instances of anomalous silicon and gold peaks are fortunately rare; however, where a high secondary X-ray flux is incident on the detector, with energy between 2 and 3 keV, the anomalous silicon peak may

appear. In electron microprobe analysis the appearance of gold absorption edges in the spectral background can complicate background calculations.[105]

If an air path exists between the X-ray tube, sample and detector, then argon present in the air can be excited, giving rise to secondary argon Kα X-rays at 2.96 keV. The occurrence of anomalous argon peaks is easily avoided by the use of either vacuum or helium paths in the spectrometer.

Scatter Peaks

There are two types of X-ray scatter, coherent (Rayleigh) and incoherent (Compton). Peaks in the X-ray spectrum are generated by scatter of the characteristic lines in the primary-excitation radiation, by the sample. Coherent scatter occurs without loss of energy and, therefore, produces a peak at the energy of the characteristic primary radiation and with a similar band width. Incoherent scatter occurs with energy loss and, therefore, produces a spectral peak at a lower energy than that of the primary-excitation radiation and with a fairly broad band width. The ratio of coherent to incoherent scatter peak intensities is a direct function of atomic number.

Spectral Background

The spectral background continuum is determined by the nature of the excitation system. With direct or primary X-ray tube excitation the spectral background is fairly high and is due mainly to scattering of the primary bremsstrahlung. Other contributions to the background are incomplete charge collection in the detector and sample-generated bremsstrahlung. With a near monochromatic secondary target or filtered X-ray excitation the background can be significantly reduced and is mainly associated with incomplete detector charge collection. With charged-particle excitation the background is due mainly to sample-generated bremsstrahlung.

Cooper[106] has discussed the features to be found in the energy-dispersive X-ray spectrum and proposed means of identification. Keith and Loomis[69] have described the origin of some of the spectral features and proposed computer programs to correct the X-ray spectra for such phenomena as escape and sum peaks. The use of computer-generated K, L and M line markers enables many of the above-mentioned spectral features to be distinguished easily from full-energy peaks.

Comparison of Wavelength- and Energy-dispersive Systems

A number of parameters must be considered when comparing energy-dispersive and wavelength-dispersive X-ray fluorescence equipment. These include resolution, counting-rate capacity, spectral interference, peak to background ratio and the time, cost and convenience when carrying out particular analytical procedures. A comparison between energy-dispersive and wavelength-dispersive X-ray spectrometers for electron microscopes has been made by Malissa *et al.*[107] but this is not completely relevant to the present discussion.

Walinga[108] has discussed the advantages and limitations of the energy-dispersive X-ray technique, in both fluorescence and diffraction, in comparison with conventional or wavelength-dispersive systems. He concluded that energy-dispersive X-ray fluorescence analysis would find its major applications in qualitative and semi-quantitative analysis. However, this viewpoint seems dated when compared with more recent publications[35] and the large number of papers appearing on quantitative analytical applications. Techniques for the analysis of samples of air pollutants have been compared by Gilfrich *et al.*[109] They investigated the use of various excitation sources such as X-rays, α-particles, radioisotopes and protons when used on energy-dispersive X-ray equipment and compared detection limits with those found using a wavelength-dispersive spectrometer. Detection limits were found to be comparable when the X-ray tube excited-energy dispersive system was used. Dewolfs *et al.*[110] compared a high-powered, secondary-target, energy-dispersive X-ray spectrometer with a commercial wavelength-dispersive X-ray spectrometer in terms of energy resolution, spectral interferences, intensity and peak to background ratio, sensitivity, reproducibility and precision. The eventual conclusion was that the energy-dispersive technique was advantageous when applied to an analytical situation requiring multi-element analysis with limited precision. In a study of energy- and wavelength-dispersive systems on the electron

micro-probe Dunham and Wilkinson[111] found that the techniques compared well in terms of accuracy and precision, but that the energy-dispersive system produced poorer limits of detection while being faster and more convenient to use.

The resolution of energy-dispersive X-ray systems is poor in comparison with wavelength-dispersive systems, with the exception of the K lines of the heavy elements with atomic number greater than 45. This produces more spectral overlaps, often requires the use of mathematical fitting procedures or forces the use of less sensitive lines. The counting-rate capacity is poorer for the solid-state Si(Li) detector and the associated electronics and this means that the sensitivity is poorer when only the number of counts per second measured is considered. This is at least partially balanced by the fact that the multi-element capacity of energy-dispersive systems allows much longer counting times to be tolerated. Peak to background ratios are generally poorer for energy-dispersive systems placing more emphasis on efficient background subtraction. Qualitative analysis is considerably simplified and less time consuming using the energy-dispersive system, especially when computer-generated markers are used. It is difficult to emphasise sufficiently the benefits of accumulating data simultaneously. For quantitative analysis the energy-dispersive technique can produce good multi-element data with reasonable precision; however, the counting statistics usually produce poorer limits of detection than is the case with wavelength-dispersive spectrometers. Inter-element absorption and enhancement effects should be similar, given similar spectrometer geometries and excitation conditions. The time taken for a particular analysis favours wavelength-dispersive systems when only a few elements are being quantified but favours energy-dispersive systems for multi-element analysis. Energy-dispersive X-ray spectrometers are somewhat cheaper than sequential wavelength-dispersive spectrometers and much cheaper than simultaneous wavelength-dispersive spectrometers. The energy-dispersive spectrometer is usually smaller and less bulky (especially true of low-power generator systems) and can be initially simpler to use for the non-X-ray spectroscopist.

The newer energy-dispersive X-ray fluorescence technique can be seen as a competitor to the wavelength-dispersive spectrometer or as a complement to it, depending on the particular analytical requirements of a given situation. For many applications the ultimate in precision is not required and the energy-dispersive system can provide an adequate, versatile and relatively inexpensive solution. When fast qualitative analysis is important then the energy-dispersive system must be carefully considered. When very high precision work is required, the simultaneous or sequential wavelength-dispersive spectrometer must still be the instrument of choice. When multi-element analysis is required on a limited budget, then the energy-dispersive system may appear advantageous when compared with a simultaneous wavelength-dispersive spectrometer. In some analytical situations the choice will be complicated by the need to satisfy a number of conflicting criteria and here the energy-dispersive system can be seen as a complement to the wavelength-dispersive system.

Applications

The last few years have seen a large increase in the number of publications dealing with the application of the energy-dispersive X-ray emission technique to practical analytical problems. For convenience, these will be detailed here in terms of the various fields of interest with which the papers have dealt. All of the applications have the solid-state Si(Li) detector in common, but excitation of the characteristic sample X-rays may be by a variety of means, as already detailed.

Atmospheric Particulates

Energy-dispersive X-ray fluorescence analysis has attracted considerable interest for the analysis of airborne particulate matter.[112] There are a number of reasons for this popularity, including its potential multi-element capability, non-destructive nature and the advantages gained when working with thin samples. A number of papers have dealt with the problems to be overcome before acceptable multi-element analyses can be obtained,[113–118] while others describe the results found in various locations and their implications.[119–121]

Air particulates are normally collected by passing a known volume of air through a filter. This results in "thin-specimen" samples and these possess a number of advantages over conventional "infinitely-thick" samples. Inter-element effects are eliminated or, at worst,

reduced considerably, peak to background ratio is normally increased, particle size effects are simplified and linear calibrations are generally found over wide ranges. The filter must be as thin as possible to reduce absorption and enhancement effects and contain no contaminants heavier than sodium. Cellulose fibre or membrane filters are popular, although weighing can be a problem owing to hygroscopicity. Using radioisotope excitation Rhodes[113] and Rhodes *et al.*[114] have investigated particle-size distribution, sampling and standardisation with respect to thin-filter samples. Adams and co-workers,[116–118] using secondary-target X-ray tube excitation, have considered a number of potential problems, including sample homogeneity and position, background subtraction and spectral overlap effects. Generator instability was compensated for by placing a thin zirconium wire below the sample surface and normalising all spectral features to the zirconium Kα X-radiation. Adams and Van Grieken[115] have also demonstrated that absorption effects cannot be ignored for elements of low atomic number and correction procedures are necessary for both the air particulate matrix and the filter material. The procedure normally adopted to correct for filter attenuation involves the measurement of front to back intensity ratios of secondary X-rays from the material deposited on the filters.[122] Ahlberg and Adams[67] demonstrated the extra sensitivity that can be obtained using proton excitation as compared with X-ray excitation, especially for the lighter elements. The use of 5-MeV protons to excite secondary X-rays from filter samples has been described by Pilotte *et al.*[121] A number of elements including sulphur, chlorine and potassium were determined with sufficient sensitivity to allow observation of time variations in elemental concentrations. The variation of elemental composition across the particle size range is of interest with respect to the determination of the source of the particulate matter. Jaklevic and co-workers[123,124] have described a "dichotomous" sampler, which is designed to separate airborne particulates above and below 2.4 μm particle diameter. The two particle-size ranges were collected separately and subjected to energy-dispersive X-ray fluorescence analysis using photon excitation. The use of energy-dispersive X-ray analysis on a scanning electron microscope for the characterisation of atmospheric particulate matter was described by Butler *et al.*[125] Specific particles can be chosen for investigation, thus allowing a correlation to be made between particle size and elemental composition. The limitation will, of course, be the lower sensitivity that is available. Calibration standards, prepared by vacuum deposition on thin films, are commercially available from Micro Matter Co., Seattle, and are most useful as an aid to the quantification of energy-dispersive X-ray fluorescence data of filter samples.

Waters

Waters can contain both dissolved solids and particulate matter. Information can be sought on one or both of these phases, or a total figure may be sufficient. For particulate matter, filtration produces thin samples similar to those obtained with atmospheric particulates and much of the above discussion applies equally. In most instances dissolved solids are present at concentrations below those directly observable using the energy-dispersive X-ray technique and some form of pre-concentration is usually employed.

In a study of the analysis of sediments and particulate matter in sea water Vanderstappen and Van Grieken[126] concluded that a 0.4-μm Nuclepore polycarbonate filter was optimum for filtration. Samples from the North Sea and Mediterranean were analysed for a number of elements at the parts per billion (10^9) level, with acceptable accuracy and precision.

The use of trace-element precipitation, by complexing with the chelating agent ammonium tetramethylenedithiocarbamate (ammonium-1-pyrrolidine dithiocarbamate, APDC) followed by filtration, is recommended for the determination of dissolved solids in natural waters.[127,128] APDC forms insoluble complexes with about 30 transition metals, but does not complex the alkali metals or the alkaline earth metals. Where only the dissolved solids are of interest, particulate matter must first be removed by filtration or centrifugation. Elder *et al.*[128] reported the analysis of a number of elements at the parts per billion level by APDC precipitation and filtration through a membrane filter, while Pradzynski *et al.*[127] determined uranium, molybdenum and thorium at the 1 p.p.b. level. Electro-deposition has been advocated as a pre-concentration technique to determine reducible metals in aqueous media by wavelength-dispersive X-ray fluorescence.[129] Boslett *et al.*[130] have proposed a similar technique for use with energy-dispersive apparatus. Zinc, copper and nickel were determined at the 2–100

p.p.b. level using potentiostatic electro-deposition on to a graphite rod, producing a thin metallic film. Special cylindrical monochromators were necessary to reduce scatter from the graphite rod and fairly long deposition times were required. Carlton and Russ[131] described the use of ion-exchange resin loaded filter-papers to pre-concentrate trace elements. An automated sample collection and preparation module was presented and sensitivities obtained were in the parts per billion range. Van Grieken *et al.*[132] have shown that Chelex-100 ion-exchange membranes can be used to pre-concentrate trace elements prior to energy dispersive X-ray fluorescence analysis, provided that the water samples contain only modest concentrations of alkali and alkaline earth metals. The use of chelating ion exchangers based on cellulose was described by Burba *et al.*[133] and illustrated by the determination of uranium in natural waters down to 0.3 p.p.b. A simple sample-spotting procedure has been proposed by Smits and Van Grieken.[134] About 1.5 ml of the sample is placed on a cellulose filter and held in position with a wax ring. The water is evaporated using an unheated air stream from below. Claimed precisions are 15–20% at the 50–100 p.p.b. level.

The choice of the pre-concentration technique depends on the elements of interest, the analysis time restrictions and sensitivity requirements. The sample-spotting procedure is probably the simplest and most widely applicable but could give problems at high concentrations where crystallisation can occur. Birks and Gilfrich[135] have evaluated seven typical energy-dispersive X-ray fluorescence instruments with respect to the determination of trace elements in polluted waters. All were considered capable of measuring elemental concentrations at levels appropriate to the problem.

Clinical and Biochemical

In many clinical and biochemical studies it is necessary to determine a number of elements in small samples of blood, urine, tissue, etc. When only one element is determined at a time, problems can be caused in terms of sample size and analysis time. The multi-element capacity of energy-dispersive X-ray fluorescence is, therefore, attractive in this field. However, its relatively poor sensitivity, compared with say atomic-absorption spectrometry, requires that more effort be devoted to sample preparation. The application of the energy-dispersive X-ray technique in this area has been discussed by a number of workers.[136–141]

The determination of trace elements in whole blood, plasma and serum has attracted considerable interest. Bearse *et al.*[142] using a plasma-ashing preparation technique, followed by proton-induced X-ray emission, determined iron, copper, zinc, selenium and rubidium in 0.1-ml samples of blood. Detection limits for elements with atomic numbers 25–45 were shown to be between 0.1 and 1 p.p.m., which should be useful for many applications. Holynska and Markowicz[143] also determined selenium in whole blood (and tissue) but used wet ashing and coprecipitation, followed by low-powered X-ray tube excitation. Levels as low as 100 p.p.b. were determined. The use of proton excitation allowed the determination of selenium in blood serum at the 10 p.p.b. level.[144] Freeze-drying and pelletising have been used[145] to prepare samples of whole blood and plasma for the determination of copper, zinc, bromine and rubidium by energy-dispersive X-ray fluorescence using secondary target X-ray excitation, with detection limits in the 100–400 p.p.b. range. Knoth *et al.*[146] suggested the use of total X-ray reflection[147] on a sample support as a means of reducing the spectral background, in the determination of copper and iron in blood serum. A 10-μl sample was dried on a support of optically flat silica glass and the incident X-ray beam adjusted to strike the support at a very low angle, such that it is "totally reflected." Agarwal *et al.*[148] applied energy-dispersive X-ray fluorescence with secondary target X-ray excitation to the analysis of copper, zinc and lead in urine. They suggested the use of an ion-exchange chelating resin as a pre-concentration step and also used yttrium as an internal standard. The method is limited to those elements chelated by the resin.

Inductively-coupled plasma-emission spectroscopy has a similar multi-element capacity to energy-dispersive X-ray fluorescence. An evaluation of both techniques for biological work has been carried out by Irons *et al.*[149] with reference to sensitivity, precision and accuracy. They conclude that the choice of method depends on the sample type, plasma emission having advantages for fluids and X-ray fluorescence for solids. The need to apply inter-element corrections in X-ray work was emphasised, hence increasing the computer size requirement relative to plasma-emission spectroscopy.

Rocks, Ores and Cement

Cooper and Schlofke[150] have described the application of energy-dispersive X-ray fluorescence, with direct X-ray tube excitation, to rock and ore analysis. Samples of this type normally receive minimal preparation prior to analysis. They are generally ground and pressed into disc form. Standardisation is achieved by using similar standard reference materials. Corrections for inter-element effects and peak overlaps must be applied to obtain acceptable results. The general utility of energy-dispersive X-ray fluorescence analysis to geochemical specimens has been demonstrated by Giauque *et al.*[151] Twenty-six trace and two major elements were determined in reference materials, use being made of the relationship between the intensity of the incoherent scattered radiation, specimen mass absorption coefficient and spectral background intensity to correct for inter-element effects. Other workers have undertaken the analysis of platinum[152] and copper[153] in ores. Hebert and Bowman[154] described a special spectrometer for the analysis of the light elements in rocks, which possessed a sensitivity of 5 p.p.m. for sodium.

In the analysis of cement-type materials both major and minor elements are determined, although the most important are aluminium, silicon, calcium and iron. Energy-dispersive X-ray fluorescence with primary X-ray tube excitation has been used to determine these four and eight other elements, in Portland cement, by Cooper and co-workers.[155,156] Once again, inter-element correction procedures were shown to improve the quality of the analytical results. Carr-Brion *et al.*[157] have described an on-stream energy-dispersive X-ray fluorescence analyser for the determination of the four main elements of interest in cement raw meal. Results appear to be sufficient for raw meal feed control requirements despite the need to analyse the raw meal "unground."

Metals and Alloys

The use of energy-dispersive X-ray emission as an alloy-sorting technique has been described.[158,159] Alloys can be quickly characterised by their spectral features in a non-destructive fashion, using a portable analyser with minimum or no sample preparation. Janssens *et al.*[160] have proposed a high-precision method for the determination of manganese in ferromanganese. Radioisotope excitation (using cadmium-109), with careful control of the instrumental conditions and standardisation, produced a relative standard deviation of 0.2%. The application of the energy-dispersive X-ray technique to multi-element analysis of nickel-alloys has been investigated by Verbeke *et al.*,[161] who found that acceptable results could be obtained only after applying inter-element corrections using a fundamental-parameters approach. The analysis of thin nickel - gold films has been examined by Franken,[162] who found that energy-dispersive X-ray fluorescence produced better data than conventional X-ray diffraction, because it was less sensitive to structural effects.

Coal and Petroleum

The multi-element analysis of coal, coke and fly-ash materials by energy-dispersive X-ray fluorescence has been shown to provide acceptable data, after application of an inter-element correction routine using multiple standards.[163] Lloyd and Francis[164] compared the results obtained for the determination of sulphur in coal by conventional ASTM procedures with energy-dispersive X-ray fluorescence results. They concluded that the instrumental technique, with proper matrix corrections, was close to meeting the ASTM standards of accuracy and precision, but was far superior in terms of speed of analysis and convenience. A different approach to the analysis of coal has been taken by De Kalb and Fassel,[165] who minimised the inter-element effects by converting the powdered coal into a thin film, using the Chung[166] technique, and obtained good results without inter-element correction procedures. The application of PIXE to coal analysis has been described by Cronch *et al.*[167]

Yousif and Al-Shahristani[168] applied energy-dispersive X-ray emission with radio-isotope excitation (using iron-55) to the determination of sulphur and vanadium in crude oils. At the concentration levels found in crude oil it was necessary to correct the vanadium data for the presence of sulphur. Vanadium was determined down to 2 p.p.m. and sulphur to 0.03%. Teller[169] has described an immersion probe, designed to determine sulphur in fuel oils or lead in refinery products, by the simultaneous measurement of scattered and transmitted low-energy X-rays.

On-stream Analysis

Energy-dispersive X-ray fluorescence possesses a number of attractive features for on-stream analysis when compared with wavelength-dispersive equipment. The use of high take-off angles and broad-beam geometry helps lessen the effects of surface roughness, and a well designed system is relatively insensitive to temperature variations. Very short path lengths can be achieved, thus increasing light-element sensitivity. The ability to use a variety of excitation systems increases the over-all system flexibility. The advantages and limitations of energy-dispersive X-ray emission and diffraction equipment in process control situations have been discussed by Carr-Brion[170] and Kawatra and Dalton.[171] On-stream systems have been described for the process control of cement raw-meal powder[157] and finished sinter.[172]

Others

Applications of the energy-dispersive technique have been both numerous and varied. Cobalt and molybdenum have been determined in hydrodesulphurisation catalysts,[173,174] noble metals in automotive exhaust catalysts,[175] silver in photographic materials,[176] thorium in optical components,[177] uranium in aqueous media,[178] technetium in nuclear fuel processing waste,[179] copper and silver in Roman silver coins[180] and in paper additives.[181] Other uses include the analysis of sedimentary pollutants[182] and agricultural wastes,[183] ion-exchange studies[184,185] and process control.[186] Hanson[187] proposed the use of energy-dispersive X-ray fluorescence as a technique to determine the authenticity of art objects. The use of the technique to determine particle sizes has been described by Tominaga *et al.*[188] while Kawamoto *et al.*[189] have designed a milli-analyser to investigate small particles of the order of 1 mm.

Future Developments

It is unlikely that any dramatic improvement in detector resolution will be made in the immediate future. Small resolution improvements, although welcome, will not significantly affect the over-all system performance. Improvements in the quality of the detector can, however, produce a lowering of the spectral background, which would be of considerable benefit. There appears to be no successor to the solid-state Si(Li) detector on the horizon.

Improvements to the stability of the X-ray generator, especially for high-powered systems, would be welcome. The use of pulsed X-ray sources, now becoming commercially available, should help to improve the counting-rate capability of the system but it is not clear whether the pulse-processing electronics are sufficiently sophisticated to allow full benefit to be gained. With many commercial systems the determination of the heavy elements can present problems. The typical X-ray generator is designed to produce a maximum of 50 kV and this does not efficiently excite the K lines of elements with $Z \approx 50$–60,[91] while the L lines are subject to a variety of possible spectral overlaps. A move toward generators capable of producing 60–80 kV would be welcome.

The most significant advances in the near future will lie in the area of computer software. The power of the dedicated mini-computer, especially when coupled to interactive disc drives, has still to be fully utilised. The identification of spectral features is primarily the work of the instrument operator, though generally aided by the computer with such devices as K, L and M markers. This task will become more and more computer dependent. The extraction of quantitative data from energy-dispersive X-ray spectra, using the fundamental parameters approach, will improve to a high degree of sophistication.[190] The techniques of deconvolution and inter-element correction, though now well documented, require further development.

Finally, although a large number of publications have appeared dealing with applications of the technique, many more studies are necessary to define the best fields of application, especially with respect to conventional infinitely thick samples.

References

1. Carr-Brion, K. G., and Payne, K. W., *Analyst*, 1970, **95**, 977.
2. Elad, E., *Nucl. Instrum. Meth.*, 1965, **37**, 327.
3. Elad, E., and Nakamura, M., *Nucl. Instrum. Meth.*, 1966, **41**, 161.

4. Bowman, H. R., Hyde, E. K., Thompson, S. G., and Jared, R. C., *Science, N.Y.*, 1966, **151**, 562.
5. Elad, E., and Nakamura, M., *I.E.E.E. Trans. Nucl. Sci.*, 1967, **14**, 523.
6. "Energy Dispersive X-Ray Analysis: X-Ray and Electron Probe Analysis," Special Publication STP 485, American Society for Testing and Materials, Philadelphia, Pa., 1971.
7. Heinrich, K. F. J., Barrett, C. S., Newkirk, J. B., and Ruud, C. O., *Editors, Advances in X-Ray Analysis*, 1972, Volume 15.
8. Heath, R. L., *Adv. X-Ray Analysis*, 1972, **15**, 1.
9. Giauque, R. D., and Jaklevic, J. M., *Adv. X-Ray Analysis*, 1972, **15**, 164.
10. Dyer, G. R., Gedcke, D. A., and Harris, T. R., *Adv. X-Ray Analysis*, 1972, **15**, 228.
11. Jaklevic, J. M., Giauque, R. D., Malone, D. F., and Searles, W. L., *Adv. X-Ray Analysis*, 1972, **15**, 266.
12. Gedcke, D. A., *X-Ray Spectrom.*, 1972, **1**, 129.
13. "Appendices on Provisional Nomenclature, Symbols, Terminology and Conventions—Number 54," *IUPAC Information Bulletin*, 1976.
14. Bertin, E. P., "Principles and Practice of X-Ray Spectrometric Analysis," Plenum Press, New York, 1970.
15. Liebhafsky, H. A., Pfeiffer, H. G., Winslow, E. H., and Zemany, P. D., "X-Rays, Electrons, and Analytical Chemistry," Wiley, New York, 1972.
16. Jenkins, R., and De Vries, J. L., "Practical X-Ray Spectrometry," Macmillan, London, 1975.
17. Birks, L. S., and Gilfrich, J. V., *Analyt. Chem.*, 1976, **48**, 273R.
18. De Vries, J. L., "X-Ray Fluorescence Spectrometry—Review of Literature," Seventh Edition, Philips, Eindhoven, 1976.
19. Jenkins, R., "An Introduction to X-Ray Spectrometry," Heyden, London, 1974.
20. Bertin, E. P., "Introduction to X-Ray Spectrometric Analysis," Plenum, New York, 1978.
21. Woldseth, R., "X-Ray Energy Spectrometry," Kevex Corp., Burlinghame, Calif., 1973.
22. Schünemann, D., *Miner. Slov.*, 1973, **5**, 569.
23. Friant, A., *Onde Elect.*, 1976, **56**, 69.
24. Russ, J. C., *X-Ray Spectrom.*, 1972, **1**, 119.
25. Friant, A., Gras, R., Lorin, A., and Saliou, C., *Bull. Instrumn Nucl.*, 1971, **42**, 34.
26. Porter, D. E., and Woldseth, R., *Analyt. Chem.*, 1973, **45**, 604A.
27. Lister, D. B., "Application of Energy-Dispersive X-Ray Fluorescence," AID 75437, Instrument Society of America, 1975.
28. Gedcke, D. A., and Elad, E., "Proceedings of the 6th International Conference on X-Ray Optics and Microanalysis, Osaka, Japan, 1971," University of Tokyo Press, Toyko, 1972.
29. Goulding, F. S., and Jaklevic, J. M., *A. Rev. Nucl. Sci.*, 1973, **23**, 45.
30. Russ, J. C., Shen, R. B., and Jenkins, R., "Energy Dispersive X-Ray Analysis of Materials: Principles and Experiments," Edax International, Prairie View, Ill., 1978.
31. Cothern, C. R., Manuel, H. L., and Millette, R. J., *X-Ray Spectrom.*, 1974, **3**, 53.
32. Jaklevic, J. M., "Proceedings of ERDA X- and Gamma-Ray Symposium, Ann Arbor, Mich., 1976," NTIS, Springfield, Va., 1977, p. 1.
33. Middleman, L. M., and Geller, J. D., "Proceedings of the 9th Annual Scanning Electron Microscope Symposium, Chicago, 1976," *Scanning Electron Microsc.*, 1976, **9**, Part 1, 171.
34. Reldy, J. J., Hutson, R. L., Daniel, H., and Springer, K., *Analyt. Chem.*, 1978, **50**, 40.
35. Gedcke, D. A., Elad, E., and Denee, P. B., *X-Ray Spectrom.*, 1977, **6**, 21.
36. Artz, B. E., and Short, M. A., "Proceedings of ERDA X- and Gamma-Ray Symposium, Ann Arbor, Mich., 1976," NTIS, Springfield, Va., 1977, p. 7.
37. Anselmo, V. C., Report, Lawrence Livermore Laboratory, UCID 17317, 1976.
38. Van Espen, P. J., and Adams, F. C., *Analyt. Chem.*, 1976, **48**, 1823.
39. Jaklevic, J. M., Goulding, F. S., and Landis, D. A., *I.E.E.E. Trans. Nucl. Sci.*, 1972, **NS19**, 392.
40. Jaklevic, J. M., Landis, D. A., and Goulding, F. S., Report, Lawrence Berkeley Laboratory, LBL 4248, 1975.
41. Howell, R. H., Pickles, W. L., and Cate, J. L., *Adv. X-Ray Analysis*, 1974, **18**, 265.
42. Kaufman, L., and Camp, D. C., *Adv. X-Ray Analysis*, 1974, **18**, 247.
43. Dzubay, T. G., Jarret, B. V., and Jaklevic, J. M., *Nucl. Instrum. Meth.*, 1974, **115**, 297.
44. Howell, R. H., and Pickles, W. L., *Nucl. Instrum. Meth.*, 1974, **120**, 187.
45. Ryon, R. W., Report, Lawrence Livermore Laboratory, UCRL 78063, 1976.
46. Aiginger, H., Wobrauschek, P., and Brauner, C., *Nucl. Instrum. Meth.*, 1974, **120**, 541.
47. Leonowich, J., Pandian, S., and Preiss, I. L., *J. Radioanalyt. Chem.*, 1977, **40**, 175.
48. Robertson, R., *Nucl. Instrum. Meth.*, 1977, **142**, 121.
49. Franzgrote, E., *Adv. X-Ray Analysis*, 1972, **15**, 388.
50. Spatz, R., and Lieser, K. H., *Z. Analyt. Chem.*, 1977, **288**, 267.
51. Fitzgerald, R., Keil, K., and Heinrich, K. F. J., *Science, N.Y.*, 1968, **159**, 528.
52. Gedcke, D. A., *in* Holt, D. B., Muir, M. D., Grant, P. R., and Boswarva, I. M., *Editors*, "Quantitative Scanning Electron Microscopy," Academic Press, New York and London, 1974, Ch. 12.
53. Birks, L. S., "Electron Microprobe Analysis," Interscience, New York, 1963.
54. Waldl, E., Wolfermann, H., Rusovic, N., and Warlimont, H., *Analyt. Chem.*, 1975, **47**, 1017.
55. Desborough, G. A., and Heidel, R. H., *Appl. Spectrosc.*, 1973, **27**, 456.
56. Reed, S. J. B., and Ware, N. G., *X-Ray Spectrom.*, 1973, **2**, 69.
57. Walter, R. L., Willis, R. D., Gutknecht, W. F., and Joyce, J. M., *Analyt. Chem.*, 1974, **46**, 843.
58. Johansson, G., Akselsson, R., Bohgard, M., Carlsson, L. E., Hansson, H. C., Lannefors, H., and Malmqvist, K., *Proc. Analyt. Div. Chem. Soc.*, 1978, **15**, 24.
59. Johansson, S. A. E., and Johansson, T. B., *Nucl. Instrum. Meth.*, 1976, **137**, 473.

60. Folkmann, F., *J. Phys. E*, 1975, **8**, 429.
61. Lochmüller, C. H., Galbraith, J. W., and Walter, R. L., *Analyt. Chem.*, 1974, **46**, 440.
62. Mangelson, N. F., Hill, M. W., Nielson, K. K., and Ryder, J. F., *Nucl. Instrum. Meth.*, 1977, **142**, 133.
63. Malmqvist, K., Akselsson, R. A., and Johansson, G., *Proc. Analyt. Div. Chem. Soc.*, 1978, **15**, 13.
64. Johansson, T. B., Van Grieken, R. E., Nelson, J. W., and Winchester, J. W., *Analyt. Chem.*, 1975, **47**, 855.
65. Reuter, W., and Lurlo, A., *Analyt. Chem.*, 1977, **49**, 1737.
66. Ahlberg, M. S., *Nucl. Instrum. Meth.*, 1977, **146**, 465.
67. Ahlberg, M. S., and Adams, F. C., *X-Ray Spectrom.*, 1978, **7**, 73.
68. Heath, R. L., *Adv. X-Ray Analysis*, 1972, **15**, 1.
69. Keith, H. D., and Loomis, T. C., *X-Ray Spectrom.*, 1976, **5**, 93.
70. Martin, G. W., and Klein, A. S., *Adv. X-Pay Analysis*, 1972, **15**, 254.
71. Laine, E., Lähteenmäki, I., and Kantola, M., *X-Ray Spectrom.*, 1972, **1**, 93.
72. Holt, S. S., *Space Sci. Instrumn*, 1976, **2**, 205.
73. Elad, E., "Energy Dispersive X-Ray Analysis: X-Ray and Electron Probe Analysis," Special Publication STP 485, American Society for Testing and Materials, Philadelphia, Pa., 1971, p. 57.
74. Goulding, F. S., Walton, J. T., and Pehl, R. H., Report, Lawrence Berkeley Laboratory, UCRL 19377, 1977.
75. Walter, F. J., "Energy Dispersive X-Ray Analysis: X-Ray and Electron Probe Analysis," Special Publication STP 485, American Society for Testing and Materials, Philadelphia, Pa., 1971, p. 82.
76. Elad, E., *I.E.E.E. Trans. Nucl. Sci.*, 1972, **19**, 403.
77. Landis, D. A., Goulding, F. S., Pehl, R. H., and Walton, J. T., *I.E.E.E. Trans. Nucl. Sci.*, 1971, **18**, 115.
78. Gedcke, D. A., Elad, E., and Dyer, G. R., "Proceedings of the 6th National Conference on Electron Probe Analysis," Electron Probe Analysis Society of America, New York, 1971, p. 5A.
79. Reed, S. J. B., *J. Phys. E*, 1972, **5**, 997.
80. Reed, S. J. B., *J. Phys. E*, 1972, **5**, 994.
81. Keenan, J. A., *Int. Lab.*, 1975, May/June, 49.
82. Fiori, C. E., Myklebust, R. L., Heinrich, K. F. J., and Yabowitz, H., *Analyt. Chem.*, 1976, **48**, 172.
83. Connelly, A. L., and Black, W. W., *Nucl. Instrum. Meth.*, 1970, **82**, 141.
84. Smith, D. G. W., Gold, C. M., and Tomlinson, D. A., *X-Ray Spectrom.*, 1975, **4**, 149.
85. Geiss, R. H., and Hwang, T. C., *X-Ray Spectrom.*, 1975, **4**, 196.
86. Russ, J. C., *X-Ray Spectrom.*, 1977, **6**, 37.
87. Nielson, K. K., *X-Ray Spectrom.*, 1978, **7**, 15.
88. Comins, N. R., and Thirlwall, J. T., *X-Ray Spectrom.*, 1978, **7**, 92.
89. Bauer, R., and Rick, R., *X-Ray Spectrom.*, 1978, **7**, 63.
90. Covell, D. F., *Analyt. Chem.*, 1959, **31**, 1785.
91. Statham, P. J., *Analyt. Chem.*, 1977, **49**, 2149.
92. Statham, P. J., *X-Ray Spectrom.*, 1978, **7**, 132.
93. Lucas-Tooth, H. J., and Price, B. J., *Metallurgia*, 1961, **64**, 149.
94. Lucas-Tooth, H. J., and Pyne, C., *Adv. X-Ray Analysis*, 1964, **7**, 523.
95. Traill, R. J., and Lachance, G. R., *Geol. Surv. Can. Pap.*, 1965, No. 64.
96. Traill, R. J., and Lachance, G. R., *Can. Spectrosc.*, 1966, **11** (3), 63.
97. Rasberry, S. D., and Heinrich, K. F. J., *Analyt. Chem.*, 1974, **46**, 81.
98. Criss, J. W., and Birks, L. S., *Analyt. Chem.*, 1968, **40**, 1080.
99. Stephenson, A., *Analyt. Chem.*, 1971, **43**, 1761.
100. de Jongh, W. K., *X-Ray Spectrom.*, 1973, **2**, 151.
101. Russ, J. C., Sandborg, A. O., Barnhart, M. W., Soderquist, C. E., Lichtinger, R. W., and Walsh, C. J., *Adv. X-Ray Analysis*, 1973, **16**, 284.
102. Ong, P. S., Cheng, E. L., and Sroka, G., *Adv. X-Ray Analysis*, 1974, **17**, 269.
103. Nielson, K. K., *Analyt. Chem.*, 1977, **49**, 641.
104. Shen, R. B., and Russ, J. C., *X-Ray Spectrom.*, 1977, **6**, 56.
105. Brombach, J. D., *X-Ray Spectrom.*, 1978, **7**, 81.
106. Cooper, J. A., *Am. Lab.*, 1976, Nov., 35.
107. Malissa, H., Grasserbauer, M., and Hoke, E., *Microchim. Acta*, 1974, **5**, 465.
108. Walinga, J., "Proceedings of the 8th Philips X-Ray Analytical Conference, Birmingham, England, 1972," Philips, Eindhoven, 1973.
109. Gilfrich, J. V., Burkhalter, P. G., and Birks, L. S., *Analyt. Chem.*, 1973, **45**, 2002.
110. Dewolfs, R., De Neve, R., and Adams, F., *Analytica Chim. Acta*, 1975, **75**, 47.
111. Dunham, A. C., and Wilkinson, F. C. F., *X-Ray Spectrom.*, 1978, **7**, 50.
112. Dzubay, T. G., *Editor*, "X-Ray Fluorescence Analysis of Environmental Samples," Ann Arbor Science Publishers, Ann Arbor, Mich., 1977.
113. Rhodes, J. R., *Am. Lab.*, 1973, July, 57.
114. Rhodes, J. R., Pradzynski, A. H., and Sieberg, R. D., *Air Qual. Instrumn*, 1974, **2**, 1.
115. Adams, F. C., and Van Grieken, R. E., *Analyt. Chem.*, 1975, **47**, 1767.
116. Adams, F. C., and Van Espen, P., "Proceedings of ERDA X- and Gamma-Ray Symposium, Ann Arbor, Mich., 1976," NTIS, Springfield, Va., 1977, p. 182.
117. Van Espen, P., and Adams, F. C., *Analytica Chim. Acta*, 1974, **75**, 61.
118. Van Espen, P., Nullens, H., and Adams, F. C., *Z. Analyt. Chem.*, 1977, **285**, 215.
119. Rhodes, J. R., Pradzynski, A. H., Hunter, C. B., Payne, J. S., and Lindgren, J. L., *Envir. Sci. Technol.*, 1972, **6**, 922.

120. Hammerle, R. H., and Pierson, W. R., *Envir. Sci. Technol.*, 1975, **9**, 1058.
121. Pilotte, J. O., Nelson, J. W., and Winchester, J. W., "Proceedings of ERDA X- and Gamma-Ray Symposium, Ann Arbor, Mich., 1976," NTIS, Springfield, Va., 1977, p. 161.
122. Davis, D. W., Reynolds, R. L., Tsou, G. C., and Zafonte, L., *Analyt. Chem.*, 1977, **49**, 1990.
123. Jaklevic, J. M., Loo, B. W., and Goulding, F. S., Report, Lawrence Berkeley Laboratory, LBL 4834, 1976.
124. Loo, B. W., Jaklevic, J. M., and Goulding, F. S., *in* Liu, B. Y. H., *Editor*, "Fine Particles: Aerosol Generation, Measurement, Sampling and Analysis," Academic Press, New York, London, 1976, p. 311.
125. Butler, J. D., MacMurdo, S. D., and Stewart, C. J., *Int. J. Environ. Stud.*, 1976, **9**, 93.
126. Vanderstappen, M., and Van Grieken, R., *Z. Analyt. Chem.*, 1976, **282**, 25.
127. Pradzynski, A. H., Henry, R. E., and Draper, E. L., "Proceedings of ERDA X- and Gamma-Ray Symposium, Ann Arbor, Mich., 1976," NTIS, Springfield, Va., 1977, p. 175.
128. Elder, J. F., Perry, S. K., and Brady, F. P., *Envir. Sci. Technol.*, 1975, **9**, 1039.
129. Vassos, B. H., Hirsch, R. F., and Letterman, W., *Analyt. Chem.*, 1973, **45**, 792.
130. Boslett, J. A., Towns, R. L. R., Megargle, R. G., Pearson, K. H., and Furnas, T. C., Jr., *Analyt. Chem.*, 1977, **49**, 1734.
131. Carlton, D. T., and Russ, J. C., *X-Ray Spectrom.*, 1976, **5**, 172.
132. Van Grieken, R. E., Bresseleers, C. M., and Vanderborght, B. M., *Analyt. Chem.*, 1977, **49**, 1326.
133. Burba, P., Gleitsmann, B., and Lieser, K. H., *Z. Analyt. Chem.*, 1978, **289**, 28.
134. Smits, J., and Van Grieken, R., *Analytica Chim. Acta*, 1977, **88**, 97.
135. Birks, L. S., and Gilfrich, J. V., *Appl. Spectrosc.*, 1978, **32**, 204.
136. Cox, H. L., Jr., and Ong, P. S., *Med. Phys.*, 1977, **4**, 99.
137. Kaufman, L., Nelson, J., Price, D., Shames, D., and Wilson, C. J., *I.E.E.E. Trans. Nucl. Sci.*, 1973, **20**, 402.
138. Mangelson, N. F., Allison, G. E., Christensen, J. J., Eatough, D. J., Hill, M. W., Izatt, R. M., and Nielson, K. K., "Proceedings of the 2nd International Symposium on Trace Element Metabolism in Animals, 1973," University Park Press, Baltimore, Md., 1974, p. 439.
139. Reuter, F. W., and Reynolds, W. L., *Adv. Exp. Med. Biol.*, 1974, **48**, 621.
140. Kaufman, L., Deconinck, F., Camp, D. C., Voegele, A. L., Friesen, R. D., and Nelson, J. A., "Proceedings of ERDA X- and Gamma-Ray Symposium, Ann Arbor, Mich., 1976," NTIS, Springfield, Va., 1977, p. 118.
141. Zombola, R. R., Kitos, P. A., and Bearse, R. C., *Analyt. Chem.*, 1977, **49**, 2203.
142. Bearse, R. C., Close, D. A., Malanify, J. J., and Umbarger, C. J., *Analyt. Chem.*, 1974, **46**, 499.
143. Holynska, B., and Markowicz, A., *Radiochem. Radioanalyt. Lett.*, 1977, **31**, 165.
144. Berti, M., Buso, G., Colautti, P., Moschini, G., Stievano, B. M., and Tregnaghi, C., *Analyt. Chem.*, 1977, **49**, 1313.
145. Stump, I. G., Carruthers, J., D'Auria, J. M., Applegarth, D. A., and Davidson, A. G. F., *Clin. Biochem.*, 1977, **10**, 127.
146. Knoth, J., Schwenke, H., Marten, R., and Glauer, J., *J. Clin. Chem. Clin. Biochem.*, 1977, **15**, 537.
147. Wobrauschek, P., and Aiginger, H., *Analyt. Chem.*, 1975, **47**, 852.
148. Agarwal, M., Bennett, R. B., Stump, I. G., and D'Auria, J. M., *Analyt. Chem.*, 1975, **47**, 924.
149. Irons, R. D., Schenk, E. A., and Giauque, R. D., *Clin. Chem.*, 1976, **22**, 2018.
150. Cooper, J. A., and Schlofke, D. B., *Skillings Min. Rev.*, 1976, **65**, 1.
151. Giauque, R. D., Garrett, R. B., and Goda, L. Y., *Analyt. Chem.*, 1977, **49**, 62.
152. Coombes, R. J., Chow, A., and Flint, R. W., *Analytica Chim. Acta*, 1977, **91**, 273.
153. Shenberg, C., Ben Haim, A., and Amiel, S., *Analyt. Chem.*, 1973, **45**, 1804.
154. Hebert, A. J., and Bowman, H. R., Report, Lawrence Berkeley Laboratory, LBL 3268, 1975.
155. Cooper, J. A., Wheeler, B. D., Bartell, D. M., and Gedcke, D. A., *Adv. X-Ray Analysis*, 1976, **19**, 213.
156. Cooper, J. A., Wheeler, B. D., and Bartell, D. M., *Cem. Technol.*, 1976, March/April, 68.
157. Carr-Brion, K. G., Kipping, P. J., New, R., Nutter, J. C., and Thomlinson, F. I., *Wld Cem. Technol.*, 1977, **8**, 123.
158. Pradzynski, A. H., and Draper, E. L., Jr., "Proceedings of the 9th Symposium N.D.E., San Antonio, 1973," Southwest Research Institute, San Antonio, Texas, 1973, p. 47.
159. Harrison, P. E., and Kenna, B. T., *Talanta*, 1972, **19**, 810.
160. Janssens, R., Maenhaut, W., and Hoste, J., *Analytica Chim. Acta*, 1975, **76**, 37.
161. Verbeke, P., Nullens, H., and Adams, F., *Proc. Analyt. Div. Chem. Soc.*, 1978, **15**, 18.
162. Franken, P. E. C., *Thin Solid Films*, 1976, **31**, 337.
163. Cooper, J. A., Wheeler, B. D., Wolfe, G. J., Bartell, D. M., and Schlafke, D. B., "Proceedings of ERDA X- and Gamma-Ray Symposium, Ann Arbor, Mich., 1976," NTIS, Springfield, Va., 1977, p. 169.
164. Lloyd, W. G., and Francis, H. E., "Proceedings of ERDA X- and Gamma-Ray Symposium, Ann Arbor, Mich., 1976," NTIS, Springfield, Va., 1977, p. 166.
165. De Kalb, E. L., and Fassel, V. A., "Proceedings of ERDA X- and Gamma-Ray Symposium, Ann Arbor, Mich., 1976," NTIS, Springfield, Va., 1977, p. 209.
166. Chung, F. H., *Adv. X-Ray Analysis*, 1976, **19**, 181.
167. Cronch, S. M., Ehmann, W. D., Laumer, H. W., and Cabbard, F., "Proceedings of ERDA, X- and Gamma-Ray Symposium, Ann Arbor, Mich., 1976," NTIS, Springfield, Va., 1977, p. 190.
168. Yousif, A. N., and Al-Shahristani, H., *Int. J. Appl. Radiat. Isotopes*, 1977, **28**, 759.
169. Teller, S., "Proceedings of ERDA X- and Gamma-Ray Symposium, Ann Arbor, Mich., 1976," NTIS, Springfield, Va., 1977, p. 194.

170. Carr-Brion, K. G., *X-Ray Spectrom.*, **1973**, **2**, 63.
171. Kawatra, S. K., and Dalton, J. L., *Canmet Rep.*, **1977**, **77**, 21.
172. Grobstück, P., Gumprich, M., Ihlefeldt, J., Kopineck, H. J., and Tappe, W., *Stahl Eisen*, **1977**, **97**, 1106.
173. Labrecque, J. J., *J. Radioanalyt. Chem.*, **1977**, **41**, 127.
174. Labrecque, J. J., Preiss, I. L., and Pandian, S., "Proceedings of ERDA X- and Gamma-Ray Symposium, Ann Arbor, Mich., 1976," NTIS, Springfield, Va., **1977**, p. 173.
175. Elgart, M. F., "Proceedings of ERDA X- and Gamma-Ray Symposium, Ann Arbor, Mich., 1976," NTIS, Springfield, Va., 1977, p. 227.
176. Ehn, E., *X-Ray Spectrom.*, **1973**, **2**, 27.
177. Keenan, J. A., *Appl. Spectrosc.*, **1975**, **29**, 63.
178. Bertrand, C. C., and Linn, T. A., Jr., *Analyt. Chem.*, **1972**, **44**, 383.
179. Metcalf, S. G., *Analytica Chim. Acta*, **1977**, **93**, 297.
180. Klockenkämper, R., and Hasler, K., *Z. Analyt. Chem.*, **1978**, **289**, 346.
181. Buchnea, A., McNelles, L. A., Sinclair, A. H., and Hewitt, J. S., "Proceedings of ERDA X- and Gamma-Ray Symposium, Ann Arbor, Mich., 1976," NTIS, Springfield, Va., 1977, p. 242.
182. Wogman, N. A., Rieck, H. G., and Kosorok, J. R., *Nucl. Instrum. Meth.*, **1975**, **128**, 561.
183. Reuter, F. W., Hautala, E., Randall, J. M., Friedman, M., and Masri, M. S., "Proceedings of the 2nd International Conference on Nuclear Methods of Environmental Research, 1974," NTIS, Springfield, Va., **1974**, p. 168.
184. Mucci, J. F., and Stearns, R. L., *Soil Sci.*, **1977**, **123**, 264.
185. Mucci, J. F., and Stearns, R. L., *J. Chem. Educ.*, **1975**, **52**, 750.
186. Delmastro, A. M., "Proceedings of ERDA X- and Gamma-Ray Symposium, Ann Arbor, Mich., 1976," NTIS, Springfield, Va., 1977, p. 215.
187. Hanson, V. F., *Appl. Spectrosc.*, **1973**, **27**, 309.
188. Tominaga, H., Enomoto, S., Senoo, M., and Tachikawa, N., "Proceedings of ERDA X- and Gamma-Ray Symposium, Ann Arbor, Mich., 1976," NTIS, Springfield, Va., 1977, p. 211.
189. Kawamoto, A., Hirao, O., Kashiwakura, J., and Gohshi, Y., "Proceedings of ERDA X- and Gamma-Ray Symposium, Ann Arbor, Mich., 1976," NTIS, Springfield, Va., 1977, p. 263.
190. Hurley, R. G., and Goss, R. L., *X-Ray Spectrom.*, **1978**, **7**, 70.

Received *July 6th*, 1978
Accepted *October 5th*, 1978

Analyst, March, 1979, Vol. 104, pp. 196–200

Analysis of Steroids

Part XXXII.* Determination of Allyloestrenol by Titrimetric, Polarographic and Gas-chromatographic Methods

Sándor Gorög, Anna Laukó and Zsófia Sziklay

Chemical Works Gedeon Richter Ltd., P.O. Box 27, H-1475 Budapest, Hungary

A titrimetric method is described for the determination of allyloestrenol based on methoxymercuration of its double bonds and titration of the acetic acid formed with standard sodium hydroxide solution. The relative standard deviation of the method is 0.29%. The polarographic reduction of the mercury addition compound on the dropping-mercury electrode is used for the determination of allyloestrenol in a tablet formulation with a relative standard deviation of 3.1%. A gas-chromatographic method with a relative standard deviation of 1.5% is also described. The applicability of these methods to the determination of the stability of allyloestrenol and of its dosage form is discussed.

Keywords: Allyloestrenol determination; titrimetry; polarography; gas chromatography

The analysis of allyloestrenol (17α-allyloestr-4-en-17-ol) and its tablet formulation sets serious problems for the analyst. The molecule of this synthetic progestogen is one of the least substituted of the steroid drugs, its functional groups being two isolated double bonds and a tertiary hydroxyl group. In addition the drug, both in bulk and in formulations, is very sensitive to atmospheric oxygen and, therefore, any reliable analytical method should enable the unchanged material to be determined in the presence of its oxidative degradation products.

Little information is available in the literature on the determination of allyloestrenol. Fokkens and Polderman[1] described its examination by thin-layer chromatography, including the detection of the degradation products. Gänshirt and Polderman[2] developed this method into a quantitative colorimetric procedure using aqueous sulphuric acid for the colour development after thin-layer chromatographic separation and spot elution. This method enabled an assay of the stability of solid dosage forms to be carried out. Another colorimetric method was described by Kato[3] using aluminium chloride as the reagent. Cavina *et al.*[4] reported on the column-chromatographic determination of the material using flame-ionisation detection for monitoring of the eluent. The gas-chromatographic separation and gas-chromatographic - mass-spectrometric investigation of allyloestrenol in biological fluids was described by Brooks and Middletich.[5]

The purpose of this study was to develop a reliable titrimetric method for the determination without the use of standards and to develop rapid polarographic and gas-chromatographic methods for examining the stability of the drug when in tablet form.

Experimental

Reagents and Apparatus

All materials and the solvent (methanol) were of analytical-reagent grade and were used without further purification.

Titrimetric method

Mercury(II) acetate solution, 0.1 M in methanol. This should be used the same day as it is prepared.

Sodium nitrate solution, saturated solution in methanol.

Sodium bromide solution, 4 M in water.

Sodium hydroxide solution, 0.1 M in water. Standardised against oxalic acid in a methanolic medium using phenolphthalein as indicator.

* For Part XXXI of this series, see *Analyst*, 1978, **103**, 346.

Polarographic method

Radelkis (Budapest) OH-105 d.c. - a.c. polarograph.
Mercury(II) acetate solution, 0.1 M in methanol containing 1 ml l^{-1} of acetic acid.
Thymol solution, 0.1% m/V in methanol.
Sodium hydroxide solution, 1 M in water.

Gas chromatographic method

Hewlett-Packard 7620 gas chromatograph with flame-ionisation detector and 3380 reporting integrator.
Internal standard. Dehydroepiandrosterone (3β-hydroxyandrost-5-en-17-one).

Materials investigated

Bulk allyloestrenol (crude and purified samples) and other steroids were products of Chemical Works Gedeon Richter Ltd., Budapest. Turinal (Richter) tablets contain 5 mg of allyloestrenol per tablet.

Procedures

Titrimetric method

An accurately weighed sample of allyloestrenol (approximately 0.12 g) is dissolved in 10 ml of methanol, 20 ml of 0.1 M mercury(II) acetate solution and 5 ml of saturated sodium nitrate solution are added and the solution is allowed to stand for 30 min. Then 2 ml of 4 M sodium bromide solution are added and the slightly turbid solution is titrated with 0.1 M sodium hydroxide solution to a phenolphthalein end-point.

A blank titration is carried out in the same manner but omitting the allyloestrenol, and this titration value (less than 0.2 ml) is subtracted from the above titre. The equivalent mass is half of the relative molecular mass (150.2).

Polarographic method

Fifteen Turinal tablets are finely powdered and a portion of the powder equivalent to about 60 mg of allyloestrenol is accurately weighed. It is triturated with 20 ml of methanol for 30 min and the solution is filtered through a filter-paper into a 25-ml calibrated flask, washed with small portions of methanol and the filtrate diluted to volume with methanol and mixed. A 10-ml volume of this solution is transferred into a 25-ml calibrated flask, 5 ml of 0.1 M mercury(II) acetate solution and 2 ml of saturated sodium nitrate solution are added and the solution is allowed to stand for 30 min. Then 2.5 ml of 1 M sodium hydroxide solution are added and the solution is diluted to volume with methanol. A 10-ml portion of the yellow, turbid solution is transferred into a polarographic cell, 1 ml of 0.1% thymol solution is added and the cell is carefully de-aerated with oxygen-free nitrogen. The solution polarographed in the a.c. mode from −1 V, using dropping-mercury and mercury-pool electrodes as the working and reference electrodes, respectively.

A standard solution is prepared by dissolving an accurately weighed amount of standard allyloestrenol (about 25 mg) in 10 ml of methanol in a 25-ml calibrated flask and treating the solution as described above beginning at ". . . 5 ml of 0.1 M mercury(II) acetate solution and 2 ml of . . ."

The allyloestrenol content of the tablets is calculated from the peak currents of sample and standard in the usual way.

Gas-chromatographic method

One accurately weighed tablet is placed in a 25-ml calibrated flask, 26 ml of methanol are added and the tablet is disintegrated by vigorous shaking. The flask is shaken for a further 15 min, 2 ml of internal standard solution containing 10 mg of dehydroepiandrosterone dissolved in methanol are added and the volume of the solution is adjusted to the mark with methanol. The solution is mixed thoroughly and allowed to stand until the tablet base has settled. A 2-μl aliquot of the clear supernatant liquid is injected into the gas chromatograph. A glass column, 6 ft × 3 mm i.d., packed with Anakrom ABS, 90–100 mesh, coated with 1% of OV-101 was used. The column temperature was 220 °C, the

vaporiser zone temperature 250 °C and the detector temperature 250 °C. The carrier gas (nitrogen) flow-rate was 30 ml min^{-1}. The retention times of allyloestrenol and dehydroepiandrosterone were 5.3 and 6.6 min, respectively.

Results and Discussion

Titrimetric method

Titrimetric methods are seldom used in the analytical chemistry of steroids.[6] The favourable results obtained in this laboratory for the titrimetric analysis of steroidal double bonds,[7–9] ethynyl,[10] keto,[11] phenolic hydroxyl[12,13] and epoxide[14] groups, 16,17-diols[15] and 21-acyloxycorticosteroids[16] encouraged us to try to develop such a method for the determination of allyloestrenol. Further, titrimetric methods in general have the advantage that no standard sample is necessary for the analysis; this is particularly important in the instance of allyloestrenol as it is one of the less stable steroid drug materials.

Our first experiments in which we aimed to base the determination on the titration of the double bonds by our earlier described catalytic bromination method,[7] failed to give acceptable results. However, good results were obtained by the addition of mercury(II) acetate and methanol to the double bonds, complexing the excess of mercury(II) acetate with sodium bromide and titration of the liberated acetic acid.

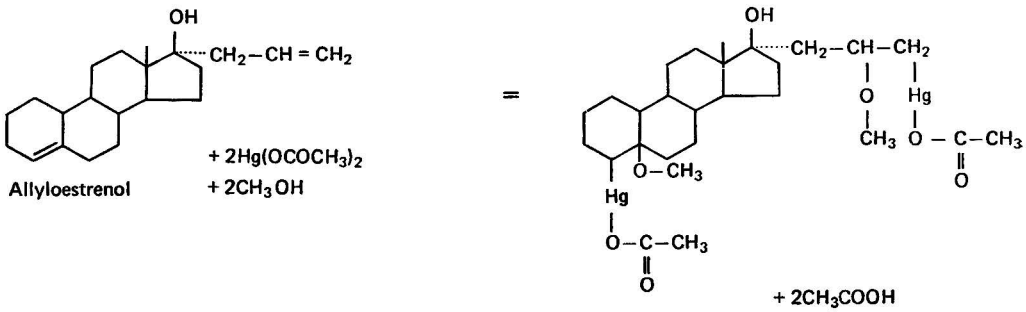

The principle of this method was described by Martin[17] and developed to its generally accepted form by Johnson and Fletcher.[18] On the basis of the papers published on the application of this method and references in standard monographs,[19–21] this method appears to be applicable mainly to olefins with three, or at least two, hydrogen atoms in the *cis* position attached to the double bond. As double bonds of this type are usually not present in steroids, no indication of the use of this method for steroids has been found in the literature.

According to our measurements 2 mol of mercury(II) acetate are consumed by 1 mol of allyloestrenol, indicating that both double bonds are involved in the reaction. If the reaction is carried out at 0 °C 1 mol is consumed instantaneously while the reaction with the second mole takes place at a measurable rate (1.15 mol after a reaction time of 2 min). The first mole of mercury(II) acetate undoubtedly reacts with the allylic double bond. The reaction between the Δ^4 double bond and mercury(II) acetate is sluggish even at room temperature and a reaction time of more than 1 h would be necessary to complete the reaction at 25 °C. The use of sodium nitrate as catalyst considerably decreases the reaction time. The use of longer reaction times does not influence the results.

By using the described method a freshly prepared standard allyloestrenol sample was found to be 100.21% pure. The relative standard deviation (eight parallel determinations) was 0.29%. Similarly good results were obtained with oestr-4-en-17β-ol and oestr-4-en-17-one where naturally only 1 mol of the reagent was consumed.

Several other steroids were also tested in order to obtain data for determining the selectivity of the method. It has been found that the most frequently occurring double bonds in steroid hormones do not react at all (5-ene-3β-hydroxy, 4-ene-3-keto, 1,4-diene-3-keto, 16-ene-20-keto, 9-ene or 11-ene derivatives) and hence the method can be regarded as being fairly specific. The most serious interference was caused by the 17α-ethynyl group and the free phenolic hydroxyl group of oestrogens. However, no stoicheiometric amounts

of acetic acid were formed in these instances (about 2.5 equivalents in the first group and 1–2 equivalents, depending on the reaction time, in the second group).

The results obtained suggest that the titrimetric method is accurate and precise enough for it to be used for the assay of bulk allyloestrenol. The relatively large sample size obviously precludes the possibility of its use for the assay of tablets.

Polarographic method

The polarographic determination of olefinic unsaturation based on methoxymercuration was described by Fleet and Jee.[22,23] The present method is a slightly modified application of the above method to the determination of allyloestrenol in tablets.

Rectilinear calibration graphs were obtained over the range of allyloestrenol concentration of 5×10^{-4} to 5×10^{-3} mol l^{-1}. The peak potential *versus* the mercury-pool electrode was found to be −1.47 V. Antioxidants such as tocopherol do not interfere in the assay.

As the polarographic method is based on the same reaction scheme, the remarks made on the selectivity of the volumetric method apply also to this method.

Gas-chromatographic method

As the molecule of allyloestrenol has few substituent and stable functional groups, the gas-chromatographic determination can be carried out without derivatisation and at not too high a temperature. Use of the internal standard technique affords a suitable method for the assay of single tablets containing allyloestrenol.

A comparison of the results for the allyloestrenol content of one batch of tablets as determined by the polarographic and gas-chromatographic methods is shown in Table I.

TABLE I

DETERMINATION OF ALLYLOESTRENOL IN TURINAL TABLETS

Each tablet had a nominal allyloestrenol content of 5 mg.

	Allyloestrenol content per tablet/mg	
	Polarographic method	Gas-chromatographic method
	4.79, 5.05, 4.86	5.01, 5.13, 4.91
	5.15, 4.76, 4.96	5.04, 5.01, 5.08
Mean	4.93	5.03
Standard deviation	0.153	0.076
Relative standard deviation ..	3.1%	1.5%

Examination of the Stability of Allyloestrenol

When allyloestrenol as such or its tablet dosage form is exposed to air, polar degradation products appear in its thin-layer chromatogram.[1,2] We examined the three methods to see whether they could measure allyloestrenol selectively in the presence of the degradation products.

The oxidative degradation product can easily be separated from a highly contaminated sample on the basis of its extremely low solubility in hexane. Analysis by thin-layer chromatography showed that it was a mixture of several components, presumably peroxides or even more highly oxidised derivatives.

When tested by the titrimetric method an allyloestranol content of about 50% was found for this material, indicating that only one of the double bonds (presumably that in the Δ^4 position) is attacked during the autoxidation. From these results we conclude that the excellent accuracy and precision of the titrimetric method make it suitable for the determination of bulk allyloestrenol but it must be remembered that a completely decomposed material shows a virtual content of 50%. The polarographic assay based on the same reaction is suitable for the rapid testing of tablets but neither method is suitable for examining the stability of samples.

The gas-chromatographic procedure appears to be suitable for this purpose. The isolated degradation product does not give gas-chromatographic peaks under the recommended

conditions or at higher temperatures, indicating that its components are further decomposed or polymerised in the vaporiser zone. Gas chromatography is therefore suitable for determining the active ingredient content of tablets that have been stored under various conditions and hence this method was used in testing the stability of Turinal tablets.

References

1. Fokkens, J., and Polderman, J., *Pharm. Weekbl.*, 1961, **96**, 657.
2. Gänshirt, H. G., and Polderman, J., *J. Chromat.*, 1954, **16**, 510.
3. Kato, K., *Chem. Pharm. Bull., Tokyo*, 1964, **12**, 578 and 824.
4. Cavina, G., Moretti, G., Mollica, A., and Antonini, R., *J. Chromat.*, 1971, **60**, 179.
5. Brooks, C. J. W., and Middletich, B. S., *Clinica Chim. Acta*, 1971, **34**, 145.
6. Görög, S., and Szász, Gy., "Analysis of Steroid Hormone Drugs," Elsevier, Amsterdam, 1978, pp. 261–262.
7. Görög, S., *Acta Chim. Hung.*, 1966, **47**, 1.
8. Görög, S., *Acta Chim. Hung.*, 1966, **48**, 121.
9. Csizér, E., and Görög, S., *J. Chromat.*, 1973, **76**, 502.
10. Görög, S., *Acta Chim. Hung.*, 1966, **47**, 7.
11. Görög, S., and Tomcsányi, L., *Acta Chim. Hung.*, 1966, **47**, 121.
12. Görög, S., and Földes, V., *Acta Chim. Hung.*, 1966, **48**, 249.
13. Görög, S., *Acta Chim. Hung.*, 1967, **51**, 221.
14. Csizér, E., Görög, S., and Gyenes, I., *Acta Chim. Hung.*, 1972, **73**, 175.
15. Csizér, E., Görög, S., and Szén, T., *Mikrochim. Acta*, 1970, 966.
16. Görög, S., *J. Pharm. Pharmac.*, 1969, **21**, 46S.
17. Martin, R. W., *Analyt. Chem.*, 1949, **21**, 921.
18. Johnson, J. B., and Fletcher, J. P., *Analyt. Chem.*, 1959, **31**, 1563.
19. Cheronis, N. D., and Ma, T. S., "Organic Functional Group Analysis," John Wiley, New York, 1964, pp. 374–375, 525–527.
20. Polgár, A., and Jungnickel, J. L., *in* Mitchell, J., Kolthoff, I. M., Proskauer, E. S., and Weissberger, A., *Editors*, "Organic Analysis," Volume III, Interscience, New York, 1956, pp. 301–310.
21. Gyenes, I., "Titrationen in nichtwässrigen Medien," Enke Verlag, Stuttgart, 1970, pp. 592–594.
22. Fleet, B., and Jee, R. D., *Talanta*, 1969, **16**, 1561.
23. Fleet, B., and Jee, R. D., *J. Electroanalyt. Chem.*, 1970, **25**, 397.

NOTE—References 7, 8, 9, 10, 11, 12, 13, 14, 15 and 16 are to Parts I, IV, XXIII, II, III, V, VI, XIX, XV and XII of this series, respectively.

Received *August 7th*, 1978
Accepted *September 27th*, 1978

Analyst, March, 1979, Vol. 104, pp. 201–207

Diffusion Assay by an Automated Procedure

J. W. Lightbown, R. A. Broadbridge and P. Isaacson*
National Institute for Biological Standards and Control, Holly Hill, Hampstead London NW3 6RB

J. E. Sharpe†
Division of Engineering, National Institute for Medical Research, Mill Hill, London NW7 1AA

and A. Jones
Research Division, Beecham Pharmaceuticals, Worthing, West Sussex BN14 8QH

Equipment is described that allows diffusion assays to be performed automatically in Petri dishes using the punch-hole technique. With a block of six dishes limits of error of approximately ±2% can be obtained consistently. Various sources of systematic errors and their elimination are discussed.

Keywords: *Automation*; *antibiotic assay*; *diffusion assay*; *systematic errors*

A systematic programme of automation of antibiotic diffusion assay was started some years ago by the Antibiotics Division, National Institute for Biological Standards and Control (NIBSC) (then Division of Biological Standards, National Institute for Medical Research). The assay consists basically of three stages: pouring of plates; application of assay solutions; and measurement of zones of inhibition.

It was considered that the third stage had the greatest content of subjective involvement of the operator and was the stage that could most easily allow the introduction of an operator bias in the measurement of potency. Most laboratories at that time measured the diameter of zones of inhibition in millimetres, using some form of magnification, either by projection of an enlarged image on to a screen or indirect magnification of the zone and scale by a lens system.

The use of a television camera in conjunction with a graticule was developed by Tatum and Lightbown[1] and has been used successfully for more than 10 years to quantitate the areas of zones of inhibition on Petri dishes carrying six zones. The six areas were measured consecutively and recorded in arbitrary units. This method removed the need for the operator to make a subjective decision regarding the position of the edge of each zone and allowed zone area measurements to be made that were independent of the operator. It was found, however, that the performance of the image analyser could deteriorate under certain conditions in such a way that a bias was introduced by the machine, which could, for example, result in the first of the six zones measured on a dish being found to be too large or small. The fault was eliminated electronically, but as it could apparently develop again, progressively, any possible effects of this bias were eliminated by reading the replicate dishes in groups of six, as a Latin square, so that any effects of the bias were systematically and evenly distributed to all responses in the assay.

Early in 1969 the Beecham laboratory started measuring inhibition zones by means of a commercial image analyser with a graticule adapted for Petri dishes. The automation of the second stage of the assay, *i.e.*, the application of the solutions to the dishes, was developed subsequently and jointly by the two laboratories and in the course of the work Quantimet Petriscopes, Models 60 and 720, were used for zone measurements (the Optomax, recently available from Micromeasurements Ltd., has also been used).

A decision to base the assay on the use of plastic Petri dishes rather than large square plates, which were currently used by NIBSC, had been taken during the development of the image analyser device for measuring the zones. Various advantages accrued from the use of such dishes. (*i*) They are disposable, thus avoiding problems arising from contamination of assay plates by antibiotics, such as occurs with neomycin and glass surfaces. Experience has shown, in one laboratory, that sufficient neomycin can be adsorbed on to the glass surface of an assay plate so that, after washing three times and dry heat sterilisation, zones of inhibition were still produced by the residual antibiotic on the glass. Steaming in

* Present address: National Biological Standards Laboratory, Canberra, Australia.
† Present address: Division of Mechanical Engineering, Queen Mary College, London, E1 4NS.

dilute acid was necessary to clean the plates. Penicillinase was also adsorbed on to glass plates and resisted washing and dry heat sterilisation, thus interfering with subsequent assays of penicillin. (*ii*) The dishes are readily obtainable with a uniform plane surface. (*iii*) Bias from edge or corner effects is minimised as each zone is equidistant from the edge. (*iv*) Automation is more readily applied to a circular array than to a Latin square. (*v*) Automation of pouring is more easily arranged for Petri dishes.

Consideration was given to the application of the assay solution. A number of possible procedures were tried, *viz.*, application of fish-spine beads and subsequent filling with solutions, delivery of precise volumes of assay solutions to the surface of the agar (fixed volume and several concentrations, or fixed concentration and several volumes), injection of assay solutions into the agar layer, assay solutions solidified with agar in tubing, then extruded and cut into plugs, and punching holes in the agar layer with subsequent delivery of assay solutions into the holes. As a result of these preliminary experiments, and in consideration of the wide variation in the nature of possible assay solutions, particularly variations caused by differences in surface tension, it was decided to concentrate on the development of a system based on holes punched in the agar. The size of the zone of inhibition that develops from the hole containing antibiotic solution is affected by a number of factors, which may vary from hole to hole: size of hole, diameter and surface area of agar to solution interface; seal of agar to surface of dish; volume of assay solution added; and period of diffusion before the zone of inhibition is defined (critical time).

Various procedures for punching six holes per dish were examined: using a single punch and rotating the dish in six steps; punching six holes simultaneously; drilling the holes with a twist drill; and removing the agar plug whole by suction, by blowing and by fragmentation and suction. Probably the most difficult problem was the removal of the plug without disturbing the seal between the agar and the dish. If this seal was disturbed the assay solution spread in the interface between agar and dish, producing distorted or enlarged zones of inhibition.

Various means of delivering the assay solutions into the holes were considered and examined using single or multiple devices; a minimum precision of $\pm 0.2\%$ was considered desirable for repeated deliveries of the chosen volume. Delivering the six volumes simultaneously had the advantage that variation in diffusion time between the assay solutions was eliminated and this design was therefore adopted.

Using Petri dishes with a nominal diameter of 90 mm, an apparatus was constructed that would cut six holes (6 mm in diameter) in the contained agar, remove the plugs and introduce equal volumes of six assay solutions, simultaneously, into the six holes.

Description and Use of Apparatus

The apparatus[2] shown in Fig. 1 consists of two units, the punch head (right) and the dispensing head (left). Both units move vertically, enabling the punches and pipette tips, both of which are plastic and disposable, to perform the various operations. The assay dish together with the reservoirs for the test and standard solutions are transported horizontally underneath the heads on a carriage. A container for the spent agar plugs is placed under the cutting head.

The apparatus normally performs automatically the sequence of operations, but can be controlled manually if required. Operation is electro-pneumatic, and vertical movements of the punch and dispenser heads are independently adjustable. The dispensed volume can readily be adjusted by means of a calibrated micrometer. Likewise, the action of the punches is adjusted to suit a wide range of gel types and thicknesses.

The sequence of operation begins with the operator placing a dish prepared for assay on to the right-hand position of the carriage. The carriage moves to the right until the dish is under the punch head and the reservoirs of test and standard are under the dispensing head. The heads move vertically down, the dispenser pipette tips are immersed in the solutions in the reservoirs and the punches penetrate the agar to the required depth. The dispenser pistons then draw a pre-determined amount of solution into each of the pipette tips, while the punching assembly rotates slightly to free the agar plugs.

Both heads are retracted, the punches carrying with them the plugs removed from the agar. The carriage returns to the left until the holes in the assay agar are under the

Fig. 1. Automatic bioassay machine.

[to face page 202

dispenser pipettes. The dispenser head descends, the pipettes discharging the solution into the holes in the agar, while the plugs remaining in the punches are ejected into the container below the punch head. The dispenser head retracts and the punched and filled assay dish is removed by the operator. The complete cycle takes approximately 15 s.

Dispensed volumes of 50 and of 70 μl are currently being used. The apparatus can be adjusted to deliver a maximum of approximately 100 μl. The dispensing unit is constructed in such a way that the tips are not completely emptied at each operation. Experience has shown that it may not be necessary to replace pipette tips or to sterilise the punches between assays of different antibiotics. In certain conditions, however, it has been found necessary to treat the punch tips with alcohol, *e.g.*, when changing from *Pseudomonas aeruginosa* to *Bacillus subtilis* as assay organism. The plastic pipette and punch tips are readily replaceable, if this is necessary.

Evaluation of the Apparatus

Variations in volumes delivered into the six holes were measured initially by collecting repeated simultaneous deliveries of an aqueous solution of albumen labelled with iodine-131 and measuring the activity in each sample. With the prototype machine (three micrometers) and using pipette tips of various sources of manufacture, coefficients of variation for a single delivery point ranged from 1.0 to 4.0%. Measurement of the movement of the six pistons showed that these were all well within the 0.1–0.2% target. Measurement of the changes in pressure within a plastic tip during the cycle of filling and emptying showed that the changes were complex and that surface tension was a major factor affecting the volume delivered. Variations were noted in the size of orifice of the pipette tip and in the effectiveness of the seal at the cone joint of the tip. It was important to adjust the movement of the pipette head so that the tips at filling and delivery were as close as possible to the base of the dish. When the base of the dish was not plane and parallel to the six tips, then variable interference with the flow of liquids occurred either at the filling or emptying stages. The adjustments had to ensure that the tips were immersed as soon as possible during delivery and, in addition, the operator had to be careful to observe that liquid remaining on the outside of the pipette tips between emptying and re-filling did not vary greatly. By careful choice of tips, control of cleanliness and care in fitting, it was readily possible to obtain coefficients of variation of approximately 1% for the volumes delivered from the six tips, as is shown in Table I. This variation was greater than hoped, but could not be improved and it was considered that by means of replication, effects of the error could be reduced.

Variation between the mean volumes delivered by the six pipettes was found to be less than 0.5% by mass. The prototype machine was designed with three micrometer adjustments in order to allow any measured bias affecting the six zones (in a circular pattern), arising from any source, to be removed by the application of an opposite bias to the volumes delivered at the six points. Experience proved that this was not practicable because bias arising independently of the machine procedures was not necessarily constant from day to day. For this reason the final engineering design ensured a uniform displacement of the six pistons and a single micrometer head allowed all six to be varied equally and simultaneously. The results given in Table I were obtained with this design of equipment and it is seen that the variation between the mean volumes delivered by each pipette was approximately 0.2%.

Variations in the size of punched holes were examined by using dishes containing nutrient

TABLE I

VARIATIONS IN DELIVERY OF PIPETTES USING WATER

	Positions					
	1	2	3	4	5	6
Mean mass of 20 volumes delivered from pipette/mg	51.59	51.55	51.71	51.52	51.60	51.61
Coefficient of variation	1.26	0.029	1.32	1.02	1.37	1.46

Grand mean mass/mg 51.60
Range of means 1–6 .. .. .. 99.90–100.2% of grand mean.
Range of individual deliveries for all positions .. 50.1–53.2 mg.

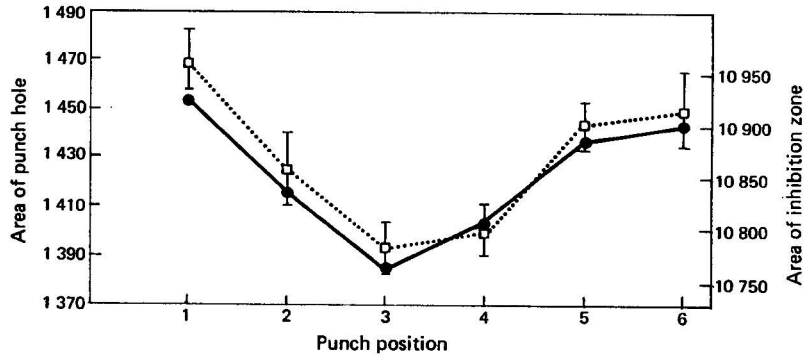

Fig. 2. Systematic bias originating from punches. □ . . . □, Area of punch holes in arbitrary units; mean of 12 plates ± 2 standard deviations of the mean for areas of punch holes. ●——●, Area of inhibition zones in arbitrary units; mean of 18 plates.

agar, flooding the plates with water and measuring the cross-sectional areas of the six holes by means of the plate reading device. The results shown in Fig. 2 were obtained using the prototype assay machine. On the same day, and with the same conditions, 18 plates were prepared and filled with solutions for a tetracycline assay (3 + 3 design). The solutions were applied to three blocks, each of six dishes, in a Latin square within each block, so that within a block each solution was delivered once into a hole produced by each cutter, as shown in Table II.

TABLE II

TEST FORMAT

	Identification of punch hole*					
Petri dish	1	2	3	4	5	6
1	SH	TM	SL	TH	SM	TL
2	TM	SL	TH	SM	TL	SH
3	SL	TH	SM	TL	SH	TM
4	TH	SM	TL	SH	TM	SL
5	SM	TL	SH	TM	SL	TH
6	TL	SH	TM	SL	TH	SM

* Solution identity: SH = standard high; SM = standard medium; SL = standard low; TH = test high; TM = test medium; TL = test low.

After normal incubation the zones were measured. The difference in response between columns represents the effects of differences in the six punch positions. Fig. 2 shows that the variation in size of the zones produced around holes from different punches follows closely the variation in the size of those holes. If holes from one punch are always used for the same assay solution, then with the pattern of distribution of assay solutions used in the two laboratories (1 SH, 2 TM, 3 SL, 4 TH, 5 SM, 6 TL) the two dose response lines for standard and test would be expected to be biased as shown in Fig. 3, with the possible introduction of non-parallelism and curvature.

Assays carried out on a proposed standard preparation, using the machine, were each composed of 36 dishes. The assay design was 3 + 3 in six blocks of six dishes per assay. The dishes within a block had a fixed relationship between the six pipette and punch stations and the six assay solutions, one block of six dishes for each of the six relationships shown in Table II for the six Petri dishes. Analysis of separate blocks of six dishes showed invalidities of curvature and non-parallelism within a number of blocks, but when the 36 dishes were taken together, as was intended, the assays were usually statistically valid. Results from six such assays are reported in Table III. Valid assays of a high degree of precision could be obtained with this assay system, but the procedure was very cumbersome in performance and statistical analysis.

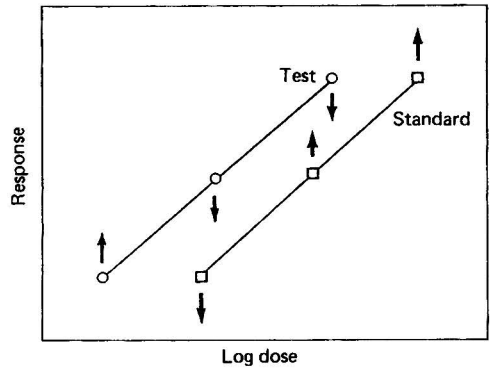

Fig. 3. Effect of systematic bias on assay under conditions shown in Fig. 2. Arrows indicate direction of bias.

One of the two laboratories developed the use of the automated apparatus in the form of two independent units, one to punch holes and the second to dispense the assay solutions. This procedure had the advantage that it allowed dishes to be punched at a more rapid rate than could be accommodated by the dispensing unit. In this way one punch unit could supply dishes for several dispensing units. After punching the holes, the dishes were mixed so that, at subsequent dispensing, a particular punch position was not tied to a particular assay solution. The randomisation thus introduced at this stage had the advantage of reducing or removing the bias which resulted from the punches. Assays performed in this way were usually free from invalidities of curvature or non-parallelism, but there was an expected reduction in precision (see Table IV). The precision obtained with 10 dishes per assay was, however, adequate for the purpose required. A higher precision could be obtained by increasing the number of dishes, but the use of the linked units, together with the systematic rotation of the solutions, is more economical if the higher precision is required.

Later assays with linked units have used a total of six Petri dishes per assay instead of 36, with one dish for each of the six positions (punch hole relative to solutions). With this arrangement valid assays with confidence limits of ± 2 to 3% are regularly obtained (Table V) with a number of different antibiotics. In this way, the precision obtained with a unit of six Petri dishes (36 zones) is better than was previously obtained using a large plate with a 6×6 or 8×8 Latin square arrangement and applying the solutions by means of fish-spine beads.

The greater part of the effort in the assay goes into the preparation of the solutions and

TABLE III

ASSAY OF CHLORTETRACYCLINE PROPOSED STANDARD USING PUNCH AND PIPETTE UNITS LINKED

3 + 3 design. Six blocks of six dishes per assay. Each solution was delivered in turn by each station to six dishes within one assay.

Day	Assay	Potency ratio	Fiducial limits ($P = 0.95$)
1	1	1.024	1.012 to 1.035
	2	1.023	1.010 to 1.036
2	3	1.023	1.006 to 1.041
	4	1.022	1.005 to 1.040
3	5	1.039*	1.025 to 1.053
	6	1.016*	1.000 to 1.033

* Significant non-parallelism.

TABLE IV

AUTOMATED BIOASSAY UNIT IN USE FOR ROUTINE ASSAY USING PUNCH AND PIPETTE UNITS SEPARATE

Ten dishes employed per assay.

Antibiotic	Assay	Penicillin content/ $\mu g\ mg^{-1}$	Departure from parallelism, F	Quadratic curvature, F	Difference of curvature, F	Limits ($P = 0.95$), %
Ampicillin trihydrate ..	A (1)	843	0.02	1.08	1.76	1
	A (2)	837	0.94	0.26	1.86	5
	A (3)	838	0.63	0.81	0.38	5–6
	B	858	0.09	1.83	0.03	3–4
Flucloxacillin— syrup preparations ..	A	36.3	0.02	0.41	1.29	3–4
	B	35.1	0.02	0.88	0.03	5
	C	35.9	0.05	1.82	0.02	4–5

dishes and there is a temptation to use a large number of replicate dishes in the assay by means of automation, in order to obtain an even higher degree of precision. This temptation should be resisted; if greater precision is necessary it should be obtained by repetition of completely independent assays. Under our own conditions there is little to be gained by using more than six dishes in a single assay with the linked apparatus.

Statistical analysis commonly used to determine confidence limits from the internal evidence of the assay is in any event of doubtful significance in such automated procedures, where the random error has been reduced to a very low level by a systematic distribution of known errors to all doses. The residual error can be reduced to an extent such that the usual analysis of variance may invite false conclusions.

TABLE V

ASSAYS WITH PUNCH AND PIPETTE UNITS LINKED

Antibiotic	Potency/ U mg^{-1}	Departure from linearity	Departure from parallelism	Fiducial limits ($P = 0.95$)	Limits, %
Neoymcin ..	95.8*	$P > 0.05$	$P > 0.05$	93.5 to 98.2	2.5
Gentamicin ..	649	$0.05 > P > 0.01$	$P > 0.05$	626 to 672	3.6
Tetracycline ..	970	$P > 0.05$	$P > 0.05$	942 to 999	2.9
Oxytetracycline ..	102.6*	$P > 0.05$	$P > 0.05$	100.5 to 104.9	2.2
Tobramycin ..	104.9*	$P > 0.05$	$P > 0.05$	102.7 to 107.2	2.2
Streptomycin ..	771	$P > 0.05$	$P > 0.05$	746 to 797	3.3
Erythromycin ..	933	$P > 0.05$	$P > 0.05$	914 to 952	2.1
Amikacin ..	926	$P > 0.05$	$P > 0.05$	906 to 947	2.3
Rolitetracycline ..	780	$0.05 > P > 0.01$	$P > 0.05$	762 to 798	2.3
Spectinomycin ..	98.2*	$P > 0.05$	$0.05 > P > 0.01$	97.4 to 98.9	0.7
Doxycycline ..	874	$P > 0.05$	$P > 0.05$	855 to 893	2.2
Nystatin	5075	$0.05 > P > 0.01$	$P > 0.05$	5045 to 5263	2.1

* Potency expressed as percentage of claim on label.

Discussion

The apparatus described has been in constant use for 6 years in the two laboratories, one concerned mainly with assays where a high precision was desirable, *e.g.*, in calibration of new standards, and the other which had the additional need for a high throughput of less precise assays. The performance of the machines has gradually improved over this period as general operating experience has been gained, both with the prototype and commercial machines. They have been operating over the past 3 or 4 years constantly and routinely with no significant operational failures, producing results in line with those described in the tables. This has involved the use of a wide range of different assay media and solvents as can be seen from Table V.

Perhaps the most important lesson to be learnt was the practical impossibility of reducing

the systematic errors to an insignificant level. It is perhaps surprising that a systematic variation in the size of the punch holes within a single dish of only approximately 0.05 mm can produce a zone error of approximately 2%; when converted into potency error this would become approximately 3%. The systematic variation in size of holes shown in Fig. 2 is difficult to explain. It is of interest that a similar circular variation was found when the holes were cut automatically and successively with a single punch. It is possible that a rapid change in the gel properties commences following the first rupture of the agar surface and is progressive during the time period necessary to complete the punching of the six holes.

Although the volumetric displacement of the six dispenser pistons was probably within 0.1% of target (represented by an error of the piston movement of 0.01 mm or an error in diameter of the pistons of 0.001 mm) the six volumes delivered varied by up to 4%. However, the dispensed volume from a single pipette was consistent to within approximately 1%.

Hence, the combined errors arising from the punching and the dispensing can be considered in two parts; systematic errors related to each station are 2 and 1%, respectively, and the random errors for the punches and pipettes approximately 1% in each instance. If no attempt is made to eliminate the deterministic errors, then an inaccuracy of up to 4% may be introduced and not revealed by statistical analysis, which may, however, demonstrate apparent invalidities arising from these deterministic errors.

If the deterministic errors are systematically eliminated as described, only the random errors remain and a precision of approximately 2% may be achieved.

Alternatively, when pre-punched plates positioned randomly under the dispenser are used, larger random errors are generated although the dispenser deterministic errors are also retained; in this instance traditional statistical analysis tends to produce valid estimates. There is a narrow dividing line between these two situations arising from the use of the machine in the two modes (punch and pipette linked or separate) and any particular assay may fall into either category.

Measurement of true machine errors is extremely difficult and therefore seldom recognised, let alone quantitatively assessed. It is, however, likely that there are many similar situations in automated biological assays where repeated multiple volume measurements and repetitive quantitative physical observations are made. These effects can only be observed in experiments specifically designed to show them. Once the deterministic and random errors within a particular assay have been quantified, it is possible by careful design of the assay systematically to remove the former. However, in weighing, solution preparation, etc., this will not usually be possible. Little is gained by using more than the minimum number of replicates; for example, in the assay described where there are six positions it is possible to remove all deterministic errors by allowing each punch position to be filled in turn from a different dispenser or with a different solution. Thus, only six dishes are required to eliminate all deterministic machine errors and assays that previously required four large 12 × 12 in plates can be replaced with six Petri dishes.

The pipette tips on the apparatus are those commonly used manually in clinical and analytical laboratories for repetitive delivery of small volumes of reagents. It is likely that the variability obtained with manual operation will be much greater than that shown in Table I.

Thanks are due to the staff of the Worthing Research Division laboratories during the long development and proving period of the equipment. Research Engineers Ltd., Orsman Road, London, N1 5KD, have been associated with the further development of the prototype machine to the commercial stage.

References

1. Tatum, F., and Lightbown, J. W., Demonstration Meeting of the Society for Applied Bacteriology, Imperial College, London, 1968.
2. Sharpe, J. E., Lightbown, J. W., and Jones, A., *in* "Second International Symposium on Rapid Methods and Automation in Microbiology, Cambridge, 1976," Learned Information (Europe) Ltd., Oxford, 1976, p. 63.

Received *August 16th*, 1978
Accepted *October 25th*, 1978

Analyst, March, 1979, Vol. 104, pp. 208–223

Mechanism of Atom Excitation in Carbon Furnace Atomic-emission Spectrometry

D. Littlejohn and J. M. Ottaway

Department of Pure and Applied Chemistry, University of Strathclyde, Cathedral Street, Glasgow G1 1XL

By consideration of electronic and vibrational excitation temperatures and the ionisation temperature, it is demonstrated that local thermal equilibrium (LTE) is established under the practical analytical conditions of interrupted gas flow in which commercial carbon furnace atomisers are used as emission sources. The electron concentration is shown to be derived from thermionic emission from the carbon tube and calculated values of 5.2×10^{10} cm^{-3} at 2558 K and 1.3×10^{11} cm^{-3} at 2766 K are reported. The processes that contribute to the establishment of LTE are considered in detail, and it is suggested that molecular collisions make the major contribution to atomic excitation under all conditions, but that radiation absorption may be significant when a monatomic gas is used as purge gas and when molecules are present as impurities at concentrations of only 0.01%.

Keywords: *Atom emission*; *carbon furnace atomisation*; *excitation mechanism*; *electron concentration*; *local thermal equilibrium*

The original introduction of electrothermal atomisers, now used extensively in analytical atomic-absorption and -emission spectrometry, can be traced back to the work of A. S. King in 1905 and 1908.[1,2] He designed a resistively heated electrothermal atomiser in order to measure emission spectra of atoms and molecules in a source, which was free from the electrical action of the current carrying vapour of an arc or spark, and where the complicated, and often unknown, chemical reactions of a combustion flame could be avoided. The measurement of atomic- and molecular-emission spectra, generated by thermal energy alone, in a source closely approximating to thermodynamic equilibrium, rendered the King furnace of great value in the study of a number of fundamental spectroscopic processes.[1–5] The King furnace has been used more recently in a number of other fundamental studies. R. B. King and co-workers used furnace-emission intensity measurements at known temperatures to calculate relative gf values for a number of atomic species,[6] and determined the distribution of CN molecules amongst the vibrational and rotational energy levels in a calculation of the relative vibration transition probabilities of the CN violet bands.[7] In studies of the vapour pressure and heat of sublimation of graphite, Brewer and co-workers[8,9] measured the emission spectrum of C_2 in a King furnace and calculated the dissociation energy of gaseous C_2. During their studies, the vapour-phase temperature was measured using zirconium line-reversal at 473.95 nm. For a tube-wall temperature of 2973 K, they obtained a vapour-phase temperature of 2963 ± 20 K, which was also in agreement with the C_2 Swan band rotational temperature.[9] The existence of thermal equilibrium within the electrically heated furnace was thus confirmed.

Despite the information derived from such studies of the King furnace, no applications of this type of atomiser in analytical emission spectrometry were reported at that time. The first analytical applications of a modified atomiser, incorporating arc atomisation, were reported only in 1959 and involved atomic-absorption measurements.[10] Since then, and notably in recent years, the development of electrothermal atomisers for use in atomic-absorption analysis has advanced rapidly,[11] but it is only since 1975 that the possibility of using a furnace as an analytical emission source has been advanced[12,13] and, as yet, only a limited number of analytical procedures have been described.[14–19]

Commercially available furnace atomisers are resistively heated like the King furnace, and it might therefore be expected that they would also act as thermal emission sources. However, differences in the design and operation of modern atomisers, compared with the King furnace, may cause deviations from thermal equilibrium during the analysis time. There has, to date, been no evaluation for a furnace of the relative importance of the various excitation processes known to populate atomic energy states. The King furnace was

generally enclosed and sealed and either operated at high pressures, up to 16 atm,[3] or at pressures below 1 atm.[5–9] Samples introduced into the furnace were spread in bulk along the hot section of the tube, often fusing to the carbon surface for the lifetime of the tube. The furnace was usually operated at the desired temperature for 10–15 min to allow equilibrium to be attained, before emission measurements were taken over a further period of several minutes.[8] In modern analytical carbon furnace atomic-absorption and -emission spectrometry, however, transient signals are measured when both the tube temperature and the concentration of atoms are changing rapidly. Under these conditions, there is a net transport of energy and mass through the system and an inhomogeneous temperature distribution exists. The chemical species in the furnace never reach over-all equilibrium as in the King furnace, and atomisation is carried out under non-isothermal conditions. However, if the rates of transport and temperature change are small, compared with the rate at which energy is partitioned over the different degrees of freedom, a state of equilibrium can be established for each volume element of the furnace in each small time interval. Each volume element at any instant can then be assigned a local temperature and local thermal equilibrium (LTE) can be achieved for each volume element in each small interval of time.

A knowledge of the vapour temperature and how this relates to the change in wall temperature is of fundamental importance in emission spectrometry, as the intensity of the analytical signal is related directly to the temperature, which controls (under LTE) the distribution of the analyte species amongst the various energy levels. To understand the processes that control this distribution, it is necessary to ascertain both the magnitude of the apparent source temperature and the effect of the temperature gradient on the measured emission intensity. In most instances, the influence of the temperature gradient will be a function of the distribution of atoms along the tube at any instant of time. In contrast, in atomic-absorption spectrometry, where resonance lines are employed for most analyses under normal experimental conditions, the magnitude of the vapour temperature and the severity of the temperature gradient are less significant spectroscopically, provided that the furnace temperature is high enough to maintain the atomic vapour. However, the vapour temperature will affect the absorption (and emission) signals because of the temperature dependence of physical parameters, such as the degree of dissociation of molecular species and the residence time of atoms in the furnace.

To investigate these processes and to assess whether LTE is established during the time required for the measurement of atomic-absorption signals, a number of workers[20–27] have compared vapour-phase temperatures with tube-wall temperatures measured at different times during atomisation. In most instances, two-line atomic-absorption methods have been applied to estimate the vapour temperature from electronic excitation temperature calculations and these, and other methods, have been reviewed recently.[20–22] The results of these investigations show a marked lack of agreement on the relationship between vapour and furnace-wall temperatures, which is significant if the occurrence of LTE is to be confirmed. Adams and Kirkbright[23] reported that the excitation temperature of indium, in a Perkin-Elmer HGA-2000 furnace, increased with increase in the furnace-wall temperature, achieved a maximum similar to the temperature of the wall at the time of peak absorbance and finally decreased to a value that was up to 700 K lower than the final wall temperature. More recently, Sturgeon and Chakrabarti[20] found that excitation temperatures calculated from indium, gallium, iron and tin absorption signals, in a Perkin-Elmer HGA-2100 furnace and a Varian Techtron CRA-63 atomiser, rose to a maximum that occurred at a different time to the absorption maximum. The excitation temperature varied with the volatility of the thermometric species and was always lower than the tube-wall temperature by as much as 1300 K (indium). In contrast, Matousek[24] reported vapour-phase temperatures in a Varian CRA-63 mini-furnace that were 300 K higher than the wall temperature over most of the absorption signal. He used a nickel two-line atomic-absorption procedure and this discrepancy was traced subsequently to the use of erroneous *gf* literature values.[22] When corrected values were applied, the average vapour temperature was found to lag behind the maximum wall temperature by only 50–100 K.[22] Van den Broek *et al.*[22] have suggested that the differences observed in the literature vapour temperature calculations for different elements can often be attributed to random and systematic errors in the methods used. From measurements of the vapour temperatures of both a Perkin-Elmer HGA-2100 furnace

and a Varian CRA-63 mini-furnace using the same nickel line-pair as Matousek,[24] they proposed[22] a model for heat transfer that indicates that, in the absence of convective flow through a furnace, the gas temperature will follow the wall temperature of the heated furnace to within a few degrees.

Electronic excitation temperatures, based on emission measurements, have also been reported and show closer agreement with the furnace-wall temperature than those based on atomic-absorption methods. Alder *et al.*[25] calculated the electronic excitation temperature of iron by a two-line atomic-emission procedure using a Perkin-Elmer HGA-70 furnace. The temperature was calculated for the time of the peak emission signal and was found to be of the order of 2450 K when the temperature of the furnace wall was 2420 K. Hutton[26] employed iron two-line atomic-emission and "slope techniques"[21] as well as two-line atomic absorption procedures involving indium and gallium, to measure the vapour temperature in argon, nitrogen and helium in a Perkin-Elmer HGA-72 furnace, at the time of maximum atomic-emission or -absorption signals. He concluded that the vapour temperature lagged behind the wall temperature by up to 250 K and that the difference was greatest in helium and least in argon. A subsequent investigation, using iron electronic excitation temperature measurements, indicated[21] that the vapour temperatures in argon, nitrogen and helium were only 80–150 K lower than the wall temperature at the tube centre throughout the duration of the emission signal. Temperatures measured using the same procedure with an HGA-2200 furnace operated with maximum power heating and temperature control have also indicated[27] close agreement between the vapour-phase temperature and the furnace-wall temperature at the centre of the tube.

Although some of the above results are conflicting, the balance of recent experimental data supports the view that LTE does exist during carbon furnace atomisation. The supporting evidence is, however, derived solely from studies of atomic species. In order to confirm the existence of LTE more conclusively, we have extended the application of emission measurements to molecular and ionic species, and present electronic and vibrational excitation temperatures, and ionisation temperatures, obtained from a detailed study using the Perkin-Elmer HGA-72 and -74 furnace atomisers. Our results support the view that a thermal process or processes seem adequate to explain analyte emission intensities.[21,25] The mechanism responsible for the establishment of a Boltzmann distribution of energy under different experimental conditions has also been examined. The relative importance of electron and molecular collisions and radiative processes are assessed in a kinetic study of sodium atom excitation and an explanation is offered for the observation[21] that similar atomic-emission intensities are obtained in argon and nitrogen furnace gases. In addition, the electron concentration during furnace atomisation has been calculated using Saha's equation and the result shown to be consistent with the hypothesis that electrons are generated from thermionic emission from the graphite surface.

Experimental

Reagents

Standard solutions were prepared from reagents of the highest purity available and distilled water was used at all times. Stock solutions of each element (1000 μg ml^{-1}) were prepared by dissolving the appropriate amount of sulphate or nitrate salt in distilled water with the addition of sufficient nitric or sulphuric acid to give a final acid concentration of 10^{-2} M. Working solutions of the required concentration were prepared from the stock standard solutions as required.

Research-grade argon (99.996% purity) was used as the furnace purge gas.

Apparatus

Two instrumental systems were used for the measurements reported in this paper.

A Perkin-Elmer HGA-72 carbon furnace atomiser was mounted in a Perkin-Elmer 306 atomic-absorption/emission spectrometer and coupled to a Servoscribe RE 541.20 strip-chart recorder. This was used for the measurement of (*i*) nickel atomic emission for calculation of the electronic excitation temperature, and (*ii*) barium, calcium, europium, strontium and ytterbium atom and ion emission for calculation of the ionisation temperature and electron concentration. The operation of this system for measurement of atomic emission

has been described previously.[12,21] Standard HGA-72 graphite tubes were used. Solutions of the required concentration were transferred to the centre of the carbon tube using a 50-μl Oxford micropipette, and were then dried for 40 s at 373 K and atomised for 10–13 s at maximum power, which gave a final temperature of approximately 2700 K, under argon gas-stop conditions. The PE 306 monochromator slit was set to give a band pass of 0.2 nm in the ultraviolet and 0.4 nm in the visible region, and emission signals were recorded at a chart speed of 2 cm s^{-1}.

A Perkin-Elmer HGA-74 carbon furnace atomiser, mounted in a Perkin-Elmer 360 atomic-absorption/emission spectrometer and coupled to the Servoscribe RE 541.20 strip-chart recorder, was used to measure the $\Delta v = 0$ series, CN band emission of the $B^2\Sigma^+ \rightarrow X^2\Sigma^+$ violet system, for calculation of the vibrational excitation temperature. Standard HGA-74 graphite tubes were used. The operation of this system for measurement of furnace-emission signals is similar to that of the HGA-2200, which has been described previously.[27] A small volume of nitrogen was introduced into the furnace with the argon purge gas to allow formation of CN molecules. This was achieved either by mixing 1–2% nitrogen with the argon supply or by operating the furnace with the end windows removed, to allow ingress of atmospheric nitrogen. Both methods gave signals of sufficient magnitude and stability to permit the measurement of CN emission over the time required to scan the wavelength region of interest from 382 to 390 nm. The HGA-74 was operated at maximum power under a continuous argon gas flow for 90 s. A maximum tube temperature of 2700 K was obtained within 8 s and remained constant for the duration of the measurement period. The CN band emission was scanned using the PE 360 wavelength drive at a rate of 5 nm min^{-1}. The spectrometer slit width was set to give a spectral band pass of 0.2 nm with reduced slit height and the emission signals were recorded at a chart speed of 1 cm min^{-1}.

For measurements of atomic and ionic emission the spectrometers were adjusted to the required wavelength using the appropriate hollow-cathode lamp. In all instances, suitable choice of slit height and aperture stops reduced the amount of tube-wall radiation directly entering the monochromator to a minimum. Residual background emission signals were recorded under the same conditions as the atomic- and ionic-emission measurements. The background emission, at the time of the maximum of the combined analyte and background signal, was then subtracted to give the net maximum atom- or ion-emission signal.

The methods employed in the calculation of the spectroscopic temperatures presented in this paper are described in the Results and Discussion section. The values obtained are compared with the tube-wall temperatures measured with an Ircon series 1100 automatic optical pyrometer, the design and application of which have been described elsewhere.[21]

Results and Discussion

The processes reponsible for the excitation and de-excitation of atoms, ions and molecules in arcs, sparks, flames and other emission sources have been well characterised by many workers (see, for example, references 28–34 and the literature cited therein). Excitation mechanisms have been classified[28] into radiative processes, collisions with electrons, atoms and molecules, and chemical reactions, and in any specific source one or some combination of these processes may make a significant contribution. The relative importance of these processes in stimulating atomic emission from a carbon or tungsten tube atomiser has not been considered previously. If, as appears likely from the earlier work cited above, local thermal equilibrium is confirmed for electrothermal atomisation, then one or more of these processes must be responsible for establishing LTE.

Atoms produced in a graphite furnace exist in a chemically inactive system. It seems unlikely, therefore, that the chemical processes that often produce suprathermal atomic emission in combustion flames will be important. However, photoreactions involving dissociation and excitation by continuum radiation from the walls, and two-body exothermic exchange reactions of gaseous carbon with molecular oxides, could conceivably take place under particular conditions. Similarly, although the furnace system does not exhibit the electrical action of highly ionised vapours, the concentration of electrons and their significance in the excitation of atoms has yet to be investigated. In order to eliminate these possible, but unlikely, excitation processes, it is important to obtain conclusive evidence of the existence of local thermal equilibrium in the furnace during the initial few seconds of

atomisation and to calculate the concentration of electrons in the furnace atmosphere in the same period.

Local Thermal Equilibrium

For a gas to be in complete thermodynamic equilibrium it is required that the various gaseous components of the system be in equilibrium mutually and with respect to the surroundings. This will normally prevail only in an enclosure whose walls and interior have a uniform temperature with respect to radiation and internal energy,[31,32] and although a situation closely approximating to this can exist under certain conditions for the King furnace,[7,9] modern commercial electrothermal atomisers do not fulfil this criterion. However, as previously mentioned, local thermal equilibrium can be established within a furnace during the normal atomisation period. This will be characterised for each volume element of the source by the following conditions[31,32]: (*a*) the velocity distribution of all species in all energy levels satisfies Maxwell's equation; (*b*) for each chemical species, the relative population of energy levels conforms to Boltzmann's distribution law; (*c*) the degree of ionisation of each species is described by Saha's equation; and (*d*) the radiation density is consistent with Planck's law.

Local thermal equilibrium can be shown to exist if the same value of temperature determines each of the above conditions at the same time in each volume element. In real sources with concentration and thermal gradients, it is impossible to consider each volume element individually and a collective measurement is obtained. This usually involves the measurement of the combined radiation emission from each volume element and the value of the resulting apparent temperature depends on the distribution of atoms along the temperature gradient of the source.[35,36]

As most of the atoms and molecules in an electrothermal tube furnace have similar mass and atmospheric pressure is normally used, translational energy will be partitioned by collisions almost instantaneously, and it can therefore be assumed that the velocity distribution will be given by Maxwell's formula. The experimental determination of the translational (or kinetic) temperature is possible from Doppler half-widths but is known to be fairly inaccurate[37] and is not considered further here.

The likelihood of LTE existing in the graphite tube furnace is enhanced by the presence of the tube-wall enclosure, which is the source of all energy subsequently transferred to the vapour phase. In most emission sources, condition (*d*) above, concerning Planck's radiation density, is not fulfilled and deviations from LTE can exist because radiation emitted by vapour species is not compensated for by absorption of an equal amount of radiation from the surroundings. In many sources, where the molecular concentration is high and collisional processes of excitation and de-excitation predominate, the effect of this outward radiation loss is minimal. Departures from LTE through radiative dis-equilibrium have, however, been observed for hydrogen - argon flames[38] and for a low current d.c. arc operated in an atomic gas (see p. 126 of reference 32). In a previously reported study,[39] we have shown that the spectral distribution of energy from a graphite tube atomiser closely fulfils the requirements of Planck's radiation law. A temperature of 2553 K was calculated from the spectral distribution of the graphite tube continuum, when the wall temperature, as measured by the optical pyrometer, was 2603 K at the tube centre, and a temperature of 2534 K was obtained from the intensity of wall radiation scattered by the components of the vapour phase when the wall temperature was measured at 2573 K.

In this investigation, we considered LTE criteria (*b*) and (*c*) above, by comparing electronic and vibrational excitation temperatures and the ionisation temperature with corresponding tube-wall temperatures in order to ascertain whether LTE holds during the initial few seconds of atomisation when both atomic-absorption and atomic-emission signals are recorded.

Excitation temperatures[31,32,37,40]

The wavelength-integrated emission intensity measured by a spectrometer when an atom or molecule undergoes a radiative transition from an energy level E_x to a lower energy state E_y can be expressed by

$$I = KA_{xy}N_x \times \frac{hc}{\lambda_{xy}} \times \frac{L}{4\pi} \quad .. \quad .. \quad .. \quad .. \quad (1)$$

where I is the intensity over the total line width, K is a machine constant, A_{xy} is the Einstein transition probability, N_x is the concentration of atoms or molecules in the upper energy level, λ_{xy} is the wavelength of the transition, L is the source length in the direction of viewing and h and c have their usual meanings and values.

If the species in question are thermally distributed amongst the various electronic, vibrational and rotational levels, N_x can be replaced with

$$N_x = N_t \times \frac{g_x}{B(T)} \times \exp\left(\frac{-E_x}{kT}\right) \quad .. \quad .. \quad .. \quad (2)$$

where k is Boltzmann's constant, g_x is the statistical weight of the upper energy level, N_t is the total species concentration in all states and $B(T)$ is the partition function or the state sum[41] and is defined as

$$B(T) = g_0 + g_x \exp\left(\frac{-E_x}{kT}\right) + g_y \exp\left(\frac{-E_y}{kT}\right) + \ldots \quad .. \quad .. \quad (3)$$

where the subscripts denote the excited states and zero the ground state.

Combining equations (1) and (2) gives

$$I = \frac{KLhcg_xA_{xy}N_t \exp\left(\frac{-E_x}{kT}\right)}{4\pi B(T)\,\lambda_{xy}} \quad .. \quad .. \quad .. \quad .. \quad (4)$$

which can be rearranged to

$$\ln\left(\frac{I\lambda_{xy}}{g_xA_{xy}}\right) = \ln\,(K'N_t) - \frac{E_x}{kT} \quad .. \quad .. \quad .. \quad .. \quad (5)$$

where K' covers all of the constants in equation (4), including the partition function $B(T)$, which is approximately constant for the species of interest over the temperature range discussed here.[42]

The value of $\ln(K'N_t)$ will vary during the atomisation cycle of a furnace, because N_t, the total concentration of atoms in the tube, varies, but will be constant for all lines of an element at any specific instant. Hence, by measuring the relative intensity of a series of spectral lines at different times during atomisation, it is possible to calculate T, the electronic excitation temperature at each moment, from the slope of $\ln\left(\frac{I\lambda_{xy}}{g_xA_{xy}}\right)$ against E_x, if the energy levels are populated in accordance with the Boltzmann equation.

The atomic-emission signals of the nickel lines listed in Table I were measured in duplicate with respect to time, using the HGA-72/PE 306 system. A 50-μl aliquot of a 0.5 μg ml^{-1} nickel solution was used in each instance. At this concentration, self-absorption effects were observed to be negligible. Correction factors for the slight variation in the spectrometer spectral response at different wavelengths were applied to the mean of the recorded intensities. The slope temperatures were then calculated, as illustrated in Fig. 1(*a*), at various times during atomisation from the least squares calculation of the slope of the graph

TABLE I

NICKEL LINES EMPLOYED FOR THE MEASUREMENT OF THE ELECTRONIC EXCITATION TEMPERATURE BY THE SLOPE METHOD[43]

Wavelength, λ/nm	Energy levels/eV	$\log_{10} gA/\lambda$
305.08	4.088–0.025	5.35
341.48	3.655–0.025	5.24
342.37	3.832–0.212	4.72
343.36	3.635–0.025	4.72
344.63	3.705–0.109	4.98
349.30	3.657–0.109	5.05

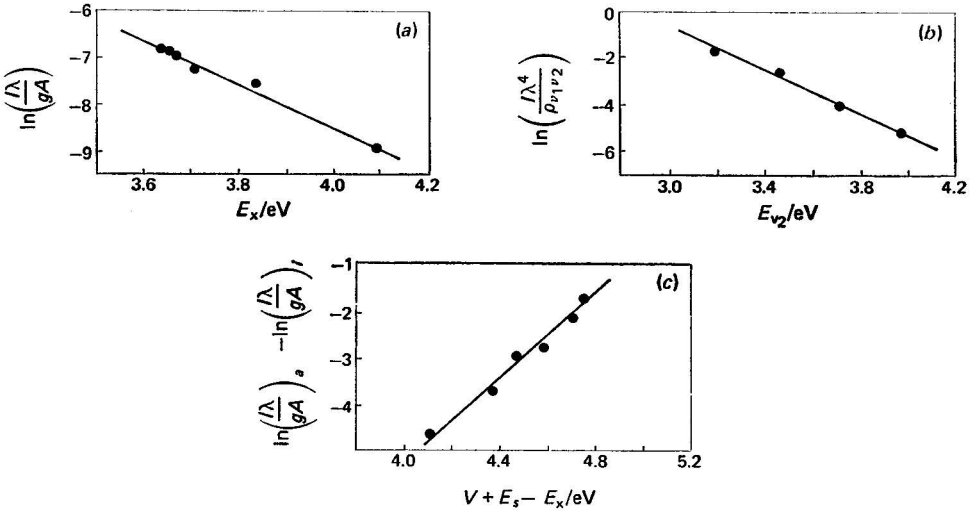

Fig. 1. Variation of the intensity of carbon furnace emission signals with excitation and ionisation energy in a calculation of (*a*) nickel electronic excitation temperature (HGA-72), wall temperature at the centre 2 670 K and slope temperature 2 568 ± 143 K; (*b*) CN vibrational excitation temperature (HGA-74), wall temperature at the centre 2 700 K and slope temperature 2 491 ± 143 K; and (*c*) ionisation temperature (HGA-72), wall temperature at the centre 2 700 K and slope temperature 2 603 ± 174 K. Measurements made in argon at maximum power (999 units). Electronic and ionisation temperature calculated from atomic and ionic emission intensities recorded, with interrupted gas flow, at 4 and 6 s, respectively, from the start of atomisation.

of $\ln\left(\frac{I\lambda_{xy}}{g_x A_{xy}}\right)$ against E_x. The $g_x A_{xy}$ values employed were those described by Corliss[43] as the best recommended values for the nickel lines in question.

The calculated temperatures at various times up to 9 s during atomisation in Fig. 2 are slightly lower than the equivalent wall temperatures at the centre of the tube owing to the temperature gradient along the carbon surface and are in agreement with our previous studies using iron as the thermometric species in Perkin-Elmer HGA-72[21] and HGA-2200[27] furnaces. The error bars in the observed temperatures were obtained by the method of least squares and represent one standard deviation of the points from the straight line, taking into account variations in sample introduction, signal measurement and errors in the

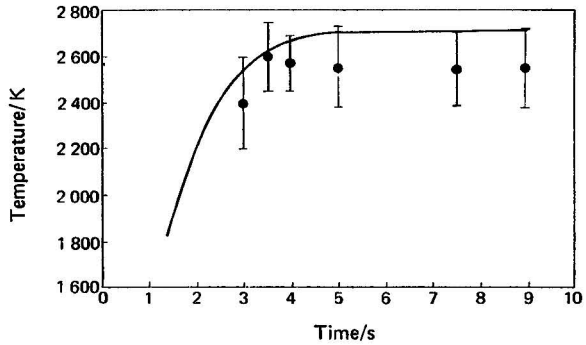

Fig. 2. Variation with time of the wall temperature at the centre of an HGA-72 graphite tube atomiser (——) with the electronic excitation temperature (●), calculated from the nickel atomic emission. Atomisation at maximum power (999 units) in argon with interrupted gas flow.

$g_x A_{xy}$ values. Close agreement between tube-wall and electronic excitation temperature was also reported by Van den Broek *et al.*,[22] who used a nickel two-line atomic-absorption procedure to calculate the vapour temperatures of a Varian CRA-63 mini-furnace and a Perkin-Elmer HGA-2100 atomiser.

When molecules are used as the thermometric species, the excitation temperature can be calculated from rotational and vibrational spectra. This requires the replacement of the transition probability, A_{xy}, in equation (4) by the expression

$$A_{xy} = \frac{16\pi^3}{3\epsilon_0 h\lambda_{xy}^3} \times \frac{1}{g_x} \times S \quad .. \quad .. \quad .. \quad (6)$$

where ϵ_0 is the permittivity of a vacuum and S is the line strength, which by definition is the square of the electric dipole transition moment.[41] Rotational lines of certain molecules, such as OH and CN, are nearly always observed as impurities in emission sources but high resolution is required to resolve the rotational structure.[41,44] Vibrational bands of unresolved rotational character can, however, be used easily to calculate the vibrational excitation temperature. In this instance, the line strength S is replaced by the vibrational transition probability $\rho_{v_2v_1}$, calculation of which requires a knowledge of the dependence of the electronic transition moment on internuclear distance.[45] Equation (4) can then be expressed in the form

$$I_{v_2v_1} = \frac{K''N_{T\rho v_2v_1} \exp\left(\frac{-E_{v_2}}{kT}\right)}{\lambda_{21}^4} \quad .. \quad .. \quad .. \quad .. \quad (7)$$

which on rearrangement becomes

$$\ln\left(\frac{I\lambda_{21}^4}{\rho_{v_2v_1}}\right) = \ln\left(K''N_T\right) - \frac{E_{v_2}}{kT} \quad .. \quad .. \quad .. \quad .. \quad (8)$$

where K'' includes all of the constants in the previous equations and E_{v_2} is the energy of the upper vibrational level of the transition of interest.

Emission spectra of a number of molecules formed during carbon furnace atomisation were described in detail by Hutton *et al.*[46] Of those molecules which are easily observed, CN seemed the most suitable, and equation (8) was applied to the vibrational spectra of the $\Delta v = 0$ sequence of the $B^2\Sigma^+ \rightarrow X^2\Sigma^+$ band system given in Table II. The CN emission was measured using an HGA-74 atomiser operated at maximum power with argon gas flow, using the wavelength drive of the spectrometer (PE 360) to scan the bands in the 385–390-nm region. As with the vibrational spectra of many diatomic molecules, the bands overlap strongly and it was necessary to extrapolate the tail of each band to the maximum of the adjacent band to subtract the overlapping background intensity and obtain the net emission intensity of each band. With these reduced band-head intensities, a graph of $\ln\left(\frac{I\lambda_{21}^4}{\rho_{v_2v_1}}\right)$ *versus* E_{v_2} was constructed, as illustrated in Fig. 1(*b*), and the vibrational excitation temperature calculated.

A period of approximately 90 s was necessary to scan the wavelength region required,

TABLE II

BANDS OF THE CN VIOLET $B^2\Sigma^+ \rightarrow X^2\Sigma^+$ SYSTEM EMPLOYED FOR THE MEASUREMENT OF THE VIBRATIONAL EXCITATION TEMPERATURE BY THE SLOPE METHOD[45]

Band	Wavelength/ nm	Energy levels/ eV	Relative vibrational transition probabilities
0,0	388.34	3.198–0.0	1000
1,1	387.14	3.462–0.253	880
2,2	386.19	3.720–0.503	790
3,3	385.47	3.973–0.750	740

and to maintain reproducible and measurable CN emission over this time nitrogen impurities were continuously introduced at a constant rate into the furnace with the argon gas flow by operating the atomiser without the end windows to allow ingress of air. As the furnace was also operated at constant temperature, the CN bands were therefore measured under equilibrium conditions. The residence time of the nitrogen in the furnace is, however, relatively short, and the establishment of equilibrium conditions therefore needs to be rapid. Temperatures calculated by this procedure give little information about changes in the vapour temperature during the initial few seconds of atomisation normally used for analysis, but do give an indication of the influence of tube-temperature gradient on the vapour-phase temperature.

Because the measured emission intensity is a combination of the photons emitted from each small volume element of the furnace, and the intensity from each section is dependent on its temperature and atom or molecule content, the deviation of the apparent vapour temperature from that of the carbon wall at the tube centre will depend on the distribution of species along the tube-temperature gradient. Under the conditions normally used for analytical atomic-emission studies, *i.e.*, interrupted gas flow (or gas stop), the concentration of atoms, etc., will always be greatest at the tube centre, but for the procedure used for the measurement of CN, an almost even distribution will exist along the tube. The vibrational excitation temperature of 2491 $\pm$ 143 K calculated from the slope in Fig. 1(*b*) is about 200 K lower than the wall temperature at the tube centre. Although this is a greater deviation than that observed for the nickel atom measurements, the difference is relatively small considering that the ends of the tube and the carbon cones will be of the order of 1000 K or lower, when the centre of the tube is at 2700 K. This suggests that an apparent temperature gradient of only a few hundred degrees from the centre to a few millimetres from the ends of the carbon tube will be effective in determining the intensity of atomic or molecular emission from an electrothermal atomiser, depending on the concentration gradient therein. This argument will be developed elsewhere[47] in a consideration of tube design and temperature on the intensity of atomic-emission signals. As far as the present work is concerned, measurements of the vibrational excitation temperature of CN indicate a thermal population of energy levels and support the contention that LTE is attained during carbon furnace atomisation.

Ionisation temperature[37,41,48]

Saha's equation for the ionisation equilibrium between the atoms and ions of one element is represented by

$$\frac{N_i N_e}{N_a} = \frac{2(2\pi m_e k)^{\frac{3}{2}}}{h^3} \times T^{\frac{3}{2}} \times \frac{B(T)_i}{B(T)_a} \times \exp\left(\frac{-V}{kT}\right) \quad .. \quad .. \quad .. \quad (9)$$

where N_a, N_i and N_e are the concentrations of atoms, ions and electrons, respectively, $B(T)_a$ and $B(T)_i$ are the partition functions of atom and ion, V is the ionisation potential, m_e is the mass of the electron and the other terms have their usual meanings and values.

The intensity of the ionic emission can be expressed in a similar manner to that for atomic emission, and combination of equation (4) for each species with equation (9) yields the relationship

$$\ln\left(\frac{I\lambda_{xy}}{g_x A_{xy}}\right)_a - \ln\left(\frac{I\lambda_{st}}{g_s A_{st}}\right)_i = \ln N_e - \ln\left[\frac{2(2\pi m_e k)^{\frac{3}{2}}}{h^3}\right] - 1.5 \ln T + \frac{(V + E_s - E_x)}{kT} \quad (10)$$

where subscripts s and t refer to the upper and lower energy levels of the ionic transition. Equation (10) requires that the emission intensities of an atom and ion line be measured for a series of elements or line pairs. At any instant in time during atomisation, the temperature and hence 1.5 ln$T$ will be constant, and a graph of the left-hand side of equation (10) *versus* $V + E_s - E_x$ for each element or line pair will be a straight line of slope $+1/kT$, from which the ionisation temperature can be calculated. Emission signals were measured with respect to time in duplicate for each of the atom and ion line pairs shown in Table III, using the HGA-72/PE 306 system at maximum furnace power and with interrupted argon

TABLE III

ATOM AND ION LINE PAIRS EMPLOYED FOR THE CALCULATION OF THE IONISATION TEMPERATURE[49]

Element	Line	Wavelength/ nm	Energy levels/ eV	Ionisation potential/ eV	$gA \times 10^{-8}$/s	Concentration of solution*/ $\mu g\ ml^{-1}$
Eu	I	321.281	3.858–0.0	5.67	9.6	5
	II	420.505	2.949–0.0		3.2	
Yb	I	377.010	5.433–2.144	6.20	8.6	50
	II	369.419	3.356–0.0		0.74	
Ca	I	430.253	4.781–1.899	6.11	7.1	40
	II	393.367	3.152–0.0		0.91	
Ca	I	445.673	4.683–1.899	6.11	7.5	40
	II	393.367	3.152–0.0		0.91	
Sr	I	496.226	4.346–1.848	5.69	4.8	10
	II	407.771	3.041–0.0		0.66	
Ba	I	611.076	3.219–1.190	5.21	5.2	20
	II	614.172	2.723–0.704		0.38	

* Injections of 50 μl.

gas flow. Similar spectrometer conditions were applied for the measurement of the atom and ion signals of each pair. Wavelengths were chosen to give emission intensities of a similar order of magnitude for both species at concentrations giving negligible self-absorption. Atom and ion lines of similar wavelength were employed where possible to minimise errors in the correction for variations in spectrometer spectral response.

The ionisation temperature was calculated at various times during atomisation as illustrated in Fig. 1(*c*) and the collated results, shown in Fig. 3, compared reasonably well with the tube-wall temperature at the corresponding time. The error bars signify the random errors for the derived temperatures as calculated with a programmable calculator by applying the method of least squares. The errors appear to be acceptable for the procedure, considering the number of measurements contributing to each calculation.

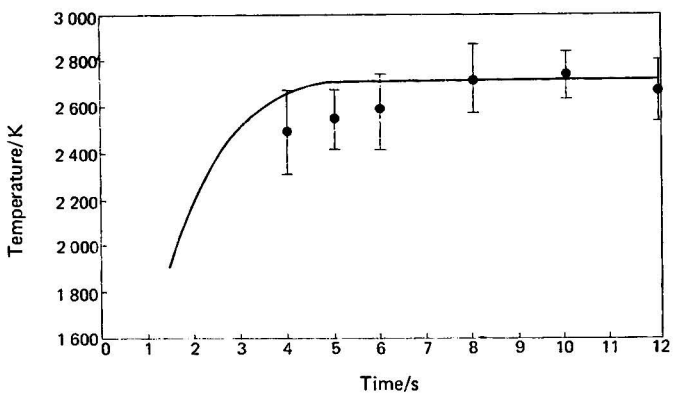

Fig. 3. Variation with time of the wall temperature at the centre of an HGA-72 graphite tube atomiser (——) with the ionisation temperature (●), calculated from the atomic and ionic emission of calcium, barium, strontium, europium and ytterbium. Atomisation at maximum power (999 units) in argon with interrupted gas flow.

Electron concentration

Once the ionisation temperature at any point during atomisation has been calculated, the abscissa of the above graph of equation (10) can be used to calculate the value of N_e,

the natural level of electrons in the furnace at the same time. The electron concentration was found to range from 5.2×10^{10} cm^{-3} at 2558 K to 1.3×10^{11} cm^{-3} at 2766 K. The errors in the electron concentrations at each point during atomisation were calculated from a knowledge of the error in the slope (and hence the abscissa) and the temperature. The errors were found to vary between ± 0.9 and ± 1.9 orders of magnitude for all the points considered. This appears to be acceptable for the procedure used, considering the degree of extrapolation required to obtain the abscissa and the dependence of the calculation of electron concentration on temperature (see p. 173 of reference 31). No comparative values for the electron concentration in electrothermal atomisers have been reported.

It is unlikely that furnace electrons will be produced through the ionisation of vapour phase carbon species as the ionisation potentials of CN, C, C_2, C_3, etc., are of the order of 11 eV or higher.[50] Graphite however, has a comparatively low thermionic work function and an indication of the concentration of electrons produced by thermionic emission as the tube surface is heated is given by the expression[51]

$$N_e = \frac{2(2\pi m_e kT)^{\frac{3}{2}}}{h^3} \times \exp\left(\frac{-W}{kT}\right) \quad .. \quad .. \quad .. \quad .. \quad (11)$$

where W is the work function for carbon, 4.6 eV. At 2760 K, the value of 2.7×10^{12} cm^{-3} obtained from equation (11) compares reasonably well with the value obtained above, from Saha's equation, and is within experimental error. Although trace impurities of sodium, potassium and other easily ionised elements present in the furnace material or purge gas will add to the partial pressure of electrons, the concentration will be much smaller (10^8 cm^{-3}) than that produced by thermionic emission,[20] which hence seems the only viable source of electrons.

Conclusion

From the preceding discussions, it appears that conditions closely approximating LTE are achieved in a carbon furnace during atomisation, excitation and ionisation of atomic and molecular species. The evidence presented above appears conclusive, at least for the presently available commercial systems investigated. Although the measurement of thermal emission from a carbon furnace precludes excitation by suprathermal chemiluminescence mechanisms, confirmation of a Boltzmann distribution of energy does not in itself identify the relative contributions of the remaining processes in establishing thermal equilibrium. To obtain information on the most likely mechanism or mechanisms, it is necessary to consider the kinetics and practical rate of each process under normal atomisation conditions.

Atom Excitation Mechanism

The competing processes that are likely to excite metal atoms (or ions)electronically in a graphite tube atomiser are therefore: (*a*) collisions with electrons involving transfer of the translational energy from electrons, (*b*) collisions with molecules, with transfer of the vibrational and rotational energy of molecules, (*c*) discrete absorption of radiation from the tube-wall continuum.

These processes can be expressed in the form of equations as follows:

$$M + e^- \rightleftharpoons M^* + e^- \quad .. \quad .. \quad .. \quad .. \quad .. \quad (12a)$$

$$M + XY \rightleftharpoons M^* + XY \quad .. \quad .. \quad .. \quad .. \quad .. \quad (12b)$$

$$M + h\nu \rightleftharpoons M^* \quad .. \quad .. \quad .. \quad .. \quad .. \quad .. \quad (12c)$$

where e represents an electron, M and M* a metal atom in the ground and excited states, respectively, XY a molecule where X may or may not be the same as Y, and $h\nu$ is a photon of discrete energy.

The excitation rate equations for these processes can then be described, respectively, as

$$\text{Rate}_e = k_e[e^-][M] \quad .. \quad .. \quad .. \quad .. \quad .. \quad (13a)$$

$$\text{Rate}_{XY} = k_{XY}[XY][M] \quad .. \quad .. \quad .. \quad .. \quad .. \quad (13b)$$

$$\text{Rate}_{RAD} = k_{RAD}[M] \quad .. \quad .. \quad .. \quad .. \quad .. \quad (13c)$$

where k is the rate coefficient or constant for each process and k_{RAD} includes a term accounting for the radiation density.

It is generally accepted that monatomic species show low efficiency in the electronic excitation of metal atoms,[28] which would be expected from classical mechanics, and this process is not considered further in this discussion. However, owing to their much smaller mass and larger mean velocity under thermal conditions, electrons are expected to be considerably more efficient than inert gas atoms in the (de-)population of atomic electronic states that lie several electronvolts above the ground state[28] and so have been considered.

Gilmore *et al.*,[29] in a review of atomic and molecular excitation mechanisms, tabulated rate coefficients for excitation, de-excitation and excitation energy transfer for a number of reactions, but in general, investigations involving metal atom species have been limited to the alkali metals. For all the processes described above, expressions were available that allowed calculation of the rate coefficients for the excitation of the sodium resonance line at 589.00 nm. These calculations are used in the following discussion as an illustrative example, using a typical furnace temperature of 2500 K. As the concentration of sodium is a constant whichever process is considered, values of Rate/[Na] will be calculated in each instance and compared.

Electron collisions

The excitation rate constant, k_e, can be obtained under thermal conditions at temperature T, by averaging over a Maxwellian distribution of electron energy, giving[28]

$$k_e = \sigma_{THR}\left(\frac{8kT}{\pi m_e}\right)^{\frac{1}{2}}\left(1 + \frac{E}{kT}\right)\exp\left(\frac{-E}{kT}\right) \quad .. \quad .. \quad .. \quad (14)$$

where E is the energy of the excited state, in this instance 2.1 eV for sodium, and σ_{THR} is the effective cross-section at energies greater than the threshold required for excitation and is of the order of 2.3×10^{-15} cm^2.[52] Substitution for the other constants in equation (14) and $T = 2500$ K gives a value for k_e of 4.4×10^{-11} cm^3 s^{-1}. An alternative expression for k_e was derived by Gilmore *et al.*,[29] based on the integration of Zapesochnyi's[52] cross-sections over a Maxwell velocity distribution for several temperatures, and fitting the data for sodium by an Arrhenius function of temperature. The resulting equation was

$$k_e = 6 \times 10^{-10}T^{0.6}\exp\left(\frac{-24540}{T}\right) \quad .. \quad .. \quad .. \quad (15)$$

which was shown to fit well over a wide temperature range from 1500 to 20000 K. With this relationship a value of 3.6×10^{-12} cm^3 s^{-1} is obtained for k_e at 2500 K in reasonably close agreement to the alternative value above.

Taking a value for k_e of 4.4×10^{-11} cm^3 s^{-1} and the value of the electron concentration of 3.1×10^{11} cm^{-3} calculated as produced by thermionic emission at 2500 K, equation (13*a*) gives a value for Rate$_e$/[Na] of 14 s^{-1}. The alternative value of k_e would result in a smaller value of Rate$_e$/Na and the above value may be considered as a possible maximum.

Molecular collisions

The concentration of molecules such as N_2, O_2, CN, C_x, etc., present in a graphite tube atomiser during the production and excitation of metal atoms, depends greatly on the conditions of operation, such as inert gas used and temperature, and the design of the furnace. Two conditions will therefore be considered that can be taken as the extremes of the maximum and minimum molecular content normally encountered in practical analysis.

When an atomiser is operated in a nitrogen atmosphere, the concentration of molecules will be totally dominated by N_2 at a level of about 3×10^{18} molecules cm^{-3} at 1 atm and 2500 K. Mentall *et al.*[53] have calculated the rate coefficient for excitation of sodium by

nitrogen to be approximately k_{N_2} 10^{-10} cm^3 s^{-1} at temperatures between 2100 and 2800 K. These two figures combined give a value of $\text{Rate}_{N_2(\text{max.})}[\text{Na}]$ from equation (13*b*) of 3×10^8 s^{-1}.

When a monatomic gas such as argon is used as purge gas in an enclosed furnace system like the IL 555 atomiser, the molecular concentration arises from nitrogen and oxygen present as impurities in the gas and from desorption from the furnace material at elevated temperatures. The argon normally used in this laboratory contains 0.004% impurity, which, if it is assumed to be exclusively O_2 and N_2, gives about 10^{14} molecules cm^{-3}. In addition, at room temperature a level of at least 10^{14} molecules cm^{-2} of nitrogen and oxygen will be adsorbed on the surface of the atomiser when opened to the air.[54] On desorption, during atomisation, this will add a further 5×10^{14} molecules cm^{-3} to the furnace volume. At 2500 K, the partial pressure of C_x species will be approximately 10^{-7} atm,[55] giving 3×10^{11} C_x molecules cm^{-3}. This is increased at 3000 K to 3×10^{14} molecules cm^{-3} (10^{-4} atm) and only at this temperature would the concentration approach that of the nitrogen and oxygen. As optimum atomic-emission signals are normally measured for sodium and many other elements at temperatures less than 3000 K,[56] it is unlikely that excitation by C_x will be significant unless the rate constant for such excitation is very large. The fact that LTE exists at temperatures at which the concentration of C_x species is very low suggests that this process cannot be the major excitation mechanism.

A value for the rate constant for the excitation of sodium by oxygen was not available. The minimum concentration of molecules under these conditions is therefore expressed exclusively as N_2 and is assigned a value of 5×10^{14} cm^{-3}. The collision cross-section of O_2 at 2000 K (given on p. 48 of reference 28) suggests that oxygen will be at least as effective as nitrogen as a molecular species capable of exciting metal atoms. The rate of excitation at this minimum concentration of molecules, expressed as nitrogen and given by equation (13*b*), $\text{Rate}_{N_2(\text{min.})}/[\text{Na}]$, will be 5×10^4 s^{-1}.

Photon absorption

Unlike other emission sources a graphite or tungsten tube atomiser will fulfil the conditions of "detailed balance" for radiative processes, irrespective of the concentration of analyte present, as loss of photons through atomic, ionic or molecular emission will be balanced by absorption of the tube-wall black-body radiation at discrete energies.

The rate constant for radiational excitation, k_{RAD}, can be expressed as (reference 28, p. 64)

$$k_{\text{RAD}} = \frac{\pi_e^2}{m_e hc^2} \times \lambda_0^3 f P_\lambda \quad .. \quad .. \quad .. \quad .. \quad (16)$$

where f is the oscillator strength for absorption and P_λ is the spectral volume density of the radiation field. For a graphite tube atomiser, $P_\lambda \approx P_{\lambda_0}^{\text{b}}$, the black-body radiation density, which is given by Wien's approximation of Planck's law[39] as

$$P_\lambda^{\text{b}} = \frac{8\pi hc}{\lambda^5} \times \exp\left(\frac{-hc}{\lambda k T}\right) \quad .. \quad .. \quad .. \quad .. \quad (17)$$

The oscillator strength, f, can be expressed in terms of the Einstein transition probability for emission A_{21} by (reference 28, p. 17)

$$f_{1-2} = \left(\frac{m_e c}{8\pi^2 e^2}\right) \lambda^2 \times \frac{g_2 A_{21}}{g_1} \quad .. \quad .. \quad .. \quad .. \quad (18)$$

Substitution of equations (17) and (18) for P_λ and f into equation (16) produces a simplified expression for k_{RAD}:

$$k_{\text{RAD}} = \frac{\text{Rate}_{\text{RAD}}}{[\text{Na}]} = \frac{g_2}{g_1} \times \text{A}_{21} \exp\left(\frac{-hc}{\lambda k T}\right) \quad .. \quad .. \quad .. \quad (19)$$

The magnitude of $(g_2/g_1)A_{21}$ is of the order of 10^8 s,[49] giving for the sodium resonance line at 589.0 nm a value of $Rate_{RAD}/[Na]$ approaching 5.8×10^3 s^{-1} at 2500 K.

Using data available in the literature, it has been possible to calculate the reaction rates for processes (12*a*), (12*b*) and (12*c*) for the sodium resonance transition at 589.00 nm. Similar data for all the processes do not seem to be available for any other atom or transition. The reaction rates for the sodium transition at 2500 K are compared in Table IV, and additional values computed for 2100 and 2800 K are given. These temperatures represent the extremes of the temperature interval over which the nitrogen rate coefficient of 10^{10} cm^3 s^{-1} can be applied. A number of conclusions can be derived from these figures regarding the mechanism of sodium excitation and atomic excitation generally in a carbon furnace atomiser.

(A) When nitrogen is used as the furnace purge gas, excitation and de-excitation of all species will be dominated by N_2 molecular collisions.

(B) Although the temperature dependence of electron concentration greatly increases the rate of electron excitation from 2100 to 2800 K, it is unlikely that electron collisions will be a significant excitation process at the temperatures at which emission signals are normally measured (less than 3000 K), irrespective of the pressure or composition of the furnace gas.

(C) When a monatomic gas such as argon is used as purge gas, at temperatures approaching 3000 K in an enclosed furnace, the contribution of photon absorption can become similar to that of nitrogen molecular impurities. In open furnaces the contribution of photon absorption is less significant than in a closed furnace, owing to the increased ingress of atmospheric nitrogen.

(D) A lack of detailed information regarding the temperature variation of the N_2 collision-rate constant leads to an unexpected trend of reduced rate with increased temperature (Table IV) for nitrogen collisions. This trend may in fact be erroneous, but it will not affect the conclusions drawn above over the most useful temperature range of presently available carbon furnace atomisers.

TABLE IV

RATES OF REACTIONS FOR PHYSICAL PROCESSES OF SODIUM EXCITATION AT DIFFERENT TEMPERATURES OF 2100, 2500 AND 2800 K

Process	Rate/[Na]/s^{-1} 2100 K	2500 K	2800 K
Electron collisions	3.08×10^{-2}	1.39×10^{1}	4.43×10^{2}
Nitrogen collisions, maximum ..	3.5×10^{3}	3.0×10^{3}	2.6×10^{3}
Nitrogen collisions, minimum ..	$\sim 5 \times 10^{4}$	$\sim 5 \times 10^{4}$	$\sim 5 \times 10^{4}$
Photon absorption	9.0×10^{2}	5.8×10^{3}	1.7×10^{4}

Although the excitation of atomic and molecular species in nitrogen can be up to 10^4 times faster than in argon (owing to the greater concentration of N_2), similar emission intensities are measured in both gases at the same furnace temperature.[21] This is explained by the principle of "detailed balance" that applies to all processes, in conditions of local thermal equilibrium. "Detailed balance" states that the total number of atoms or other species leaving an excited state per second, by any process (collision, radiation, etc.), just equals the number arriving in that state per second, by the exact reverse process.[34] Hence, in nitrogen the de-excitation rate will be also about 10^4 times faster than in argon.

In carbon furnace atomic-emission spectrometry reduction of the molecular concentration from 100% nitrogen to approximately 0.01% does not appear to disturb conditions of local thermal equilibrium, as indicated previously by a comparison of atomic-emission intensities in argon and nitrogen gases. In contrast, departures from LTE arise in a d.c. arc operated in an inert gas with less than 1% molecular impurity, and infrathermal emission is encountered in combustion flames of low molecular concentration (see pp. 126–131 of reference 32). This can be understood from a comparison of the number of molecular collisions that a metal atom suffers during the average residence time in the observation zone of each source. At atmospheric pressure, the number of collisions between sodium and nitrogen

is about 10^9 s^{-1} at 2500 K[28] (assuming 100% nitrogen). The residence time of a metal atom in an air - acetylene flame or d.c. arc is of the order of milliseconds,[32] and therefore each sodium atom will take part in 10^5–10^6 collisions in this time. At 2000 K at least one out of every 10^5 colliding molecules has an energy of about 3 eV,[34] and the collision frequency therefore seems sufficient to establish an equilibrium population of the excited state. At lower nitrogen concentrations this is less likely to be true. However, the residence time of metal atoms in a HGA-72 furnace operated with interrupted gas flow is about 1 s,[57] and therefore, even at nitrogen concentrations as low as 0.01%, sodium and other atoms will still make 10^5–10^6 collisions with nitrogen molecules while present in the furnace atmosphere. The existence of LTE under such conditions is therefore likely even without the contribution of tube-wall radiation. It is also interesting to note that when the molecular concentration, in a d.c. arc or combustion flame, falls below the level at which molecular collisions dominate all other processes, departures from thermal populations arise through radiative disequilibrium, as photons emitted by atoms are not balanced by the absorption of photons at an equal rate from the radiation field. In a furnace atomiser, the semi-enclosure of the tube wall, which radiates as a black body, ensures that radiative disequilibrium does not occur and LTE is maintained.

Similar conclusions to the above will apply to most furnace tube atomisers operated under interrupted gas flow conditions, including those made from other materials such as tungsten. The thermionic work function for tungsten, 4.52 eV,[50] is similar to that of carbon, and will give a similar electron concentration, and Kirchoff's law[28] ensures that an approximate black body radiation density will exist in the tungsten-tube atomiser. The conclusions reached above may not necessarily apply under conditions of convective gas flow where vapour-phase temperatures may differ substantially from tube-wall temperatures.[22]

The work described in this paper indicates that the graphite furnace is unique amongst emission sources in that local thermal equilibrium exists under normal working conditions. In achieving this state, molecular collisions appear to make the major contribution, but radiation absorption may be of minor importance when argon is used as purge gas. Although some of the fundamental properties of the King furnace have been known for many years, the possibility of applying the technique of furnace emission more widely in analytical chemistry is only now being investigated in detail. While the carbon furnace remains a relatively cool source, compared with other currently available emission sources, the signal to background ratios, signal stabilities and atom residence times are such that very low detection limits have already been achieved for a wide range of elements,[27,58] and spectral interferences are much reduced in complexity. The fundamental origin of the observed emission signals established in this paper will contribute to the development of the technique, and to considerations of the most suitable design of atomisation source.

The authors thank the Salters' Company for the award of a Scholarship to D.L. and The Royal Society for the award of a research grant to J.M.O. for the purchase of the HGA-72 atomiser. The gift of the HGA-74/PE 360 system by the British Steel Corporation, Ravenscraig Works, and helpful discussions with many colleagues, particularly C. Th. J. Alkemade, are also gratefully acknowledged.

References

1. King, A. S., *Astrophys. J.*, 1905, **21**, 236.
2. King, A. S., *Astrophys. J.*, 1908, **27**, 353.
3. King, A. S., *Astrophys. J.*, 1912, **35**, 183.
4. King, A. S., *Astrophys. J.*, 1913, **37**, 239.
5. King, A. S., *Astrophys. J.*, 1922, **56**, 318.
6. King, R. B., Parnes, B. R., Davis, M. H., and Olsen, K. H., *J. Opt. Soc. Am.*, 1955, **45**, 350.
7. Floyd, A. L., and King, R. B., *J. Opt. Soc. Am.*, 1955, **45**, 249.
8. Brewer, L., Gilles, P. W., and Jenkins, F. A., *J. Chem. Phys.*, 1948, **16**, 797.
9. Brewer, L., Hicks, W. T., and Krikorian, O. H., *J. Chem. Phys.*, 1962, **36**, 182.
10. L'vov, B. V., *J. Eng. Phys. (USSR)*, 1959, **2**, 44.
11. Fuller, C. W., "Electrothermal Atomization for Atomic Absorption Spectrometry," *Analytical Sciences Monographs, No. 4*, Chemical Society, London, 1977.
12. Ottaway, J. M., and Shaw, F., *Analyst*, 1975, **100**, 438.
13. Molnar, C. J., Chuang, F. S., and Winefordner, J. D., *Spectrochim. Acta*, 1975, **30B**, 183.
14. Shaw, F., and Ottaway, J. M., *Analyt. Lett.*, 1975, **8**, 911.

15. Epstein, M. S., Rains, T. C., and O'Haver, T. C., *Appl. Spectrosc.*, 1976, **30**, 324.
16. Littlejohn, D., and Ottaway, J. M., *Analyst*, 1977, **102**, 393.
17. Hutton, R. C., Ottaway, J. M., Rains, T. C., and Epstein, M. S., *Analyst*, 1966, **102**, 429.
18. Ebdon, L., Hutton, R. C., and Ottaway, J. M., *Analytica Chim. Acta*, 1978, **96**, 63.
19. Epstein, M. S., Rains, T. C., Brady, T. J., Moody, J. R., and Barnes, I. L., *Analyt. Chem.*, 1978, **50**, 874.
20. Sturgeon, R. E., and Chakrabarti, C. L., *Spectrochim. Acta*, 1977, **32B**, 231.
21. Littlejohn, D., and Ottaway, J. M., *Analyst*, 1978, **103**, 595.
22. Van den Broek, W. M. G. T., de Galan, L., Matousek, J. P., and Czobik, E. J., *Analytica Chim. Acta*, 1978, **100**, 121.
23. Adams, M. J., and Kirkbright, G. F., *Analytica Chim. Acta*, 1976, **84**, 79.
24. Matousek, J. P., "Proceedings of the 17th Colloquium Spectroscopicum Internationale, Florence, 1973," Volume I, Adam Hilger, Bristol, 1975, p. 57.
25. Alder, J. F., Samuel, A. J., and Snook, R. D., *Spectrochim. Acta*, 1976, **31B**, 509.
26. Hutton, R. C., *PhD Thesis*, University of Strathclyde, 1977.
27. Littlejohn, D., and Ottaway J. M., *Analytica Chim. Acta*, 1978, **98**, 279.
28. Alkemade, C. Th. J., and Zeegers, P. J. Th., *in* Winefordner, J. D., *Editor*, "Spectrochemical Methods of Analysis. Quantitative Analysis of Atoms and Molecules," John Wiley, New York, 1971, Ch. 1.
29. Gilmore, F. R., Bauer, E., and McGowan, J. W., *J. Quant. Spectrosc. Radiat. Transfer*, 1969, **9**, 157.
30. Caller, A. B., *Appl. Opt., Suppl. Chem. Lasers*, 1965, 145.
31. Boumans, P. W. J. M., "Theory of Spectrochemical Excitation," Hilger and Watts, London, 1966.
32. Boumans, P. W. J. M., *in* Groves, E. L., *Editor*, "Analytical Emission Spectroscopy, Part II," Marcel Dekker, New York, 1972, Ch. 6.
33. Boumans, P. W. J. M., and De Boer, F. J., *Spectrochim. Acta, B*, in the press.
34. Alkemade, C. Th. J., "Proceedings of the 10th Colloquium Spectroscopicum Internationale, Maryland, 1962," Spartan, Washington, D.C., 1963, p. 143.
35. Reif, I., Fassel, V. A., and Kniseley, R. N., *Spectrochim. Acta*, 1973, **28B**, 105.
36. Reif, I., Fassel, V. A., and Kniseley, R. N., *Spectrochim. Acta*, 1974, **29B**, 79.
37. De Galan, L., and Winefordner, J. D., *J. Quant. Spectrosc. Radiat. Transfer*, 1967, **7**, 703.
38. Hooymayers, H. P., and Alkemade, C. Th. J., *J. Quant. Spectrosc. Radiat. Transfer*, 1966, **6**, 501, 847 and 912.
39. Littlejohn, D., and Ottaway, J. M., *Analyst*, 1977, **102**, 553.
40. Winefordner, J. D., McGee, W. W., Mansfield, J. M., Parsons, M. L., and Zacha, K. E., *Analytica Chim. Acta*, 1966, **36**, 25.
41. Thorne, A. P., "Spectrophysics," Chapman and Hall, London, 1974, Ch. 9 and 11.
42. De Galan, L., Smith, R., and Winefordner, J. D., *Spectrochim. Acta*, 1968, **23B**, 521.
43. Corliss C. H., *J. Res. Natn. Bur. Stand.*, 1965, **69A**, 87.
44. Smit, J. A., *Physica*, 1946, **12**, 683.
45. Nicholls, R. W., *Proc. Phys. Soc.*, 1956, **69**, 51.
46. Hutton, R. C., Ottaway, J. M., Epstein, M. S., and Rains, T. C., *Analyst*, 1977, **102**, 658.
47. Littlejohn, D., and Ottaway, J. M., *Analyst*, submitted for publication.
48. Mavrodineanu, R., and Boiteux, H., "Flame Spectroscopy," John Wiley, New York, 1965.
49. Corliss, C. H., and Bozmann, W. R., "Experimental Transition Probabilities for Spectral Lines of Seventy Elements," *Nat. Bur. Stand. Monogr.*, No. 53, 1962.
50. Weast, R. C., *Editor*, "Handbook of Chemistry and Physics," 56th Edition, Chemical Rubber Company, Cleveland, Ohio, 1976.
51. Page, F. M., and Woolley, P. E., *Combust. Flame*, 1974, **23**, 121.
52. Zapesochnyi, I. P., *High Temp.*, 1967, **5**, 6.
53. Mentall, J. E., Krause, H. F., and Fite, W. L., *Discuss. Faraday Soc.*, 1967, **44**, 157.
54. Ehrlich, G., *J. Phys. Chem.*, 1956, **60**, 1388.
55. Palmer, H. B., and Shelef, M., *in* Walker, P. L., Jr., *Editor*, "Chemistry and Physics of Carbon, Volume 4," Edward Arnold, London, 1968, p. 85.
56. Littlejohn, D., and Ottaway, J. M., *Analytica Chim. Acta*, in the press.
57. Sturgeon, R. E., Chakrabarti, C. L., and Bertels, P. C., *Analyt. Chem.*, 1975, **47**, 1250.
58. Littlejohn, D., and Ottaway, J. M., *Analyst*, 1978, **103**, 662.

Received *June 12th*, 1978
Accepted *October 11th*, 1978

Analyst, March, 1979, Vol. 104, pp. 224–231

Determination of Chromium in Natural Waters and Sewage Effluents by Atomic-absorption Spectrophotometry Using an Air - Acetylene Flame

K. C. Thompson and K. Wagstaff

Severn–Trent Water Authority, Malvern Regional Laboratory, 141 Church Street, Malvern Worcestershire WR14 2AN

A simple method for the determination of chromium in natural waters and sewage final effluents by atomic-absorption spectrophotometry using an air - acetylene flame is described. The sample is concentrated by evaporation by a factor of five. Interference effects were minimised by the addition of ammonium perchlorate and were further reduced by working with a flame on the verge of luminosity rather than a distinctly luminous flame.

Keywords: Chromium determination; atomic-absorption spectrophotometry; air - acetylene flame; natural waters and sewage effluents

The World Health Organization European Standard[1] quotes a limit for chromium(VI) in potable waters of 0.05 μg ml^{-1}, and a European Economic Community Directive,[2] concerning the quality required of surface waters intended for abstraction of drinking water, quotes a total chromium limit of 0.05 μg ml^{-1}. There is a requirement for a routine atomic-absorption spectrophotometric method suitable for the determination of chromium at these levels in a wide range of natural waters and sewage effluents. Ideally, the method should have a sample preparation stage that will allow subsequent analysis for other toxic metals of interest. The proposed method should have a detection limit of about 0.005 μg ml^{-1} of chromium.

Most manufacturers of atomic-absorption spectrophotometers quote detection limits for chromium in pure solution, when calculated as 4.65 times the within-batch standard deviation of the blank,[3] of between 0.007 and 0.01 μg ml^{-1} in the luminous air - acetylene flame. Under these flame conditions, inter-element effects for chromium are severe,[4,5] and it appears that some form of pre-concentration and also some method of minimising potential inter-element effects are necessary. The commonly used solvent-extraction technique using ammonium tetramethylenedithiocarbamate - 4-methylpentan-2-one is very sensitive but suffers from several disadvantages.[6,7] A pre-treatment step utilising acid digestion is required to break down any insoluble or organically bound chromium. A potassium permanganate oxidation step is necessary to convert chromium(III) into chromium(VI). Reduction of the excess of permanganate and careful pH adjustment must be made before the extraction is performed. The pH adjustment step is critical if co-extraction of manganese with subsequent emulsion formation is to be avoided. Overnight standing of the extract prior to nebulisation is recommended.[6]

This paper describes a simple atomic-absorption spectrophotometric method that utilises a concentration by evaporation technique, in which ammonium perchlorate is incorporated into the sample solution in order to minimise inter-element effects from the sample matrix. The determination is carried out in an air - acetylene flame.

Experimental

Apparatus

Atomic-absorption spectrophotometer. A Varian Techtron 1200 fitted with a standard high-solids air - acetylene burner (titanium burner grid) and a corrosion-resistant nebuliser was used.

Borosilicate glass beakers and test-tubes. Tall-form 100-ml beakers with a spout, and engraved at the 5 ml level. These beakers were initially boiled in 50% *V/V* hydrochloric acid (36% *m/m*) and were reserved for this work. Calibrated (0.1 ml) 10-ml tubes with ground-glass stoppers (Exelo Ltd.), which were initially soaked in 50% *V/V* hydrochloric acid and regularly cleaned using laboratory detergent, were used.

Reagents

Hydrochloric acid, 25% *V/V*. Dilute 250 ml (±2 ml) of hydrochloric acid (36% *m/m*) (analytical-reagent grade) to 1 l (±2 ml) with de-ionised water.

Ammonium perchlorate solution, 10% *m/V*. Dissolve 50 g (±0.1 g) of ammonium perchlorate (Fisons Ltd.) in about 450 ml of de-ionised water and dilute to 500 ml (±1 ml) with de-ionised water.

Caution—Ammonium perchlorate is a potentially hazardous chemical and any solution spillage should be dealt with immediately in order to avoid any subsequent fire risk.

Hydrogen peroxide, 6% *m/m*. BDH Chemicals, analytical-reagent grade (20 volume).

Aluminium oxide anti-bumping granules. BDH Chemicals. These granules were boiled with nitric acid, washed with de-ionised water and dried prior to use.

Standard chromium(III) chloride solution (1000 μg ml^{-1} *of chromium*). BDH Chemicals.

Standard potassium dichromate solution (1000 μg ml^{-1} *of chromium*). Hopkin and Williams.

Optimisation of the Method

Choice of flame and flame conditions

It is well known that chromium determinations in the air - acetylene flame are prone to inter-element effects[4,5,8–12] and that the chromium sensitivity is dependent on the oxidation state of the chromium.[4,13,14] These problems can be avoided by using the dinitrogen oxide - acetylene flame but the use of this flame results in a decrease in the detection limit of approximately 4–5-fold compared with the luminous air - acetylene flame. Many laboratories prefer to avoid the routine use of the dinitrogen oxide - acetylene flame for their standard toxic metal analyses and for these reasons a method utilising the air - acetylene flame was developed.

Inter-element effects in the air - acetylene flame can be minimised by setting the acetylene flow so that a non-luminous flame is obtained.[4,5,10] However, this results in a significantly decreased detection limit compared with the luminous-flame conditions that are normally used for this determination. Previous work[14] has shown that under luminous-flame conditions chromium calibration graphs over the range 0–20 μg ml^{-1} exhibited inflexions and well defined maxima. The effect was especially pronounced for chromium(III) solutions; it appeared to depend upon the age of the solutions and was also observed in solutions containing 10% *V/V* nitric acid (70% *m/m*).

For this study, the acetylene flow was set so that a flame on the verge of luminosity was obtained. The chromium characteristic concentration under these conditions (0.10 μg ml^{-1}) was just over twice that observed in the luminous flame (0.043 μg ml^{-1}).

Choice of interference suppressor

Various reagents have been recommended for minimising inter-element effects in the atomic-absorption spectrophotometric determination of chromium in the air - acetylene flame. These include lanthanum chloride,[15] sodium sulphate,[8] ammonium chloride,[4,9] ammonium bifluoride[4,10] and quinolin-8-ol.[4,11] The incorporation of 5000 μg ml^{-1} of lanthanum (as the chloride) in all the solutions was found not to overcome many inter-element effects and resulted in a significant background-absorption signal. The addition of 5000 μg ml^{-1} of sodium sulphate actually enhanced the suppression caused by 1000 μg ml^{-1} of calcium and magnesium on a 10 μg ml^{-1} chromium solution.[8] Recently, the addition of ammonium perchlorate has been recommended for minimising inter-element effects of elements other than chromium.[16–19] It was decided, therefore, to compare the addition of ammonium chloride with the addition of ammonium perchlorate to various synthetic solutions so that the final solutions contained 2% *m/V* of the added salt, as recommended by Barnes[9] for ammonium chloride. Ammonium salts, as expected, were found not to increase significantly the background-absorption signal. Table I shows that an interference suppressant is essential and that ammonium perchlorate is better than ammonium chloride. All the results in Table I were obtained using a flame on the verge of luminosity. If the acetylene flow was increased so as to obtain the maximum chromium response (a distinctly luminous flame), inter-element effects were significantly increased in all instances. Ammonium perchlorate, at a concentration of 2% *m/V* in the final nebulised solution, was used in all further work. Increasing the ammonium perchlorate concentration

TABLE I

COMPARISON OF AMMONIUM CHLORIDE AND AMMONIUM PERCHLORATE AS INTERFERENCE SUPPRESSORS OF INTER-ELEMENT EFFECTS

All solutions contained 2 μg ml^{-1} of chromium(III) and 10% *V*/*V* hydrochloric acid (36% *m*/*m*). Sequential background correction was applied.

Interfering substance added	Concentration*/ μg ml^{-1}	Signal with no suppressant added	Relative signal with 2% *m*/*V* of added suppressant	
			Ammonium chloride	Ammonium perchlorate
None	—	100	100	100
Ca (as Cl)	2000			
SO_4 (as H_2SO_4)	1000	74	92.5	95.3
Na (as Cl)	480			
Ca (as Cl)	4000			
Mg (as Cl)	1000	79.5	85.9	90.1
Ca (as Cl)	2000			
Fe (as Cl)	200	85	89.9	98.4
Mg (as Cl)	200			
Mg (as Cl)	1000	66.2	92.7	100.8

* The concentrations shown represent the final concentrations in the nebulised solution and should be divided by 5 when related to the analyte solution.

to 3% *m*/*V* did not appear to offer any further significant reduction in the inter-element effects.

Instrumental operating conditions

Table II gives the optimised instrumental operating conditions. Automatic background correction at the 357.9-nm chromium line is not to be recommended, as balancing the hydrogen and chromium lamp intensities at this wavelength is not easy and a severely degraded chromium detection limit is normally observed. Sequential background correction using the lead 357.3-nm non-resonance line was used and found to be satisfactory. Table III gives the typical background-absorption signals (expressed as a chromium concentration) from the main matrix elements and from some typical samples. It can be seen that the presence of sulphate significantly enhances the background absorption from calcium and magnesium. However, this table shows that the background-absorption signals for most natural-water and sewage-effluent samples are relatively small.

TABLE II

OPTIMISED INSTRUMENTAL OPERATING CONDITIONS

Wavelength	357.9 nm
Background correction wavelength	357.3 nm (Pb)
Slit width	0.5 nm
Air flow	As recommended in handbook
Acetylene flow	Flame on verge of luminosity (no yellow luminosity visible)
Distance from top of burner grid to position where the grid just intercepted the light beam (0.01 absorbance)	3.5 mm
Integration period	3 s
Wash solution	3% *V*/*V* hydrochloric acid (36% *m*/*m*)

TABLE III

TYPICAL BACKGROUND-ABSORPTION SIGNALS USING THE 357.3-nm LEAD NON-RESONANCE LINE

All solutions contained 2% *m/V* ammonium perchlorate and 10% *V/V* hydrochloric acid (36% *m/m*).

Substance added or sample	Concentration/ $\mu g\ ml^{-1}$	Background-absorption signal/$\mu g\ ml^{-1}$ of chromium
Ca (as Cl)	10000	0.09
Ca (as Cl)	10000	0.22
SO_4 (as H_2SO_4) ..	9600	
Na (as Cl)	10000	0.03
Na (as Cl)	10000	0.035
SO_4 (as H_2SO_4) ..	9600	
Mg (as Cl)	10000	0.17
Mg (as Cl)	10000	0.26
SO_4 (as H_2SO_4) ..	9600	
SO_4 (as H_2SO_4) ..	19200	<0.01
Tap water 1*	See Table V	<0.002
River water 2* ..		0.0070
River water 3* ..		0.0090
Sewage effluent 6* ..		0.0060

* The background-absorption signals were measured after the samples were concentrated by evaporating to one fifth of volume. The observed signals were then divided by 5.

Concentration technique

A five-fold concentration step of 50 ml to 10 ml was found to result in an acceptable detection limit (less than 0.005 $\mu g\ ml^{-1}$), tolerable inter-element effects and very low background absorption. The time for the evaporation step was approximately 1.5 h.

Hydrochloric acid was used rather than nitric acid, as previous work had shown that the background-absorption signal at 357.3 nm from 10000 $\mu g\ ml^{-1}$ of calcium (as the chloride) was increased approximately four-fold in the presence of 10% *V/V* nitric acid (70% *m/m*), but was unaffected by the presence of 10% *V/V* hydrochloric acid (36% *m/m*). Also, a small, but significant, negative background-absorption signal had been observed with strong nitric acid solutions at 357.9 nm. However, nitric acid is the preferred acid for other types of samples (*e.g.*, sewage sludge).[20]

Method

NOTE—
This method should not be used with trade wastes or any unknown samples for safety reasons. An alternative method is given below (see Alternative Method).

Volumes (50 ± 0.5 ml) of the samples, standards and blanks were placed in 100-ml borosilicate glass beakers and 4 ml (±0.1 ml) of 25% *V/V* hydrochloric acid, 2 ml (±0.05 ml) of 10% *m/V* ammonium perchlorate solution and some aluminium oxide anti-bumping granules were added. The beakers were then placed on a hot-plate with the temperature set such that gentle simmering occurred. The evaporation step was carried out in a fume cupboard and all normal safety precautions were observed. When the volume of the solution had decreased to 20 ml (±5 ml), 0.5 ml (±0.05 ml) of hydrogen peroxide (6% *m/m*) was then added. This ensured that any chromium(VI) would be converted into chromium(III).[21] The evaporation was then continued until the final volume was about 5 ml (±1 ml) and this took approximately 1.5 h. The solutions were allowed to cool and the contents transferred into the 10-ml calibrated borosilicate glass tubes. The beakers were

carefully washed out using three approximately 1.5-ml washes with de-ionised water from a wash-bottle with a very fine nozzle. The contents of the tube were then diluted to volume and shaken and any suspended matter was allowed to settle prior to nebulisation.

The final acid concentration during the evaporation step, in conjunction with the addition of hydrogen peroxide, should ensure adequate digestion of particulate and organically bound chromium in natural waters and effluents. The solutions in the beakers do not boil dry if the temperature of the hot-plate is carefully set because the presence of the ammonium perchlorate significantly increases the boiling-point of the liquid, and hence decreases the rate of evaporation as the solution approaches dryness.

It is not normal practice to heat solutions of perchlorate in the presence of organic matter, but it should be stressed that each beaker contains only 200 mg of ammonium perchlorate (equivalent to 170 mg of perchloric acid). The method is applicable only to river samples, potable waters and sewage final effluents and the solution in the beaker should not boil dry. In order to attempt to evaluate the risk of explosion, 10 ml of an industrial digested sludge containing 6% of dry solids with levels of over 3000 $\mu g\ g^{-1}$ of copper and zinc were added to three beakers, diluted to 50 ml and carried through the procedure. When the evaporation stage was nearly completed the temperature of the hot-plate was increased to the maximum and the solutions in the beakers were allowed to boil dry. Although violent spitting and some deflagration were observed, no explosive reaction occurred. Numerous similar tests with 50 ml of 5000 and 10000 $\mu g\ ml^{-1}$ glucose solutions and 50 ml of a 1000 $\mu g\ ml^{-1}$ glucose solution containing 0.5 ml of vegetable oil yielded similar results. It is generally agreed that carbohydrates, and vegetable oils and fats constitute a particular hazard in the presence of perchloric acid.[22] The use of 10-ml calibrated stoppered tubes rather than 10-ml calibrated flasks was considered accurate enough for this type of analysis and facilitated solution transfer and storage of large numbers of samples.

Some laboratories will prefer to avoid boiling down a solution containing ammonium perchlorate and an alternative method was tested. This involved using a larger initial volume so that the ammonium perchlorate could be incorporated after the evaporation stage and allow efficient washing of the beaker used for the evaporation.

Caution—During the whole course of this study no violent reactions were observed, but if the technique was scaled up the risk would almost certainly increase.

Alternative Method

Volumes (100 $\pm$ 1 ml) of the samples, standards and blanks were placed in 150-ml borosilicate beakers and 8 ml ($\pm$0.2 ml) of 25% *V/V* hydrochloric acid and some aluminium oxide anti-bumping granules were added. The beakers were then placed on a hot-plate and gently simmered until the solution volume had decreased to 40 ml ($\pm$10 ml), then 1 ml ($\pm$0.1 ml) of hydrogen peroxide (6% *m/m*) was added. The evaporation was continued until the final volume was about 8 ml ($\pm$2 ml). The solutions were allowed to cool, 4 ml ($\pm$0.1 ml) of 10% *m/V* ammonium perchlorate then added and the contents transferred into 20-ml calibrated borosilicate glass tubes. The beakers were carefully washed using four approximately 2-ml washes with de-ionised water from a wash-bottle with a very fine nozzle. The contents of the tube were then diluted to volume and shaken and any suspended matter was allowed to settle prior to nebulisation.

All the results quoted in this paper were obtained by using the original method except for some precision measurements.

No significant blanks were observed but prior to this work base-line noise and drift were observed during chromium determinations on humid days. Water droplets could be seen in the tube connecting the air supply from the air compressor water trap to the atomic-absorption spectrophotometer. This problem was overcome by inserting an additional water trap in the air line.

Inter-element Effects

Table IV (in addition to Table I) shows the effect of various substances on the chromium response. It can be seen that for typical levels of the main matrix elements in natural waters and sewage effluents, the method would appear to be satisfactory. Aliquots of tap water, sample 1 (see Table V), were spiked with equal amounts (0.04 and 0.4 $\mu g\ ml^{-1}$) of

TABLE IV

EFFECT OF VARIOUS SUBSTANCES ON THE CHROMIUM RESPONSE

All solutions contained 2% *m/V* ammonium perchlorate and 10% *V/V* hydrochloric acid (36% *m/m*). Instrumental conditions as in Table II.

Interfering substance*	Concentration of interfering substance†/ $\mu g\ ml^{-1}$	Chromium concentration*/ $\mu g\ ml^{-1}$	Relative signal
None	—	2	100.0
Ca	1000	2	98.7
Mg	100		
Ca	2000	2	96.6
Mg	200		
PO_4 (as P)	100		
Ca	2000	2	95.0
Mg	200		
Cu	100		
Zn	100		
Ca	1000	2	97.4
Mg	100		
Fe	200		
None		1	100.0
Ca	500	1	100.0
Mg	100		
SiO_2	100		
Ca	500	1	96.1
Mg	100		
Detergent (Mannoxol)	50		
Ca	500	1	99.6
Mg	100		
SO_4	500		
Ca	500	1	100.8
Mg	100		
PO_4 (as P)	50		
Ca	500	1	99.5
Mg	100		
NH_4 (as N)	900		
NO_3 (as N)	900		
Ca	500	1	99.7
Mg	100		
SiO_2	100		
Ca	1000	1	97.1
Mg	100		
Zn	100		
Mn	100		

* All cations were added as chlorides. SO_4 was added as H_2SO_4, SiO_2 as sodium silicate, phosphates as $(NH_4)_2HPO_4$ and NH_4 and NO_3 as NH_4NO_3.

† The concentrations shown represent the final concentrations in the nebulised solution and should be divided by 5 when related to the analyte solution.

chromium(III) and chromium(VI) and taken through the procedure, and no significant difference in response for the two oxidation states was detected.

Results

The technique was initially tested using a sample of tap water with a moderate total

TABLE V

ANALYTICAL RESULTS ON SAMPLES USED, PRIOR TO CONCENTRATION BY EVAPORATION

Sample No.	Source	Content/μg ml^{-1} Total hardness ($CaCO_3$)	Mg	Na	Total Fe	SO_4^{2-}	Cl^-	Conductivity/ μS cm^{-1}
1	Tap water	238	12	11	<0.03	50	18	405
2	River water	516	43	35	0.38	302	34	986
3	River water	538	51	460	0.20	403	800	2900
4	River water	327	15	25	1.7	119	37	587
5	Sewage works final effluent	563	24	44	0.65	348	39	1093
6	Sewage works final effluent	593	27	78	0.41	296	94	1431

hardness value (see Table V). A large sample of the tap water was acidified with hydrochloric acid to pH 2.5 and split into four aliquots, three of which were then spiked with 0.02, 0.2 and 0.4 μg ml^{-1} of chromium(III). The resulting samples were then analysed in duplicate over nine days and Table VI gives the results of these analyses. The alternative method, in which the ammonium perchlorate was added after the evaporation stage, showed within-batch standard deviations comparable to those in the original method (see Table VII).

TABLE VI

TYPICAL PERFORMANCE DATA FOR TAP WATER, SAMPLE NO. 1, ANALYSED IN DUPLICATE OVER NINE DAYS

Sample	Added chromium/ μg ml^{-1}	Mean chromium result/μg ml^{-1}	Standard deviation/ μg ml^{-1}
Unknown standard (0.2 μg ml^{-1})	—	0.197	0.00494
Tap water	—	0.0013	0.00093
Tap water	0.02	0.0204	0.0012
Tap water	0.2	0.200	0.00437
Tap water	0.4	0.396	0.0111
Blank	—	—	0.00092*

* The within-batch standard deviation (s) of the blank was calculated using the nine sets of paired blank results.[3] Hence, the 4.65 s detection limit is 0.0043 μg ml^{-1}.

Recovery tests using the original method were then carried out using three river-water samples and two sewage works final effluents. These samples were selected as they exhibited high conductivities and high sulphate levels and would be expected to give a good indication of maximum potential inter-element effects. Table V gives the main matrix element concentrations for these samples.

Table VIII shows the recoveries obtained after the addition of 0.04 and 0.4 μg ml^{-1} of chromium(III) to these samples, and also shows some recoveries obtained in the absence of ammonium perchlorate. The natural chromium level in the samples, except for sample 2, was below the detection limit. Sample 2 was found to contain 0.015 μg ml^{-1} of chromium. Using the electrothermal atomisation technique utilising the standard additions method of calibration, a chromium level of 0.016 μg ml^{-1} was found in this sample. It can also be

TABLE VII

COMPARISON OF ORIGINAL AND ALTERNATIVE METHODS

Sample	Added chromium/ μg ml^{-1}	Within-batch standard deviation/μg ml^{-1} (9 degrees of freedom) Original method	Alternative method
Standard	0.2	0.0020	0.0018
Tap water	0.2	0.0022	0.0019

seen from Table VIII that the proposed method would appear to be satisfactory for natural water and sewage final effluent analysis and that in the absence of ammonium perchlorate poor recoveries were observed, especially if the flame conditions were set for maximum response (*i.e.*, a distinctly luminous flame).

TABLE VIII

RECOVERY TEST RESULTS

		Chromium recovered/μg ml^{-1}			
		Flame on verge of luminosity (Table II)			
Sample	Sample No.	Chromium added (0.04 μg ml^{-1}) plus ammonium perchlorate	Chromium added (0.4 μg ml^{-1}) plus ammonium perchlorate	Chromium added (0.4 μg ml^{-1}) and no ammonium perchlorate	Luminous flame with chromium added (0.4 μg ml^{-1}) and no ammonium perchlorate
River water ..	2	0.040	0.380	0.293	0.188
River water ..	3	0.0371	0.379	0.296	0.184
River water ..	4	0.0396	0.404	0.332	0.230
Sewage final effluent ..	5	0.0386	0.387	0.312	0.243
Sewage final effluent ..	6	0.0382	0.370	0.306	0.246

Conclusions

The concentration by evaporation technique with the addition of ammonium perchlorate and hydrochloric acid would appear to be a rapid pre-concentration technique for the atomic-absorption spectrophotometric analysis of total chromium in natural waters and sewage final effluents using the air - acetylene flame. A detection limit of 0.0043 μg ml^{-1} (4.65 *s*) was obtained and inter-element effects were considered acceptable. The proposed technique has the additional advantage that other elements can also be determined.

The authors thank Mr. W. F. Lester, Director of Scientific Services, Severn–Trent Water Authority, for permission to publish this work.

References

1. "World Health Organization European Standards for Drinking Water," Second Edition, 1970.
2. EEC Directive, *Official Journal of the European Communities*, 75/440/EEC, July 1975.
3. Wilson, A. L., and Cheeseman, R. V., "Manual on Analytical Quality Control for the Water Industry," Water Research Centre Technical Report TR66, Water Research Centre, Medmenham, 1978.
4. Rawa, J. A., and Henn, E. L., *Am. Lab.*, 1977, **9** (8), 31.
5. Thompson, K. C., and Reynolds, R. J., "Atomic Absorption, Fluorescence and Flame Emission Spectroscopy, A Practical Approach," Griffin, London, 1978.
6. Midgett, M. R., and Fishman, M. J., *Atom. Absorption Newsl.*, 1967, **6**, 128.
7. Gilbert, T. R., and Clay, A. M., *Analytica Chim. Acta*, 1973, **67**, 289.
8. Hurlbut, J. A., and Chriswell, C. D., *Analyt. Chem.*, 1971, **43**, 465.
9. Barnes, L., *Analyt. Chem.*, 1966, **38**, 1083.
10. Purushottam, A., Naidu, P. P., and Lal, S. S., *Talanta*, 1973, **20**, 631.
11. Ottaway, J. M., and Pradhan, N. K., *Talanta*, 1973, **20**, 927.
12. Kodama, M., Shimizu, S., Sato, M., and Tominaga, T., *Analyt. Lett.*, 1977, **10**, 591.
13. Kraft, G., Lindenberger, D., and Beck, H., *Z. Analyt. Chem.*, 1976, **282**, 119.
14. Thompson, K. C., *Analyst*, 1978, **103**, 1258.
15. Tenny, A. M., *Instrum. News*, 1967, **18**, 14.
16. Burke, K. E., and Albright, C. H., *Dev. Appl. Spectrosc.*, 1970, **8**, 33.
17. Oguro, H., *Nippon Kagaku Kaishi*, 1976, **7**, 1409.
18. Oguro, H., *Nippon Kagaku Kaishi*, 1977, **8**, 225.
19. Oguro, H., *Nippon Kagaku Kaishi*, 1977, **8**, 218.
20. Thompson, K. C., and Wagstaff, K., "Development of a Technique for the Analysis of Certain Toxic Metals in Sewage Sludges," Internal Report No. TP116/ML19, Severn–Trent Water Authority, Malvern.
21. Vogel, A. I., "A Text Book of Macro and Semimicro Qualitative Inorganic Analysis," Longmans, Green, London, 1955.
22. Gorsuch, T. T., "The Destruction of Organic Matter," Pergamon Press, Oxford, 1970.

Received *September 7th*, 1978
Accepted *October 17th*, 1978

Analyst, March, 1979, Vol. 104, pp. 232–240

Determination of Selenium in Soil Digests by Non-dispersive Atomic-Fluorescence Spectrometry Using an Argon - Hydrogen Flame and the Hydride Generation Technique

J. Azad, G. F. Kirkbright and R. D. Snook

Department of Chemistry, Imperial College, London SW7 2BP

The determination of selenium at submicrogram levels by atomic-fluorescence spectrometry, based on the evolution of hydrogen selenide into an argon - hydrogen air-entrained flame, is described. Using a simple purpose-built non-dispersive atomic-fluorescence spectrometer a detection limit of 10 ng cm^{-3} of selenium is obtained. The technique has been applied to the determination of selenium in soil digests and experiments have been carried out in order to study the interference of other elements on the determination. Procedures for the elimination of interferences from copper are recommended.

Keywords: Selenium determination; atomic-fluorescence spectrometry; hydride generation; soil digests

The volume of literature published on the flame spectrometric determination of selenium is small compared with that available for many other elements. The determination of selenium by flame spectrometry presents some problems; for example, the selenium resonance lines lie in the far ultraviolet region of the spectrum below 200 nm and this frequently leads to unfavourable signal to noise ratios resulting from atmospheric and background absorption of these selenium lines. Rann and Hambly,[1] however, obtained a sensitivity (for 1% absorption) of 1.0 $\mu g\ cm^{-3}$ of selenium by atomic-absorption spectrometry (AAS) using the 196.1-nm selenium resonance line and an air - acetylene flame. With the introduction of the argon - hydrogen air-entrained flame[2] the problem of flame absorption was greatly reduced but more severe interference effects were observed in AAS for selenium in this cooler flame. In order to provide higher sensitivity and to overcome some of these interferences chemical separation procedures have been developed that are based on the evolution of hydrogen selenide into the flame.[3–5] The original method for the determination of selenium by AAS in this way employed reduction with metallic zinc, and a collection and storage device was used for the evolved hydrogen selenide prior to its introduction into the flame for AAS.[6] Pollock and West[7] extended the technique to the determination of bismuth, antimony and tellurium by AAS using a magnesium metal - titanium(III) chloride mixture as reductant. Schmidt and Royer[8] reported the determination of selenium, arsenic, bismuth and antimony by AAS using the hydride generation technique in a procedure in which a solution of sodium tetrahydroborate(III) was employed as the reductant; this reagent had previously been shown by other workers[9,10] to provide rapid and efficient reduction. Sodium tetrahydroborate(III) has been employed in this work for the generation of hydrogen selenide prior to the determination of selenium by atomic-fluorescence spectroscopy (AFS) in an argon - hydrogen air-entrained diffusion flame using a simple non-dispersive atomic-fluorescence spectrometer. This paper reports the development of a reliable, simple method for the determination of selenium in aqueous solution by this technique and a study of the chemical interference effects encountered.

The atomic-fluorescence spectrometric determination of selenium was first reported by Dagnall *et al.*[11] using a dispersive spectrometer equipped with an air - propane flame giving a detection limit of 0.25 $\mu g\ cm^{-3}$ of selenium on aspiration of aqueous solutions using a pneumatic nebuliser. Fluorescence from the 204.0-nm selenium resonance line was observed when the flame was irradiated by radiation from a selenium electrodeless discharge lamp, the optical axis of which was aligned at 90° to the optical axis of the monochromator. In this study a similar experimental arrangement has been employed using a non-dispersive

spectrometer with which it was possible to observe fluorescence from the 196.1-, 214.3- and 204.0-nm lines simultaneously, thus enabling a detection limit of 10 ng cm^{-3} to be observed using discrete sample introduction via the hydride generation technique.

Two procedures have been investigated for the suppression or elimination of the well known interference of copper[12,13] on the determination of selenium by the hydride generation technique. In the first procedure the copper and other interfering ions are removed when selenium is coprecipitated with lanthanum from alkaline medium and the precipitate containing selenium is taken for analysis by the procedure developed. In the second procedure the interference from copper is suppressed by utilising the addition of tellurium(IV) to the analyte solution; stable copper telluride is formed and the interference of copper on the hydrogen selenide generation step is suppressed. The chemical pre-treatment and atomic-fluorescence spectrometric procedures developed have been applied to the determination of selenium in soil digests obtained after digestion with a perchloric acid - nitric acid mixture.

Experimental

Apparatus

The instrumentation employed in this work was a purpose-built non-dispersive atomic-fluorescence spectrometer and a simple hydride generation apparatus. A schematic diagram of the equipment employed is shown in Fig. 1 and the details of the components employed are listed in Table I. Radiation from a microwave-excited selenium electrodeless discharge lamp (EDL) was focused on to a rotating sector and then refocused into the argon - hydrogen flame. The atomic-fluorescence radiation stimulated from selenium atoms in the flame was then observed at 90° to the incident radiation by passage through a focusing lens to the solar-blind end-window photomultiplier. The output from the photomultiplier was taken to a lock-in amplifier whose reference signal was provided by the rotating sector in the incident radiation beam from the EDL source. The analytical atomic-fluorescence signals for selenium observed at the output from the lock-in amplifier were displayed at the potentiometric chart recorder.

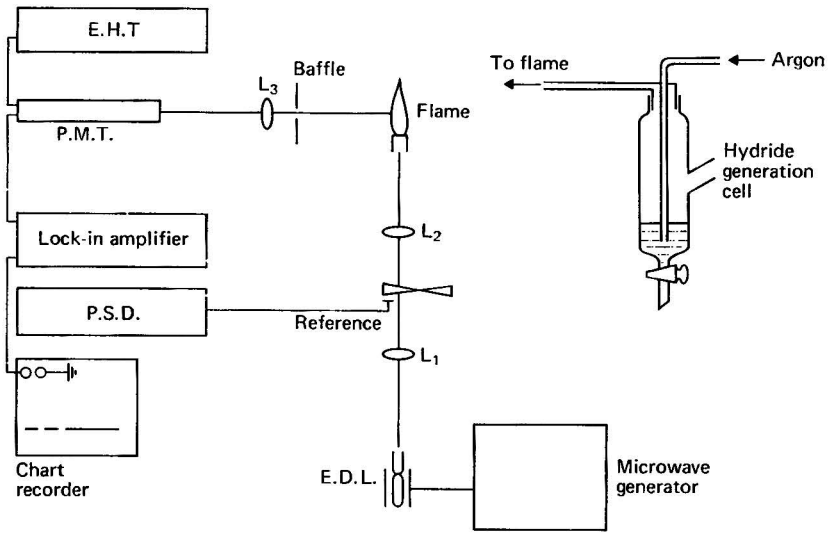

Fig. 1. Schematic diagram of equipment employed.

Reagents

Selenium(IV) standard solutions were prepared by dissolving pure elemental selenium (Specpure grade, Johnson Matthey Ltd.) in a minimum volume of concentrated nitric acid and diluting to volume with 5 M hydrochloric acid. The sodium tetrahydroborate(III)

reagent was used as a freshly prepared 5% (*m*/*V*) solution in 1% sodium hydroxide solution. Analytical-reagent grade lanthanum nitrate, tellurium(IV) oxide, perchloric acid, hydrochloric acid, nitric acid and concentrated ammonia solution were used in all experiments.

TABLE I

INSTRUMENTATION EMPLOYED

Source	Selenium microwave electrodeless discharge lamp operated at 2450 MHz in a ¾-wave resonant cavity. Radiation modulated with an eight-sector mechanical chopper
Chopper..	Programmable Rofin, Model 7500, 3–800 Hz (Rofin Ltd., Egham, Surrey)
Microwave generator	Microtron 200 (EMS Ltd., Wantage, Berkshire)
Photomultiplier	Solar blind, Type R431, Hamamatsu Co., Japan
Lock-in amplifier	Brookdeal Electronics, Type 450S (Brookdeal Ltd., Bracknell, Berkshire)
Phase sensitive detector ..	Brookdeal Electronics, Type 411 (Brookdeal Ltd.)
Optics	Source focused as 1:1 image on the flame using two 7.5-cm focal length fused silica convex lenses (L_1 and L_2). Flame focused as inverted 1:1 image on PMT using 7.5-cm focal length lens (L_3)
Chart recorder	Servoscribe, Model RE 511.20 (Smiths Industries Ltd.)

Procedure

With the flame ignited and argon passing through the hydride generation cell, sufficient time (approximately 20 s) was allowed for the replacement of any air in the apparatus. A 2-cm^3 volume of sodium tetrahydroborate(III) reagent solution was then transferred into the generation cell through the side-arm. Acidified selenium standard solution (or sample solution) (1 cm^3) was then pipetted into the sodium tetrahydroborate(III) solution using a syringe pipette whose tip was fitted with a rubber sleeve to ensure a gas-tight fit with the side-arm of the cell during sample introduction. The hydrogen selenide generated was then swept into the argon - hydrogen flame by the argon supply to the flame. The selenium atomic-fluorescence signal was recorded at the potentiometric chart recorder; the signal duration observed was approximately 8 s for a 5 μg cm^{-3} selenium standard solution. The optimum operating conditions established for the procedure, with the particular instrumental arrangement employed, are summarised in Table II.

TABLE II

OPTIMUM OPERATING CONDITIONS FOR DETERMINATION OF SELENIUM

Microwave power to source	50 W
Reflected power from cavity	12 W
Applied voltage to PMT	600 V
Hydrogen flow-rate	3.3 dm^3 min^{-1}
Argon flow-rate	6.0 dm^3 min^{-1}
Hydride generation cell volume	46 cm^3
Sodium tetrahydroborate(III) reagent volume (5% *m*/*V*) ..	2 cm^3
Selenium sample solution volume	1 cm^3

Determination of Selenium in Soil Digests

One-gram amounts of soil samples were weighed into a series of test-tubes, 3.5 cm^3 of oncentrated nitric acid were added to each sample and the test-tubes were covered and llowed to stand overnight. A few glass boiling beads were added to each tube and then

1.5 cm³ of concentrated perchloric acid (72% *m*/*V*) were added to each. The tubes were then transferred into a cold aluminium digestion block, the temperature of which was increased steadily to 100 °C over a period of 30 min. The block was maintained at this temperature for 30 min and then the temperature was increased to between 190 and 200 °C and maintained at this temperature until digestion of the soil was complete. The final temperature of 200 °C should not be exceeded if charring and the loss of selenium by volatilisation are to be avoided. The test-tubes were then removed from the digestion block and allowed to cool. A 2-cm³ volume of potassium bromide solution (2% *m*/*V*) was added to each and the test-tubes were allowed to stand in boiling water for 15 min to ensure complete reduction of selenium(VI) to selenium(IV). The solutions were then centrifuged and the residues rejected. The supernatant solution was taken for analysis; either the lanthanum nitrate - ammonia or the tellurium(IV) addition procedure was applied in order to eliminate interference from copper. The solutions were then made 5 M with respect to hydrochloric acid and analysed by the hydride generation technique using the atomic-fluorescence spectrometer.

Procedures for Suppression of Interferences

Lanthanum nitrate coprecipitation procedure

Lanthanum nitrate (0.5 cm³ of a 5% *m*/*V* solution) was added to each solution prepared for analysis using the digestion procedure described above, 2 cm³ of ammonia solution were then added and the solutions were mixed. After standing for 1 min the solutions were centrifuged and the liquid discarded. The precipitate was then dissolved in the appropriate amount of 5 M hydrochloric acid.

Tellurium(IV) procedure

Tellurium(IV) oxide (0.3 cm³ of a 0.1 M solution) was added to each solution prepared using the digestion procedure described above and then diluted to 5 cm³ with 5 M hydrochloric acid.

Results and Discussion

Optimisation of Experimental Parameters

Pure aqueous standard selenium(IV) solutions were used in order to optimise the experimental variables in the instrumental system, and to provide the best attainable sensitivity and precision in the determination of selenium by the atomic-fluorescence spectrometric technique, utilising the generation of hydrogen selenide for introduction of the analyte into the argon - hydrogen air-entrained flame. The operating power for the microwave-excited EDL source, argon and hydrogen gas flow-rates to the flame, photomultiplier operating voltage, hydride generation cell volume and sodium tetrahydroborate(III) and selenium sample solution volumes used were each varied independently in order to establish optimum conditions for the determination of selenium. The optimum conditions established in this way are summarised in Table II.

Effect of hydrochloric acid and sodium tetrahydroborate(III) concentrations

The effect on the intensity of the atomic-fluorescence signal, observed for 0.5 μg of selenium introduced into the hydride generation cell in 1 cm³ of solution, of variation in the concentration of hydrochloric acid in the sample solution was investigated. The sodium tetrahydroborate(III) concentration was maintained constant at 5% (*m*/*V*) for this experiment. The results obtained are shown in Fig. 2. Variation in the acid concentration present in the selenium sample solution has a pronounced effect on the efficiency of generation of hydrogen selenide only when the solution is less than 0.8 M with respect to hydrochloric acid; in all further work the hydrochloric acid concentration of solutions to be analysed was maintained at 5 M.

Using 1 cm³ volumes of solution containing 0.5 μg of selenium, which were 1 M with respect to hydrochloric acid, the effect on the selenium atomic-fluorescence signal of variation in the concentration of sodium tetrahydroborate(III) solution in the generation cell

was investigated. The results obtained are shown in Fig. 3; little variation in hydride generation efficiency was observed over the concentration range 2–5% (*m*/*V*) of sodium tetrahydroborate(III). A concentration of 5% sodium tetrahydroborate(III) was chosen for use in all further work.

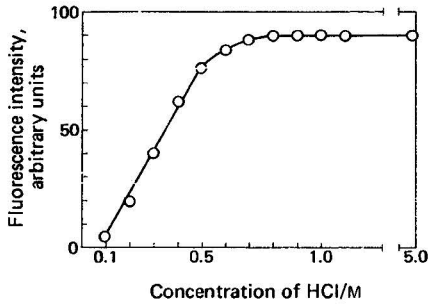

Fig. 2. Effect of hydrochloric acid concentration on the determination of 0.5 μg cm^{-3} of selenium.

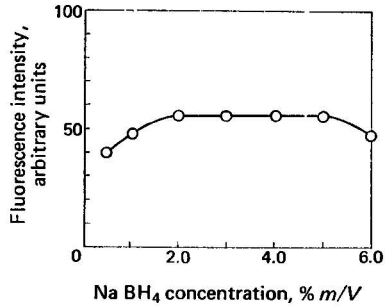

Fig. 3. Effect of sodium tetrahydroborate(III) concentration on the determination of 0.5 μg cm^{-3} of selenium.

Calibration graph, limit of detection and precision

With the optimum instrumental operating conditions and reagent concentrations, analytical calibration graphs for selenium were found to be rectilinear for selenium solutions containing between 10 and 500 ng cm^{-3} of selenium in 1 cm^3 sample volumes, *i.e.*, 10–500 ng of selenium (Fig. 4). The relative standard deviation obtained in the repetitive determination of selenium in a solution containing 100 ng cm^{-3} was 2.5%. The detection limit for selenium, defined as that mass of selenium required to produce a signal to noise ratio of 2 for the atomic-fluorescence signal, was 10 ng of selenium under the conditions employed. A significant background blank signal was observed for selenium, equivalent to approximately 16 ng cm^{-3} of selenium, caused by the presence of selenium as impurity in the sodium tetrahydroborate(III) reagent; this blank was corrected for by subtraction in all quantitative analytical work undertaken.

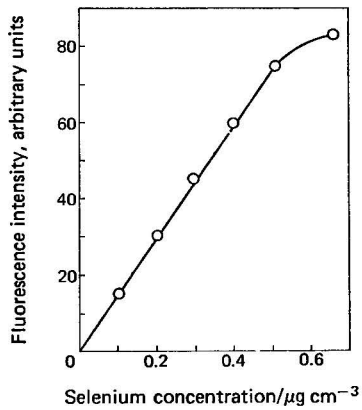

Fig. 4. Aqueous calibration graph for the determination of selenium by non-dispersive atomic-fluorescence spectrometry.

Interference effects and their suppression and elimination

The determination of selenium by atomic-absorption spectrometry utilising the hydride generation technique is well known to be subject to interference from a number of heavy metal ions, and in particular copper(II), which depress the efficiency of the hydrogen selenide generation by sodium tetrahydroborate(III). Similar interferences were expected in the atomic-fluorescence spectrometric procedure developed here and were confirmed in experiments in which the effects of metal ions on the atomic-fluorescence signal produced for 500 ng of selenium were recorded. Table III illustrates typical results of the depressive effects of the presence of some metal ions on the analytical signals observed for 1 μg cm^{-3} selenium solutions. It is clear that the presence of copper(II) as a concomitant element causes serious interference; in the presence of 1000 μg cm^{-3} no atomic-fluorescence signal was obtainable for selenium. As copper(II) concentrations in soil digests were expected to be sufficiently high to interfere with the selenium determination, two procedures were investigated to minimise or eliminate interference from copper.

TABLE III

DEPRESSIVE EFFECT OF METAL IONS ON THE ANALYTICAL SIGNALS OBSERVED FOR 0.5 μg cm^{-3} OF SELENIUM

Concentration of interfering element 1000 μg cm^{-3}.

Element	Depression of signal, %	Element	Depression of signal, %
Na(I)	0	Fe(II)	36
K(I)	2	Fe(III)	20
Mg(II)	0	Pb(II)	40
Mn(II)	0	Zn(II)	21
Ca(II)	2	Co(II)	20
Hg(II)	0	Cu(II)	99
Ba(II)	0	Ag(I)	80
Al(II)	0	Ni(II)	65

The procedure reported by Bedard and Kerbyson,[12] in which the interference of copper on the determination of selenium, by AAS via generation of hydrogen selenide, was eliminated by removal of the selenium from sample solutions by coprecipitation from an alkaline medium with lanthanum, was investigated. This procedure was observed to give good recovery of selenium using a double precipitation; the mean recovery for 10 replicate analyses was 99% with a relative standard deviation of 2.5%. The procedure was found to be most efficient when the lanthanum hydroxide precipitate was filtered off as soon as possible after precipitation. The effect on the recovery of selenium, monitored as the selenium atomic-fluorescence signal intensity, of elapsed time between precipitation and filtration is shown in Fig. 5. The effect of variation in pH of the solution on the selenium recovery by the coprecipitation procedure was found not to be critical provided that the pH was maintained above 9.0.

The second procedure investigated for suppression of the interference from copper utilises the addition of tellurium(IV) to sample solutions immediately before the hydride generation procedure; this procedure has been described elsewhere by Kirkbright and Taddia.[13] In this procedure the interference from copper is suppressed by formation of copper telluride, which is more stable than copper selenide. The addition of excess of tellurium(IV) results in some suppression of the atomic-fluorescence signal observed for selenium; Fig. 6 shows the effect of variation in the tellurium(IV) concentration added to 0.5 μg cm^{-3} selenium sample solutions on the signal recorded. A constant suppression of approximately 30% is attained at tellurium(IV) concentrations between 0.06 and 0.08 M. The presence of 0.06 M tellurium(IV) enables relatively high concentrations of copper to be tolerated in the determination of selenium; Fig. 7 shows the effect of increasing copper concentration on the atomic-fluorescence signal observed from 0.5 μg cm^{-3} selenium sample solutions containing 0.06 M tellurium(IV) solution. Copper does not cause interference at levels up to 50 μg cm^{-3} although at higher concentrations the selenium recovery decreases. Addition of a concentration of tellurium(IV) greater than 0.06 M to sample solutions would permit extension

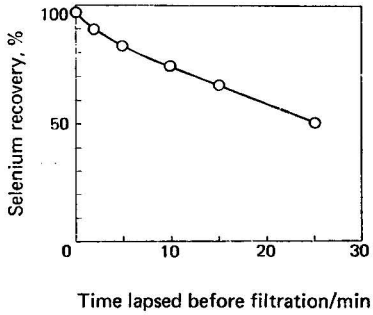

Fig. 5. Effect of time elapsed before filtration on the recovery of selenium observed when using the lanthanum nitrate coprecipitation procedure to remove interferences.

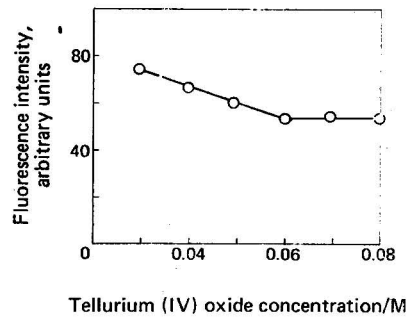

Fig. 6. Effect of tellurium(IV) concentration, added to 0.5 μg cm^{-3} of selenium solutions, on the generation of selenium hydride.

of the tolerance of the procedure to higher concentrations of copper(II). Fig. 8 shows a comparison of the analytical calibration graphs obtained for aqueous selenium solutions in the presence and absence of copper utilising tellurium(IV) to suppress copper interference. These results confirm the restoration of the selenium signal to approximately 70% of its value in the absence of copper when tellurium(IV) is employed to suppress copper interference.

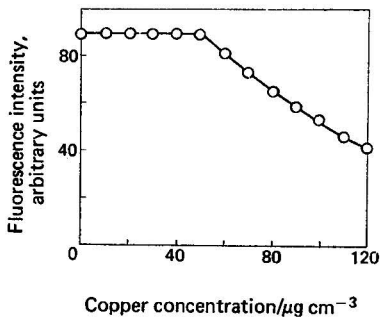

Fig. 7. Effect of copper on the determination of 0.5 μg cm^{-3} of selenium in the presence of 0.06 M tellurium(IV).

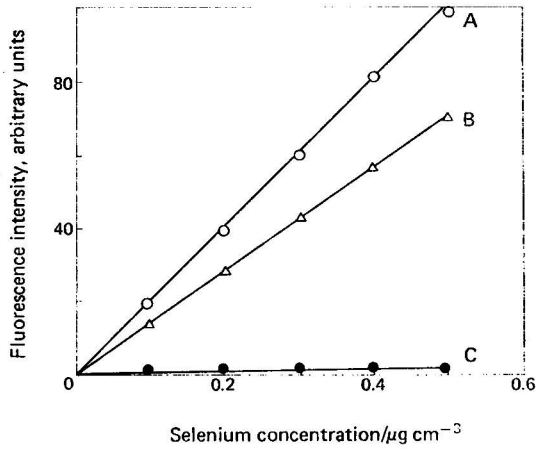

Fig. 8. Comparison of analytical calibrations in the presence and absence of 0.06 M tellurium(IV) oxide. A, Aqueous selenium; B, aqueous selenium + 0.06 M tellurium(IV) + 20 μg cm^{-3} of copper; and C, aqueous selenium + 20 μg cm^{-3} of copper.

Determination of Selenium in Soil Digests

Soil samples were digested using a mixture of perchloric and nitric acid; care was taken not to char the sample during digestion at 200 °C and to avoid loss of selenium by volatilisation. As the hydride generation procedure is only applicable to selenium in its oxidation state of four it was necessary to reduce any selenium(VI) produced in the strongly oxidising digestion mixture by the addition of potassium bromide solution after digestion. Sample digestion recoveries were evaluated by adding to 1-g soil samples a known amount of selenium prior to their digestion. The recovery of the added selenium was then determined. The results of these experiments are shown in Table IV.

TABLE IV

RECOVERY OF SELENIUM ADDED TO SOIL SAMPLE NO. 4

Selenium concentration in sample/$\mu g\ g^{-1}$	Selenium added/ μg	Selenium determined/ μg	Recovery, %
0.7 ± 0.014	0.1	0.83	104
0.7 ± 0.014	0.2	0.87	97
0.7 ± 0.014	0.3	0.94	94
0.7 ± 0.014	0.4	1.18	107

Nine soil samples were digested using the procedure described. Each sample was then analysed by both the lanthanum coprecipitation and the tellurium(IV) methods of interference suppression. The results obtained for the selenium content of the soils analysed are shown in Table V for both methods of interference suppression. As can be seen from the table there is no appreciable quantitative difference between the results obtained by both methods. These results also show extremely good agreement with those obtained by the hydride generation technique and optical-emission spectrometry using an inductively coupled argon plasma source.

TABLE V

COMPARISON OF RESULTS FOR THE SELENIUM CONTENT OF SOIL DIGESTS

	Selenium found						
	Lanthanum nitrate method			Tellurium(IV) method			
Soil sample	Mean, p.p.m.	SD, p.p.m.	RSD, %	Mean, p.p.m.	SD, p.p.m.	RSD, %	ICP* method, p.p.m.
1	0.37	0.017	4.5	0.35	0.009	2.6	0.38
2	0.36	0.016	4.4	0.35	0.012	3.4	0.33
3	0.24	0.010	4.1	0.23	0.015	6.5	0.23
4	0.70	0.014	2.0	0.68	0.015	2.2	0.69
5	18.7	0.64	3.4	18.6	0.49	2.6	19.2
6	111	2.93	2.6	110	2.45	2.2	—
7	0.29	0.014	4.8	0.28	0.012	4.2	0.28
8	0.31	0.020	6.4	0.30	0.015	5.0	—
9	0.30	0.023	7.6	0.29	0.018	6.2	—

* ICP = optical-emission spectrometry using an inductively coupled argon plasma source.

Conclusion

It has been demonstrated that selenium can be determined in soil digests using the technique of non-dispersive atomic-fluorescence spectrometry. The technique is both sensitive and precise. Although the hydride generation procedure is normally subject to severe interference from copper, this effect has been eliminated by employing chemical pre-treatment of the samples, using lanthanum hydroxide as a coprecipitant or the addition of tellurium(IV) to form stable copper telluride during reduction. Both methods have been applied successfully to the determination of selenium in soil digests. It is difficult to recommend which procedure is the most suitable for selenium determinations as each has its own advantages; the lanthanum hydroxide coprecipitation is well established and with care leads to excellent recoveries of selenium even in the presence of high concentrations of copper (approximately 2000 $\mu g\ cm^{-3}$). In order to obtain good recoveries of selenium, however, re-precipitation must be employed. The tellurium(IV) procedure is a simple method but lowers the detection limit by 30% and at the concentrations employed in this study is only effective in removing interferences from copper up to a concentration of 50 $\mu g\ cm^{-3}$ of copper. This limitation may not be a serious disadvantage, however, as copper levels in soil digests should seldom exceed this figure.

References

1. Rann, C. S., and Hambly, A. W., *Analytica Chim. Acta*, 1965, **32**, 346.
2. Kahn, H. L., and Schallis, J. E., *Atom. Absorption Newsl.*, 1968, **7**, 5.
3. Fernandez, F. J., and Manning, D. C., *Atom. Absorption Newsl.*, 1971, **10**, 86.
4. Clinton, O. E., *Analyst*, 1977, **102**, 187.
5. Siemer, D., and Hagemann, L., *Analyt. Lett.*, 1975, **8**, 323.
6. Yamamoto, Y. Y., Kumamaru, Y., Hayashi, Y., and Kanke, M., *Analyt. Lett.*, 1972, **5**, 717.
7. Pollock, E. N., and West, S. J., *Atom. Absorption Newsl.*, 1972, **11**, 104.
8. Schmidt, F. J., and Royer, J. L., *Analyt. Lett.*, 1973, **6**, 17.
9. Pierce, F. D., Lamoreaux, T. C., Brown, H. R., and Fraser, R. S., *Appl. Spectrosc.*, 1976, **30**, 38.
10. Fernandez, F. J., *Atom. Absorption Newsl.*, 1973, **12**, 93.
11. Dagnall, R. M., Thompson, K. C., and West, T. S., *Talanta*, 1967, **14**, 557.
12. Bedard, M., and Kerbyson, J. D., *Can. J. Spectrosc.*, 1975, **21**, 64.
13. Kirkbright, G. F., and Taddia, M., *Atom. Absorption Newsl.*, in the press.

Received *September 7th*, 1978
Accepted *October 17th*, 1978

Analyst, March, 1979, Vol. 104, pp. 241–247

Investigations on Reaction Mechanisms in the Determination of Non-ionic Surfactants in Waters as Potassium Picrate Active Substances

L. Favretto, B. Stancher and F. Tunis

Istituto di Merceologia, Università di Trieste, 34100 Trieste, Italy

The two-phase extraction and spectrophotometric determination of polyoxyethylene non-ionic surfactants in water at trace levels is examined in detail by considering both monodisperse and polydisperse surfactants of the type $RO(CH_2CH_2O)_nH$, where R = *p-tert*-nonylphenyl and n is the degree of polymerisation. Potassium picrate is used as a reagent for the polyoxyethylene chain and 1,2-dichloroethane as an extracting phase.

Monodisperse surfactants with n from 4 to 15 were isolated by liquid - solid absorption chromatography. Their purity was checked by temperature-programmed gas - liquid chromatography. Their reactivity to the reagent is explained qualitatively by considering the equilibria involved in the extraction.

Polydisperse surfactants with $\bar{n}$ (number-average degree of polymerisation) ranging from 3.3 to 21.5 are also considered and compared with other polydisperse surfactants in which R = dodecyl. The concentration of these non-ionics in waters is conveniently expressed as potassium picrate active substances (PPAS). It can be referred to the standard synthetic monodisperse surfactant $RO(CH_2CH_2O)_6H$, where R = dodecyl, which gives a spectrophotometric response acceptably near to that of the examined series of commercial surfactants.

Keywords: *Polyoxyethylene alkylphenyl ether non-ionic surfactant trace determination*; *water analysis*; *spectrophotometry*; *potassium picrate*; *reaction mechanism*

Potassium picrate has recently been suggested as a sensitive reagent for the extraction and spectrophotometric determination of polyoxyethylene non-ionic surfactants in water at trace levels (less than 1 mg kg^{-1}).[1] The method is based on the coordination reaction between the polyether chain and the potassium cation.[2,3] The cation complex is extracted into 1,2-dichloroethane as an ion pair with picrate, which is the anionic chromophore measured in the spectrophotometric determination at 378 nm.[4] Distinct advantages of the picrate anion over the classical tetrathioisocyanatocobaltate(II) at 620 nm are the higher molecular absorbance and the greater stability with time and towards the extraction solvent.[5]

Although the maximum at 321 nm in 1,2-dichloroethane at 20 °C of the tetrathioisocyanatocobaltate(II) ($\log \epsilon = 4.06$) is higher than that at 620 nm ($\log \epsilon = 3.25$), absorbance measurements at 321 nm are less accurate than those at 620 nm, because ethylene thiocyanate is also extracted into the organic phase and it has a broad absorbance maximum at 240 nm, which causes appreciable blanks in the ultraviolet region.

Pre-extraction of non-ionic surfactants from water with 1,2-dichloroethane and purification of the organic extract are essential steps in the trace analysis of actual samples.[1] The polyoxyethylene non-ionic surfactants are then determined on an aqueous solution of the residue of the extract with the potassium picrate reagent. The most common commercial polyoxyethylene non-ionics are polydisperse mixtures having the formula $RO(CH_2CH_2O)_{\bar{n}}H$, where R is an alkyl or alkylaryl group and $\bar{n}$ the number-average degree of polymerisation. Only if R is known and $\bar{n}$ is directly evaluable in some way (for instance, by gas - liquid chromatography, at least up to a certain value of $\bar{n}$), is an absolute determination of the surfactant concentration in the aqueous phase possible. Otherwise the concentration of potassium picrate active substances (PPAS) is conveniently referred to a standard monodisperse surfactant.[1]

In this paper, the determination of monodisperse ($4 \leqslant n \leqslant 15$) and polydisperse ($3.3 \leqslant \bar{n} \leqslant 21.5$) surfactants in which R = *p-tert*-nonylphenyl is discussed, with the aim of determining the reactivity toward potassium picrate and the factors controlling this effect.

Experimental

Apparatus

Unicam SP500 and Perkin-Elmer 402 (with 5× scale expansion) ultraviolet - visible light spectrophotometers were used with matched silica cells of various path lengths for the measurement of the absorbance of the solutions. The pH values of aqueous solutions were determined with a Beckman 4500 digital pH meter using Fisher ACS certified buffer solutions.

Monodisperse surfactants ($4 \leqslant n \leqslant 15$) were isolated by preparative gradient-elution adsorption chromatography with an LKB Ultrorac 7000 fraction collector at 20 °C. By means of a glass column of 2 cm i.d., 50–100 mg of surfactant at 70–80% purity was obtained and this was further purified by repeated chromatography in a 1-cm i.d. column. Silica gel (AR grade, Mallinckrodt, St. Louis, Mo.), 30–50 μm, activated at 190 °C, was used as an adsorbent, packed to a length of 15 cm in the first column and 30 cm in the second. Elution was carried out with mixtures of propan-2-one in dichloromethane of composition given by the expressions $P = 0.083V$ (first column) and $P = 0.040V$ (second column), where P is the concentration of propan-2-one (% V/V at 20 °C before mixing) and V ml is the volume of the eluting agent at the top of the column. The composition of 5-ml fractions was systematically checked by gas - liquid chromatography after evaporation of solvent under nitrogen.

A Pye Unicam 104 double-column chromatograph with flame-ionisation detectors was used. Pyrex glass columns (35 cm × 1.7 mm i.d.) were packed with 80–100-mesh Gas-Chrom Q coated with 3% *m/m* OV-1 (Applied Science Laboratories, State College, Pa.). At temperatures above 300 °C, this phase gives a better performance than GE SE-30, which is extensively used for high-temperature gas - liquid chromatographic analyses.[6] Fractionation was carried out with a linear temperature programme of 10 °C min^{-1} from 100 to 370 °C and with injector and detector temperatures of 400 °C. Flow-rates of the gases were nitrogen 45, hydrogen 45 and air 400 ml min^{-1}. Peak areas were determined by means of a Hewlett-Packard 3380A integrator.

Reagents

1,2-Dichloroethane. E. Merck, extra-pure grade, freshly distilled.

Potassium nitrate solution, 2.50 M. In a 100-ml calibrated flask, dissolve 25.28 g of potassium nitrate (AnalaR grade) in water and dilute to the mark with water.

Potassium picrate solution, 0.020 M. Dissolve 0.534 g of potassium picrate [re-crystallised from an aqueous solution and dried with phosphorus(V) oxide] in water in a 100-ml calibrated flask.

Monodisperse surfactants

Monodisperse surfactants with $4 \leqslant n \leqslant 15$ were separated from commercial polydisperse materials having a number-average degree of polymerisation of $\bar{n} = 5.4$, 6.5, 7.5 and 8.6.

The gas - liquid chromatographic purities of the surfactants are shown in Table I. Aqueous stock solutions containing 1–20 mg l^{-1} (depending on solubility of surfactants) were prepared weekly by weighing the compounds [dried with phosphorus(V) oxide] on a Mettler M5 microbalance. The 1 mg l^{-1} solution was prepared daily and was used immediately.

Polydisperse surfactants

Stock solutions of polydisperse surfactants were prepared by following the above procedure from commercial products (Chemische Werke Hüls) with $\bar{n} = 3.3$, 5.4, 6.5, 7.5, 8.6, 9.7, 10.8, 12.9, 15.0 and 21.5. All of the surfactants were previously dried at 80 °C under vacuum (1 mmHg) for 4 h. The value of $\bar{n}$ was checked by vapour-pressure osmometry at 37 °C in 1,2-dichloroethane with a Hewlett-Packard Mechrolab vapour pressure osmometer.

Procedures

Spectrophotometric calibration graphs

Calibration graphs were obtained at 20 °C by means of the following procedure. In a 50-ml calibrated flask 20.00 ml of potassium nitrate solution were added to an aliquot of the standard solution of surfactant. The aliquots were chosen in order to have 0.10–1.00 mg l^{-1}

TABLE I

GAS - LIQUID CHROMATOGRAPHIC PURITY OF THE MONODISPERSE SURFACTANTS $RO(CH_2CH_2O)_nH$ (R = *p-tert*-NONYLPHENYL)

The purity of the surfactants was calculated from measurements of the peak areas.

n	Purity, %	Amounts of surfactants* present as impurities, %
4	98.05	1.35 (3), 0.60 (5)
5	98.75	1.05 (4), 0.20 (6)
6	99.82	0.18 (5)
7	97.50	0.98 (6), 1.52 (8)
8	98.99	0.77 (7), 0.24 (9)
9	98.24	0.91 (8), 0.85 (10)
10	96.32	2.81 (9), 0.87 (11)
11	98.38	1.62 (10)
12	97.0	2.8 (11), 0.2 (13)
13	98.6	0.5 (11), 0.9 (12)
14	97.8	1.6 (13), 0.6 (15)
15	98.5	0.3 (13), 0.4 (14), 0.8 (16)

* *n* values of impurities are given in parentheses.

of surfactant in the final 50-ml volume of aqueous phase. After mixing and allowing to stand for 1 h, 5.00 ml of the potassium picrate solution were added and the volume was made up to the mark with water. The mixed solution (pH approximately 7) was allowed to stand for 15 min and then transferred into a separating funnel with a PTFE stop-cock. A 5.00-ml volume of 1,2-dichloroethane was added and the mixture was shaken for 5 min. The organic layer was transferred dropwise into a conical centrifuge tube fitted with a polyethylene stop-cock and centrifuged at 1000 *g* for 5 min. The absorbance (A) of the clear organic extract was measured at 378 nm in a 1-cm (or 2-cm) cell against the reagent blank.

Calibration graphs were also obtained at pH values from 7 to 11 by the addition of a few microlitres of 6 M potassium hydroxide solution to the potassium nitrate solution.

Data processing

Statistical analysis of the regression was performed on an Olivetti P 6040 desk calculator. Linearity was tested by the analysis of variance for the regression, using R^2 and F ratios as criteria of adequacy,[7] where R^2 is the ratio between the sum of squares attributable to regression and the total sum of squares and F is the ratio between the variance attributable to regression and the variance attributable to the deviation from the regression.

Results and Discussion

Monodisperse Surfactants

When the absorbance (A) of the 5 ml of organic extract is plotted against the surfactant concentration (c') existing in 50 ml of aqueous phase before the extraction, straight lines passing through the origin are obtained ($A = abc'$), at least in the c' range 1–0.1 mg l^{-1}. Table II indicates the values of the slope (a) of the calibration lines obtained at 20 °C. The slope represents the absorbance [cell length (b) = 1 cm] of the 5.00 ml of extract from 50.0 ml of aqueous phase containing 1.00 mg l^{-1} of monodisperse surfactant. At least in the range $5 \leqslant n \leqslant 15$ (the surfactant with $n = 4$ does not respond appreciably to the picrate reagent under the proposed experimental conditions), the linearity of the calibration lines is demonstrated by the analysis of variance for the linear regression. The value of R^2 is higher than 0.999 and that of F is higher than 6000 except for the surfactants with $n = 5$ ($R^2 = 0.9637$, $F = 160$) and $n = 6$ ($R^2 = 0.9970$, $F = 2171$). However, the latter surfactants have too low a response to the reagent to allow statistical calculations to be performed comparable to those on results obtained with the others.

If the polyether surfactant is determined at trace-level concentration, the linearity of the relationship between the absorbance of the organic extract and the concentration in the aqueous phase can be derived simply from the equilibrium expressions. For instance, the basic equilibria involved in the extraction of a monodisperse surfactant ligand (L) reacting

TABLE II

SLOPES OF THE CALIBRATION STRAIGHT LINES FOR MONODISPERSE AND POLYDISPERSE POLYOXYETHYLENE *p-tert*-NONYLPHENYL ETHER SURFACTANTS

a is the slope ($a = A/bc'$) obtained by linear regression from a monodisperse surfactant with degree of polymerisation n; $\bar{a}$ is the slope ($\bar{a} = \bar{A}/bc'$) obtained from a polydispersed surfactant with number-average degree of polymerisation $\bar{n}$; R^2 is the ratio between the sum of squares attributable to regression and the total sum of squares; F is the ratio between the variance attributable to regression and the variance attributable to the deviation from the regression. In all instances eight observations were processed by regression.

Monodisperse surfactants				Polydisperse surfactants			
n	a	R^2	F	$\bar{n}$	$\bar{a}$	R^2	F
5	0.030	0.9637	160	3.3	0.036	0.9870	475
6	0.081	0.9970	2171	5.4	0.121	0.9974	2402
7	0.224	0.9994	9808	6.5	0.191	0.9985	4078
8	0.287	0.9991	6590	7.5	0.211	0.9988	5187
9	0.293	0.9994	11698	8.6	0.228	0.9992	7096
10	0.289	0.9997	22030	9.7	0.236	0.9988	5129
11	0.280	0.9997	19807	10.8	0.240	0.9986	4168
12	0.264	0.9991	6647	12.9	0.243	0.9992	8074
13	0.251	0.9993	8636	15.0	0.244	0.9993	8813
14	0.248	0.9993	9241	21.5	0.245	0.9987	4521
15	0.247	0.9996	17357				

1 + 1 with picrate (A^-) are the following (a ratio of organic to aqueous phase of 1:1 is assumed for sake of simplicity):

$$\begin{array}{ccccc} \text{Aqueous phase} & L + K^+ \overset{K_{KL^+}}{\rightleftharpoons} KL^+ & KL^+ + A^- \overset{K_{KLA}}{\rightleftharpoons} KLA & (\text{pH } 7\text{–}11) \\ \text{———} \; \beta_L \Updownarrow & \text{———————} & \Updownarrow \beta_{KLA} \; \text{———} \\ \text{Organic phase} & L & KLA \end{array}$$

Assuming that the extraction is performed at a constant alkaline pH, the A^- is also constant and the side AH - A equilibrium can be neglected. It is also assumed that the ionisation of KLA in the organic phase is negligible.

In the aqueous phase activity coefficients are unity for non-ionic compounds at trace concentrations. Therefore, the distribution of the surfactant between the organic (org) and aqueous (aq) phases is $\beta_L = [L]_{org}/[L]_{aq}$ and that of the chromophore compound is $\beta_{KLA} = [KLA]_{org}/[KLA]_{aq}$, where equilibrium concentrations (mol l^{-1}) are indicated in brackets for every species considered ($[KLA]_{org}$ is proportional to the absorbance).

As the ionic strength is constant ($\mu \approx 1$), the activity coefficients of non-ionic species are also constant. Therefore, $K_{KLA} = f[KLA]_{aq}/([KL^+]_{aq}[A^-]_{aq})$, where $f = 1/(f_{KL} + f_{A^-})$ is a constant and $K_{KL^+} = f'[KL^+]_{aq}/([K^+]_{aq}[L]_{aq})$, where $f' = f_{KL^+}/f_{K^+}$ is also a constant.

If the above expressions are introduced into the mass-balance equation of the surfactant ($c_L = [L]_{org} + [L]_{aq} + [KL^+]_{aq} + [KLA]_{aq} + [KLA]_{org}$, where c_L is total surfactant concentration in the aqueous phase), the following expression is obtained by resolving for $[KLA]_{org}$:

$$[KLA]_{org} = c_L \Big/ \left\{ 1 + \frac{ff'(\beta_L + 1)}{K_{KL} + K_{KLA}\beta_{KLA}[K^+]_{aq}[A^-]_{aq}} + \frac{f}{K_{KLA}\beta_{KLA}[A^-]_{aq}} + \frac{1}{\beta_{KLA}} \right\}$$

At trace levels of surfactant and with an excess of potassium picrate, $[K^+]_{aq} \approx c_{K^+}$ (total concentration of the co-ordinating cation in the aqueous phase) and $[A^-]_{aq} \approx c_{A^-}$ (total concentration of picrate in the aqueous phase at pH $\geqslant$ 7). As c_{K^+} and c_{A^-} are constant, the above expression is reduced to an equation that represents a straight-line graph passing through the origin and with a constant slope.

Linearity of the calibration graph is always observed in the determination of both monodisperse and polydisperse polyoxyethylene compounds at trace levels with various extraction reagents, for instance, sodium picrate[5] and ammonium tetrathioisocyanatocobaltate(II).[8]

With the monodisperse surfactant considered in this work, a single extraction was adopted, as a negligible absorbance ($A < 0.003$) occurred in the organic phase when an aliquot of the

centrifuged aqueous phase was further extracted with 1,2-dichloroethane in the same 1:10 organic to aqueous phase ratio.

The variation of a as a function of n is shown in Fig. 1. Starting with the surfactant with $n = 5$, the slope a increases with n up to a maximum at $n = 9$, then decreases to a constant limiting value ($a = 0.247$), which is also observed in a binary mixture consisting of $n = 16$ (60%) and $n = 17$ (40%) (the composition of the mixture is approximate, as the gas-chromatographic analysis is beyond the limit of complete resolution of the peaks).

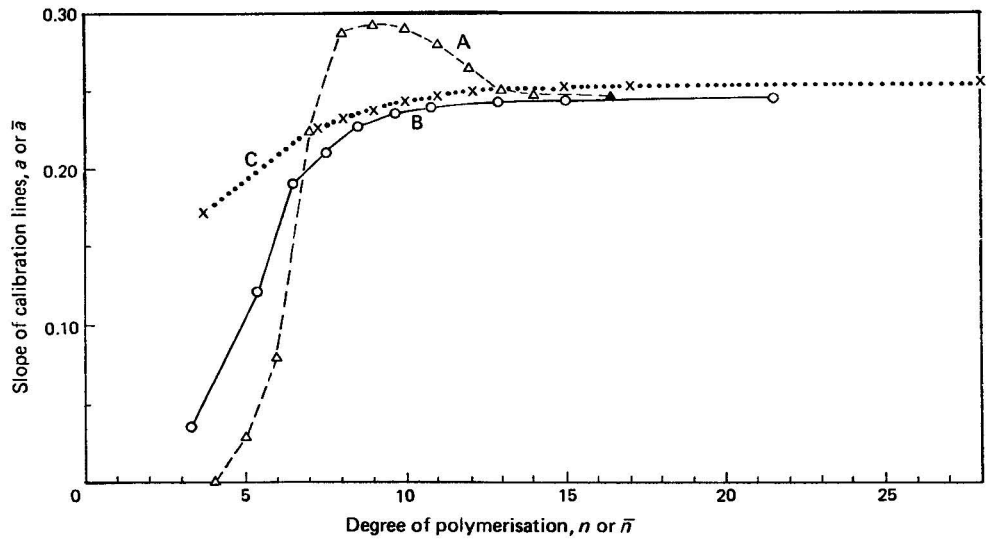

Fig. 1. Graphs of the slopes of the calibration straight lines *versus* degree of polymerisation of the surfactant. A, Slope (a) of the calibration straight lines *versus* the degree of polymerisation (n) for monodisperse surfactants $RO(CH_2CH_2O)_nH$ where R=*p-tert*-nonylphenyl; ▲ indicates the mixture $n = 16 + 17$. B, Slope ($\bar{a}$) of the calibration straight lines *versus* the number-average degree of polymerisation ($\bar{n}$) for the polydisperse surfactants $RO(CH_2CH_2O)_nH$, where R=*p-tert*-nonylphenyl. C, Slope ($\bar{a}$) of the calibration straight lines *versus* the number-degree of polymerisation ($\bar{n}$) for the polydisperse surfactants $RO(CH_2CH_2O)_nH$, where R=dodecyl.

At least in the range of n considered, the variation of a as a function of n can be explained qualitatively by considering the equilibria existing in the two-phase extraction of the poly-oxyethylene non-ionic surfactant with potassium picrate. The analytical expression for $[KLA]_{org}$ shows that the increasing reactivity with n up to 9 is dominated by (*i*) the distribution equilibrium of the surfactant between the phases and (*ii*) the co-ordinating equilibrium of the surfactant with the potassium cation. Hydrophobic polyethers with $n<5$ are almost completely extracted into the organic phase ($\beta_L>20$ at 25 °C)[6] and in aqueous solution they do not co-ordinate appreciably with potassium. Although the surfactant with $n = 5$ has $\beta_L>20$, it shows an appreciable reactivity, as the ligand has at least five polyether oxygen atoms for the co-ordination. The same limiting value is also observed with ammonium as the co-ordinating cation.[9] The co-ordination equilibrium reasonably assumes a 1 + 1 reaction between the polyether ligand and the potassium cation (the possible side equilibrium $2L + K^+ \rightleftharpoons KL_2^+$ is not considered, because the molar ratio $L/K^+ \approx 1/1000$ is unfavourable to the formation of KL_2^+). There are no direct equilibrium data available on this ligand in an aqueous phase. However, a 1 + 1 stoicheiometry was observed for $L = CH_3O(CH_2CH_2O)_5CH_3$ reacting with K^+ in methanol; in this solvent the value of the concentration stability constant ($K' = [KL^+]_{aq}/[K^+]_{aq}[L]_{aq}$ at 25 °C) is 158 l mol^{-1} but in water a lower value is expected. A 1 + 1 reversible reaction was also found potentiometrically for the monodisperse polyether $RO(CH_2CH_2O)_nR$ (R = phenyl, $6 \leqslant n \leqslant 10$) reacting in methanol[2] with Na^+, K^+ and Rb^+; with these cations, log K' increases almost linearly with n.[3] This fact suggests that in polyoxyethylene *p-tert*-nonylphenyl ethers from $n = 6$ to 9 the increment in the sensitivity mainly reflects the increase in K_{KL^+}.

The maximum at $n = 9$ is probably related to a maximum in the stability of KL^+, which probably corresponds to the complete wrapping of the K^+ by the polyether chain.

In order to evaluate the amount of surfactant extracted from an aqueous into an organic phase by means of potassium picrate, the molar absorbance coefficient at 378 nm of the picrate in 1,2-dichloroethane was first determined, using re-crystallised dodecyltrimethylammonium picrate as a standard. In the 300–700-nm region, this ion-pair compound has the same absorbance spectrum as that of the KLA compound, and it is assumed that its picrate chromophore has the same molar absorbance coefficient as that of the KLA ion pair. By use of this coefficient the theoretical absorbance at 378 nm ($b = 1$ cm) that 1.00 mg l^{-1} of surfactant in aqueous phase would give if the surfactant was totally extracted into the organic phase was calculated. The further assumption was made that surfactant and picrate were in a 1 + 1 stoicheiometric ratio in the extracted compound. The comparison with the observed adsorbance gives the proportion of surfactant extracted.

The results are shown in Fig. 2 as a function of n. For $n = 5$ the extraction efficiency is poor (7.3%), but it increases up to $n = 9$, when it reaches 100%. In the range $10 \leqslant n \leqslant 13$ the efficiency gradually increases to a constant value of 110%, but for longer chain monodisperse surfactants ($n = 14$ and 15) the rise is gradual; this effect is also confirmed by the behaviour of the binary mixture $n = 16 + 17$ (extraction efficiency = 128%). This behaviour showing more than 100% recovery can be explained only by assuming the formation of the K_2L^{2+} bivalent cation with the surfactants with $n > 9$.

The progressive formation of a polycation with the increase in the length of the polyoxyethylene chain seems to be reasonable. In the structure of KL^+ the potassium cation is progressively wrapped by the polyether chain with the oxygen atoms stretched inwards and the ethylene groups outwards. At $n = 9$ just one K^+ is co-ordinated by the polyether, whereas at higher values of n a second K^+ begins to be progressively co-ordinated. There is no direct information regarding the n value at which the bication K_2L^{2+} reaches maximum stability. Assuming that the limiting slope value ($a = 0.247$) is constant, an extraction efficiency of 200% would be reached at about $n = 27$. As the minimum chain length for complete wrapping of the first K^+ is only 9 polyoxyethylene groups, about 18 would be required to wrap the second K^+. Eighteen oxyethylene groups may be the number required for co-ordinating every other K^+ after the first in the K_mL^{m+} polycation.

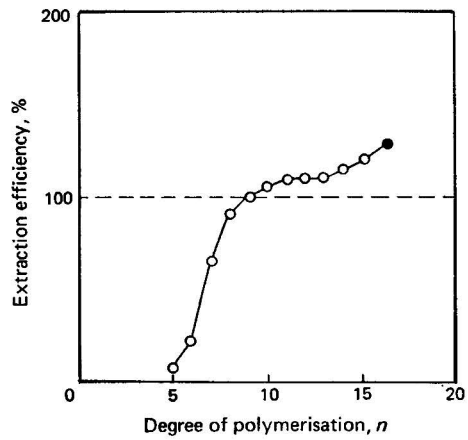

Fig. 2. Graph of extraction efficiency *versus* degree of polymerisation (n) for the monodisperse surfactants $RO(CH_2CH_2O)_nH$, where R=*p-tert*-nonylphenyl. ● Indicates the mixture $n = 16 + 17$.

Polydisperse Surfactants

Table II indicates the $\bar{a}$ values observed for these surfactants. The calibration graphs are ays straight lines through the origin with $F > 2000$, except for $\bar{n} = 3.3$ ($F = 475$); in

this surfactant the absorbance response is so low that the experimental error makes a significant contribution to the variance attributable to the deviation from the regression, thus lowering the F value. In Fig. 1 the slope of the calibration lines is shown as a function of $\bar{n}$. Increasing the pH of the aqueous phase from 7 to 11 does not change either the zero intercept or the slope of the calibration graphs.

In comparison with the behaviour of the monodisperse surfactants, the trend of $\bar{a}$ *versus* $\bar{n}$ is slightly different. At low values of $\bar{n}$, the response of the polydisperse surfactants is higher than that of corresponding monodisperse materials, but with increasing $\bar{n}$ this feature inverts and no maximum is observed. The limiting value for $13 \leqslant \bar{n} \leqslant 22.5$ appears to approach that observed with the monodisperse surfactants.

The slope of the calibration lines observed in the polyoxyethylene dodecyl ether non-ionic surfactants under the same experimental conditions[1] is also shown in Fig. 1 as a function of $\bar{n}$. The trend is similar to that found in the polyoxyethylene *p-tert*-nonylphenyl ethers and the limiting value is nearly the same for surfactants. An absolute determination of these commercial surfactants is thus possible for $\bar{n} \geqslant 8$, using a mean slope as a calibration graph. However, as the evaluation of $\bar{n}$ is possible only in special instances, and no information can be obtained on the R group at trace levels, it is convenient to express the concentration of non-ionics as "potassium picrate active substances" (PPAS).[1] It has been proposed to refer the concentration of PPAS to the standard monodisperse surfactant hexaoxyethylene dodecyl ether. The slope ($a = 0.268$) of this compound is acceptably near to those observed in both surfactant series at $\bar{n} > 10$.

The slope for a dodecyl ether is always higher than that for the corresponding *p-tert*-nonylphenyl ether, but this effect becomes more pronounced at $\bar{n} < 9$. At least two facts can possibly contribute to explain this difference. If two monodisperse potassium picrate reactive surfactants $RO(CH_2CH_2O)_nH$ with same n are compared it will be found that over the range $5 \leqslant n \leqslant 9$ the β_L constant with R = dodecyl is systematically lower than that with R = *p-tert*-nonylphenyl, that is the former is slightly more hydrophilic (more reactive) than the latter. Moreover, the K_{KL^+} constant with R = dodecyl is systematically higher than that with R = *p-tert*-nonylphenyl, as a consequence of the possible steric hindrance of the *p-tert*-nonylphenyl group to the co-ordination of K^+ by means of the phenoxy oxygen atom. When R = dodecyl, the ether oxygen atom bridging this group can also participate in the co-ordination, and therefore the surfactant probably reacts as an $n + 1$ polyoxyethylene compound. Further studies are still in progress on monodisperse *n*-alkyl ethers in order to confirm these speculations.

References

1. Favretto, L., Stancher, B., and Tunis, F., *Analyst*, 1978, **103**, 955.
2. Calzolari, C., Favretto, L., Pertoldi Marletta, G., and Favretto Gabrielli, L., *Annali Chim.*, 1974, **64**, 463.
3. Favretto, L., *Annali Chim.*, 1976, **66**, 621.
4. Calzolari, C., Favretto, L., and Tunis, F., *Analyst*, 1974, **99**, 171.
5. Favretto, L., and Tunis, F., *Analyst*, 1976, **101**, 198.
6. Stancher, B., Tunis, F., and Favretto, L., *J. Chromat.*, 1977, **131**, 309.
7. Draper, N. R., and Smith, H., "Applied Regression Analysis," John Wiley, New York, 1966, pp. 7–26.
8. Favretto, L., and Bruni, G., "Proceedings of the 6th Congress on Quality," Genoa, 11–13 September 1967, pp. 259–274.
9. Crabb, N. T., and Persinger, H. F., *J. Am. Oil Chem. Soc.*, 1968, **45**, 611.
10. Frensdorff, H. K., *J. Am. Chem. Soc.*, 1971, **93**, 600.

Received *September 11th*, 1978
Accepted *September 20th*, 1978

Limit of Detection in Analysis with Ion-selective Electrodes

Derek Midgley

Central Electricity Research Laboratories, Kelvin Avenue, Leatherhead, Surrey KT22 7SE

The limit of detection in analysis with ion-selective electrodes is discussed and definitions that are based only on the deviation of an electrode's calibration from the theoretical, and take no account of the random errors of measurement, are shown to be inadequate. Equations are derived that express the limit of detection in terms of the random error of measurement and the factors determining the deviation of the electrode response from the Nernstian value, *i.e.*, reagent blanks, solubility products and interferences. The equations enable one to predict (*a*) the degree of precision with which the e.m.f. has to be measured if an electrode is to attain a desired limit of detection in specified conditions or (*b*) whether changing the conditions might bring the desired limit of detection within reach of a given precision of measurement. Practical examples with ion-selective electrodes justify the proposed statistical treatment of limit of detection and demonstrate that the errors for electrodes operating in the non-Nernstian region are normally distributed.

Keywords: *Ion-selective electrodes*; *potentiometry*; *limit of detection*

The limit of detection of an ion-selective electrode has been defined in terms of the extent of the deviation of its calibration from the theoretical Nernstian response, but in such definitions[1,2] the critical deviation has been assigned in an arbitrary way.

In the IUPAC definition,[1] the limit of detection is taken as the concentration at the point of intersection of the extrapolated linear segments of a graph of e.m.f. against the logarithm of the concentration. In an earlier recommendation,[2] the limit of detection was the concentration at which the calibration deviated by $k\log 2/z$ mV from the extrapolated Nernstian response (k being the Nernst slope factor for a univalent electrode and z being the ionic charge). Although such definitions may be useful as rule-of-thumb characteristics of electrode performance, they are not rigorously related to analytical performance, in contrast to the statistically based definitions of limit of detection that have been applied to other techniques of chemical analysis.[3] The limit of detection should not be arbitrarily determined from the calibration graph without consideration of the random errors associated with the measurement but should be decided on a statistical basis that allows a solution containing a given concentration of determinand to be discriminated, with a specified degree of confidence, from a blank solution. A rigorous definition is needed for ion-selective electrode methods, not only for consistency with other methods of analysis, but on the practical grounds that ion-selective electrodes are routinely used to determine chloride[4–6] at levels below the IUPAC limit of detection for the electrode concerned and have been demonstrated to be of use for determining other species at comparable levels.[7]

This paper shows that when a statistical approach is adopted the limit of detection can be expressed as a function of the factors determining the deviation of the electrode response from the Nernstian value, *i.e.*, reagent blanks, solubility products and interferences. Such equations enable one to predict (*a*) the degree of precision with which the e.m.f. has to be measured if an electrode is to attain a desired limit of detection in specified conditions or (*b*) whether changing the conditions might bring the desired limit of detection within reach of the precision of measurement, *e.g.*, by working at a low temperature in order to reduce a solubility product.

Theory

The approach adopted is that of Roos,[8] combined with the conventional choice of 5% probability. The criterion of detection is then defined as the level of determinand corresponding to the analytical result that will not be exceeded on more than one occasion in

20 unless determinand is present in the sample, *i.e.*, there is a 5% chance of claiming that a determinand has been detected when none is present. The limit of detection is defined as the concentration for which there is a 5% probability that the analytical result will be less than the criterion of detection, *i.e.*, at which there is a 5% chance of failing to detect the determinand.

The criterion of detection, Q, for 95% confidence is

$$Q = 1.645\,\sigma_Q \quad .. \quad .. \quad .. \quad .. \quad .. \quad (1)$$

where σ_Q is the within-batch standard deviation of the result, *i.e.*, the difference between the sample reading, A, and the blank reading, B. Thus,

$$\sigma_Q = \sigma(A - B) = \sqrt{\sigma_A^2 + \sigma_B^2}$$

When Q is estimated empirically, we do not know beforehand the value of A at which measurements should be made. It is convenient, therefore, to make the assumption

$$\sigma_A \approx \sigma_B \quad .. \quad .. \quad .. \quad .. \quad .. \quad (2)$$

and so to write $\sigma_Q = \sqrt{2}\sigma_B$ and

$$Q = 2.33\sigma_B \quad .. \quad .. \quad .. \quad .. \quad .. \quad (3)$$

Once Q has been estimated from equation (3), a first estimate of A is obtained and the validity of the assumed equality (2) tested with standard deviations for results in the vicinity of A.

By a similar process and assuming the approximate equality (2) is still valid, it can be shown that the limit of detection, L, for 95% confidence is

$$L = 1.645\sigma_L = 4.65\sigma_B$$

If the concentration is linearly related to the experimentally observed quantity, as in titrimetric or photometric methods, L and σ_L can be expressed equally well in either concentration units or experimental units. When this linear relationship does not hold, as in potentiometry, L and σ_L should be expressed in the units in which the errors have a normal distribution. It is shown below that in the instances where data are available the distribution can be assumed to be normal irrespective of the units chosen, but for the following reasons it is better to use e.m.f. units in the absence of experimental proof of the nature of the distribution.

1. The blank reading cannot be plotted as a point on a graph of e.m.f. against the logarithm of the concentration, which is the usual representation of the calibration of an ion-selective electrode, and hence the standard deviation in concentration terms cannot be obtained from such a graph. By using the standard deviation in e.m.f. units and drawing the lines corresponding to $2.33\,\sigma_B$ and $4.65\,\sigma_B$ on the calibration graph (as in Fig. 1), the criterion and limit of detection can be obtained in concentration terms. Although it is possible to plot the blank reading as a point in other forms of calibration graph[4,5,9] and so to use the standard deviations in concentration units, standard deviations in e.m.f. have the advantage of being applicable in all instances.

2. On the basis of the small amount of data available for ion-selective electrodes operating near their limits of detection, the assumed equality (2) is more readily satisfied by taking standard deviations in e.m.f. units. Applying the F-test to the within-batch standard deviations in Table I shows that at the $P = 0.05$ level the hypothesis that the variances are equal throughout the range covered would be rejected only for the sodium electrode for measurements in e.m.f. units and for the sodium, fluoride and silver - silver chloride electrodes for measurements in concentration units.

3. The use of standard deviations in e.m.f. units is consistent with practice at concentrations in the Nernstian response range, *e.g.*, in testing the significance of recovery tests,[14] where the standard deviations in concentration units increase so much with concentration (even

TABLE I

WITHIN-BATCH STANDARD DEVIATIONS (s.d.) FOR ION-SELECTIVE ELECTRODES OPERATING IN THE NON-NERNSTIAN RANGE

						Degrees of freedom	Determinand	Electrode material	Reference
Concentration/μg l^{-1}	20	5	1	0	5	Cl^-	Hg_2Cl_2 - HgS	9
S.d./μg l^{-1}	0.35	0.37	0.52	0.75				
S.d./mV	0.19	0.20	0.29	0.41				
Concentration/mg l^{-1}	10	3.38	0.74	0.1	5	Cl^-	Ag - AgCl	4
S.d./mg l^{-1}	0.23	0.10	0.02	0.01				
S.d./mV	0.48	0.67	0.38	0.45				
Concentration/μg l^{-1}		25	2.5	0.25	11*	Na^+	Glass	10
S.d./μg l^{-1}		1.5	0.6	0.5				
S.d./mV		1.5	2.7	3.0				
Concentration/μg l^{-1}		20	10	0	4	NH_4^+	Glass	11
S.d./μg l^{-1}		2.6	1.2	1.4				
S.d./mV		1.73	1.00	1.65				
Concentration/mg l^{-1}		1.0	0.1	0.05	9	F^-	LaF_3	12
S.d./mg l^{-1}		0.057	0.011	0.008				
S.d./mV		1.23	2.35	2.18				
Concentration/μg l^{-1}		45.5	18.2		3/5	S^{2-}	Ag_2S	13
S.d./μg l^{-1}		3.2	1.8					
S.d./mV		0.9	1.8					

* These results include between-batch variation.

though the relative standard deviations decrease) that combination or comparison of errors expressed in concentration units would be misleading.

When e.m.f. units are adopted, the criterion of detection, Q, is the positive value of the difference between e.m.f. E_B, given by the blank solution, and e.m.f. E_Q, given by a sample containing such a concentration of determinand, C_Q, that

$$E_Q = E_B + iQ$$

where $i = +1$ for a cation-selective electrode and -1 for an anion-selective electrode.

The limit of detection, L, is defined in an analogous way. Thus,

$$E_L = E_B + iL$$

at a concentration of determinand C_L.

Normal Distribution of Error in E.m.f. Measurements

Within-batch errors of e.m.f. measurements made with various electrodes near their limits of detection have been analysed by means of the Lilliefors test for normality[15,16] (using the corrected table given by Conover[17]). The electrodes used and the conditions of measurement are given in Table II. The only instances in which the hypothesis that the distribution was normal was rejected at the 5% level were for the sodium-responsive glass electrode at 25 μg l^{-1} and the mercury(I) chloride - mercury(II) sulphide chloride-selective electrode at 10 μg l^{-1} and 25 °C. In no instance did acceptance or rejection depend on whether the errors were expressed in the original e.m.f. units or the derived concentration units. The use of parametric statistics in the calculations below is, therefore, justified, as are the definitions of limit and criterion of detection in e.m.f. terms.

TABLE II

ION-SELECTIVE ELECTRODES TESTED FOR DISTRIBUTION OF ERRORS IN THE NON-NERNSTIAN RESPONSE RANGE

Determinand	Electrode material	Concentrations tested/ μg l^{-1}	No. of results	Conditions	Reference
Cl^-	Hg_2Cl_2 - HgS	50	10	25 °C, 0.01 mol l^{-1} HNO_3	18
Cl^-	Hg_2Cl_2 - HgS	1, 2, 5, 10	10	25 and 4 °C, 0.01 mol l^{-1} HNO_3, flow cell	9
Cl^-	Ag - AgCl	100, 1760, 5940	10	25 °C, pH 4.7 (CH_3COONH_4 buffer)	4
NH_4^+	Glass	0, 10, 20	5	pH 8.2 (triethanolamine buffer)	11
Na^+	Glass	0.25, 2.5, 25	12	29 °C, pH 11 (NH_3)	10
S^{2-}	Ag_2S	18.2, 45.5	4/6	0.6 mol l^{-1} NaOH - 0.1 mol l^{-1} Na_2H_2EDTA	13
Cu^{2+}	CuS - Ag_2S	6.3	5	22 °C, no added salts	19

Calculation of Limits and Criteria of Detection for Ion-selective Electrodes

Measurements with ion-selective electrodes are usually made in the region of Nernstian response, where the e.m.f. can be expressed by the equation

$$E = E^\circ + k\log C \quad .. \quad .. \quad .. \quad .. \quad .. \quad (4)$$

where E° is the standard potential, $k = RT\ln 10/zF$ is the slope factor and C is the concentration of determinand from the sample. Near the limit of detection, however, other factors influence the e.m.f., which can be expressed by the equation

$$E = E^\circ + k\log(C + s + b_r + \Sigma b_i) \quad .. \quad .. \quad .. \quad (5)$$

where s is the contribution of determinand from dissolution of the materials of the electrode itself, b_r is the concentration of determinand in the reagent blank and b_i is the interference effect of the ith interfering species.

The criterion (C_Q) and limit (C_L) of detection in concentration terms can be calculated from b_r, b_i, s and K, the solubility product governing s, together with the values of Q or L. If, as is usual in potentiometric analysis, the ionic strength of the samples is adjusted to a constant value, the activity coefficients are constant and can be included in the E° and K terms of the equations derived below; concentrations have, therefore, been used throughout instead of activities.

The derivation of equations (7), (9), (11), (13) and (15) for electrodes with non-ideal responses has been described by Midgley.[20] The equations are shown for cation-selective electrodes only; those for anion-selective electrodes are identical except for the signs before the logarithmic terms in the equations for e.m.f.

Response not limited by solubility product

In this instance $b_r + \Sigma b_i = b \gg s$. The e.m.f., E_B, is given by equation (5) with $C = 0$ and $s = 0$:

$$E_B = E^\circ + k\log b$$

At the criterion of detection $C = C_Q$ and $E = E_Q$, given by

$$E_Q = E^\circ + k\log(C_Q + b)$$

By definition, $Q = | E_Q - E_B |$ and, therefore,

$$Q = k\log[(C_Q + b)/b]$$

Hence,

$$C_Q = (10^{Q/k} - 1)b \quad .. \quad .. \quad .. \quad .. \quad (6)$$

Similarly,

$$C_L = (10^{L/k} - 1)b \quad .. \quad .. \quad .. \quad .. \quad (6')$$

Response limited by solubility product

In this instance $b_r = \Sigma b_i = 0$. For electrodes whose response is governed by the solubility product of a crystalline phase with 1:1 stoicheiometry, the e.m.f. can be expressed as follows[20]:

$$E = E^\circ + k\log\left[\frac{C}{2} + \left(\frac{C^2}{4} + K\right)^{\frac{1}{2}}\right] .. \quad .. \quad .. \quad .. \quad (7)$$

At $C = 0$,

$$E_B = E^\circ + k\log K^{\frac{1}{2}}$$

At $C = C_Q$,

$$E_Q = E^\circ + k\log\left[\frac{C_Q}{2} + \left(\frac{C_Q^2}{4} + K\right)^{\frac{1}{2}}\right]$$

Hence,

$$Q = k\log\left[\frac{C_Q}{2K^{\frac{1}{2}}} + \left(1 + \frac{C_Q^2}{4K}\right)^{\frac{1}{2}}\right]$$

Expanding by the binomial theorem for $C_Q \ll K^{\frac{1}{2}}$, we obtain

$$Q \approx k\log\left(1 + \frac{C_Q}{2K^{\frac{1}{2}}} + \frac{C_Q^2}{8K}\right)$$

Exponentiating and solving the resultant quadratic, we obtain

$$C_Q = 2K^{\frac{1}{2}}[(2 \times 10^{Q/k} - 1)^{\frac{1}{2}} - 1] \quad .. \quad .. \quad .. \quad (8)$$

Similarly,

$$C_L = 2K^{\frac{1}{2}}[(2 \times 10^{L/k} - 1)^{\frac{1}{2}} - 1] \quad .. \quad .. \quad .. \quad (8')$$

Response limited simultaneously by solubility product and interference

When $b_r = 0$ and $\Sigma b_i \neq 0$, we have,[20] with the same conditions as for equation (7)

$$E = E^\circ + k\log\left[\frac{C}{2} + \Sigma b_i + \left(\frac{C^2}{4} + K\right)^{\frac{1}{2}}\right] \quad .. \quad .. \quad .. \quad (9)$$

Proceeding as from equation (7) to equation (8), we obtain

$$C_Q = 2K^{\frac{1}{2}}\{[1 - 2(1 - 10^{Q/k})(1 + b/K^{\frac{1}{2}})]^{\frac{1}{2}} - 1\} \quad .. \quad .. \quad (10)$$

and

$$C_L = 2K^{\frac{1}{2}}\{[1 - 2(1 - 10^{L/k})(1 + b/K^{\frac{1}{2}})]^{\frac{1}{2}} - 1\} \quad .. \quad .. \quad (10')$$

Response limited simultaneously by solubility product and reagent blank determinand

When $b_r \neq 0$ and $\Sigma b_i = 0$ and with the same conditions as for equation (7), we obtain[14]

$$E = E^\circ + k\log\left\{\frac{b_r + C}{2} + \left[\frac{(b_r + C)^2}{4} + K\right]^{\frac{1}{2}}\right\} \quad .. \quad .. \quad (11)$$

Proceeding as from equation (7) to equation (8), we obtain

$$C_Q = (2K^{\frac{1}{2}} + b)\left\{\left[10^{Q/k} + \frac{(10^{Q/k} - 1)\,4K}{(2\,K^{\frac{1}{2}} + b)^2}\right]^{\frac{1}{2}} - 1\right\} \quad .. \quad .. \quad (12)$$

$$C_L = (2K^{\frac{1}{2}} + b)\left\{\left[10^{L/k} + \frac{(10^{L/k} - 1)\,4K}{(2K^{\frac{1}{2}} + b)^2}\right]^{\frac{1}{2}} - 1\right\} \quad .. \quad .. \quad (12')$$

Response limited by solubility product with 2:1 *stoicheiometry*

Univalent electrodes. With $b_r = \Sigma b_i = 0$ and $(c + s)^2 s/2 = K$, the e.m.f. can be written as follows[20]:

$$E = E^\circ + k\log[(2K/s)^{\frac{1}{2}}] \quad .. \quad .. \quad .. \quad .. \quad (13)$$

At $C = 0$,

$$E_B = E^\circ + k\log[(2K)^{\frac{1}{2}}]$$

At $C = C_Q$,

$$E_Q = E^\circ + k\log[(2K/s_Q)^{\frac{1}{2}}]$$

$$Q = k\log\left[\frac{(2K)^{\frac{1}{2}}}{s_Q^{\frac{1}{2}}}\right]$$

Hence,

$$s_Q = (2K)^{\frac{1}{2}} \times 10^{-2Q/k}$$

and

$$C_Q = -s_Q + (2K/s_Q)^{\frac{1}{2}} \quad .. \quad .. \quad .. \quad .. \quad (14)$$

The calculation of s_L and C_L is exactly analogous.

Divalent electrodes. With $b_r = \Sigma b_i = 0$ and $(C + s)(2s)^2 = K$, the e.m.f. can be written as follows[14]:

$$E = E^\circ + k\log(K/4s^2) \quad .. \quad .. \quad .. \quad .. \quad (15)$$

At $C = 0$,

$$E_B = E^\circ + k\log[(K/4)^{\frac{1}{3}}]$$

At $C = C_Q$,

$$E_Q = E^\circ + k\log(K/4s_Q^2)$$

$$Q = k\log(K^{\frac{1}{3}}/4^{\frac{1}{3}}s_Q^2)$$

Hence,

$$s_Q = (K/4)^{\frac{1}{3}} \times 10^{-Q/2k}$$

and

$$C_Q = -s_Q + K/4s_Q^2 \quad .. \quad .. \quad .. \quad .. \quad (16)$$

The equation for C_L is exactly analogous.

Applicability to Different Types of Electrodes

Equation (6) is valid for all electrodes, regardless of mechanism, provided that $b \gg s$, *i.e.*, the presence of the reagent blank or interferences is the only cause of deviation from the Nernstian response at the observed criterion of detection. This can be checked by the procedure described by Midgley.[20]

Equations (8)–(16) are valid for electrodes with crystalline phases that participate in solubility equilibria with the adjacent solution but not for electrodes in which the active component dissolves as a result of an irreversible chemical reaction, such as the oxidation of sulphide in the copper(II) sulphide - silver sulphide membranes of copper-selective electrodes.[21] The validity of equations (8)–(16) does not depend on how the crystalline phase is incorporated into an electrode, *e.g.*, for electrodes based on silver chloride, the equations describing the e.m.f. are equally valid for silver - silver chloride electrodes, heterogeneous (Pungor-type) membrane electrodes and mixed-crystal (silver sulphide - silver chloride) membrane electrodes.[20] With mixed-crystal membrane electrodes the more soluble component determines the choice of equation, *e.g.*, for silver sulphide - silver chloride electrodes, the greater solubility of silver chloride means that equation (8) is used, not equation (14).

In theory,[20] liquid ion-exchange electrodes can be accommodated to equations (7)–(16) by replacing K by K_L, where K_L is equal to $(C^*)^2/K_D$ for equations (7)–(12), $0.5(C^*)^3/K_D$ for equation (14) and $4(C^*)^3/K_D$ for equation (16). In each instance C^* is the concentration of exchanger in the membrane phase and K_D is the appropriate distribution coefficient between the aqueous and membrane phases. This model has not been tested experimentally.

Influence of Blanks, Interferences and Solubility Products on Limits and Criteria of Detection

Fig. 1 shows the calibration graphs for different types of hypothetical ion-selective electrodes. All of the electrodes respond to univalent cations, have standard potentials of 337.15 mV and calibration slopes of 59.16 mV per decade at concentrations well above the limit of detection. Line N represents the extrapolation of the Nernstian portions of the calibrations of all the electrodes. To show the comparative effects of the various causes of non-Nernstian behaviour, the solubility products, interferences and reagent blanks were chosen so that the potential of each electrode at zero nominal determinand concentration was 0.0 mV, corresponding to an apparent concentration of 2×10^{-6} mol l^{-1} on the extrapolated Nernstian graph N. In all instances, σ_E was taken as 1.0 mV, resulting in the lines $E_Q = 2.3$ mV and $E_L = 4.6$ mV.

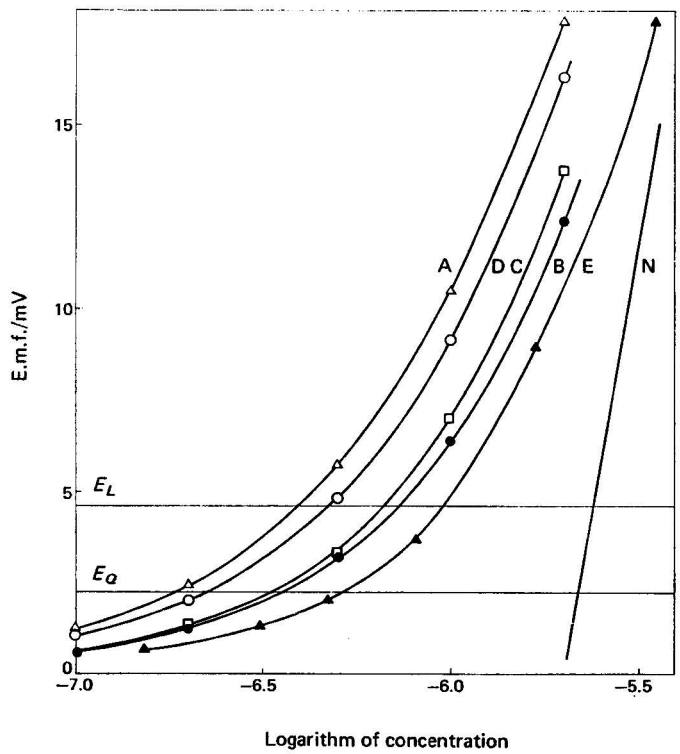

Fig. 1. Limit and criterion of detection for hypothetical univalent electrodes with non-Nernstian calibrations. A, $b = 2 \times 10^{-6}$ mol l^{-1} (interference or reagent blank determinand, no solubility effect); B, $K = 4 \times 10^{-12}$ mol^3 l^{-3} (solubility effect only); C, $b_i = 10^{-6}$ mol l^{-1}, $K = 10^{-12}$ mol^3 l^{-3} (solubility effect and interference); D, $b_r = 1.5 \times 10^{-16}$ mol l^{-1}, $K = 10^{-12}$ mol^3 l^{-3} (solubility effect and reagent blank); E, $K = 4 \times 10^{-18}$ mol^3 l^{-3} [non-isovalent (2:1) solubility effect] and N, ideal Nernstian response. Lines E_Q and E_L show the criterion and limit of detection in e.m.f. terms.

In Fig. 1 the abscissa represents the blank e.m.f. reading and the lines E_Q and E_L the criterion and limit of detection in e.m.f. terms. The intersections of E_Q and E_L with the calibration graphs give the criteria and limits of detection in concentration terms, which vary widely between electrodes even though all have identical responses at $C = 0$ and $C \gg C_L$ and identical standard deviations in e.m.f., *i.e.*, the lines E_Q, E_L, N and the abscissa are common to all the electrodes. Table III shows the limits and criteria of detection obtained for these electrodes both from Fig. 1 and by use of equations (6)–(14). The differences between the two sets of figures arise from the approximations involved in deriving the equations. Better agreement would be obtained at lower values of σ_B, because the errors from the approximations become smaller at concentrations more removed from the Nernstian region.

TABLE III

CRITERIA AND LIMITS OF DETECTION FOR UNIVALENT ELECTRODES WITH $\sigma_B = 1.0$ mV

	Curve in Fig. 1				
	A	B	C	D	E
$10^6 b_r$/mol l^{-1}	*	0	0	1.5	0
$10^6 \Sigma b_i$/mol l^{-1}	*	0	1	0	0
$10^{12} K$	—	4	1	1	4×10^{-6}
Equation used	(6)	(8)	(10)	(12)	(14)
$10^7 C_Q$/mol l^{-1}—					
Graphical	1.90	3.63	3.43	2.29	5.25
Calculated	1.90	3.47	4.28	1.99	5.21
$10^7 C_L$/mol l^{-1}—					
Graphical	3.98	7.41	6.76	4.79	9.66
Calculated	3.97	7.28	8.23	4.03	10.05

* $10^6(b_r + \Sigma b_i) = 2$.

Table III also shows that the ratio L/Q (equal to 2.0 in the conditions adopted) need not equal C_L/C_Q; this arises from the nature of the calibration of e.m.f. against the logarithm of the concentration. When the calibration reaches the limiting stage where the e.m.f. is linearly related to concentration,[5,9] the two ratios will be equal.

In practice, σ_B is obtained from a series of measurements with standard solutions, including a zero standard as a blank, but the water used to prepare these standard solutions will itself contain some concentration of determinand, b_W, which can be termed the water blank. The value of σ_B obtained will not, therefore, be the standard deviation of the true blank, but only the best approximation we can make. Because, for convenience, we have already assumed that the standard deviations are constant over the range $C = 0$ to $C = C_L$, any error in σ_B from this source should be negligible. The values of Q and L, which are multiples of σ_B, are, therefore, unaffected by the existence of the water blank.

If the value of b in equations (6) and (12) is derived from the potentiometric data, *e.g.*, by any of the methods described by Midgley,[20] it will be overestimated by the amount of the water blank unless b_W is determined in an independent experiment and then subtracted. In practice both b_r and b_W may be negligible, *e.g.*, some of the chloride results quoted by Midgley.[20]

Discussion

By the IUPAC definition,[1] the limits of detection for all the hypothetical electrode responses shown in Fig. 1 would be 2×10^{-6} mol l^{-1} regardless both of the factors governing the response and of the precision of the measurements. In contrast, the statistical definition yields a different limit of detection for each electrode, reflecting the different sources of non-Nernstian behaviour for the various electrodes. With real electrodes the limits of detection might have appeared to be higher in both instances, because of the experimental difficulty of identifying the equilibrium e.m.f. at low concentrations. With the IUPAC limit there is also the problem of identifying precisely the linear non-Nernstian segment of the calibration graph.

Even as a qualitative guide, a non-statistical definition may be misleading. For instance, chloride-selective electrodes have lower IUPAC limits of detection at lower temperatures, because the calibration graph changes as a result of the temperature dependence of the solubility product. When the two sets of calibration data are analysed statistically, it is possible for the limit of detection to be no better or even worse at the lower temperature because the increased sensitivity of the calibration may be offset by a loss of precision. An example[9] of this is the operation of a mercury(II) sulphide - mercury(I) chloride membrane electrode at 25 and 4 °C, where the limits of detection were almost the same at the two temperatures, despite the 3-fold increase in sensitivity at 4 °C.

The use of the equations for calculating C_L enables one to predict the effect that changes in the solubility product or in the purity of the reagents might have on the limit of detection. The same equations can be used to predict the precision required (in e.m.f. units) if a given limit of detection is to be attained under specified conditions.

IUPAC and statistical limits of detection are compared in Table IV for different types of electrodes. When, as with the glass electrodes,[10,11] the precision of measurement is poor (standard deviations of 1.5–3 mV) and there is a high reagent blank, the two definitions differ little, but when measurements are made more precisely (standard deviations of 0.04–0.4 mV) and the reagent blank is small, as with the two types of chloride electrode,[5,9] the IUPAC definition gives an unrealistic indication of the performance of an electrode in analysis.

TABLE IV

LIMITS OF DETECTION OF ION-SELECTIVE ELECTRODES

Electrode	Determinand	IUPAC limit/ $\mu g\ l^{-1}$	Statistical limit/ $\mu g\ l^{-1}$	Reference
Hg_2Cl_2 - HgS	Cl^-	60	1	9
Ag - AgCl	Cl^-	530	15	5
Glass	Na^+	3	1.4	10
Glass	NH_4^+	13	6	11

Both the IUPAC and statistical limits arise from the performance of the electrode itself, but in considering an analytical method as a whole, other factors may make these limits irrelevant. For instance, if the concentration is obtained from the measured e.m.f., not by use of a calibration graph but from the Nernst equation, either explicitly as equation (4) or implicitly through the use of a pIon or direct-activity scale on a pH meter, the limit of detection of the method is given by the limit of the Nernstian response. A statistical procedure for finding this limit has been given by Liteanu *et al.*,[22] although it might be improved by the use of weighted data in calculating the linear regression line representing the Nernstian calibration and in the subsequent tests for goodness of fit.

In certain circumstances,[19,23,24] *e.g.*, when high (10^{-4}–10^{-2} mol l^{-1}) concentrations of metal ion are in equilibrium with an excess of a strong complexing agent, electrodes can respond to low determinand activities (10^{-15}–10^{-9} mol l^{-1}), but the existence of this response does not contradict the above definition of limit of detection, which is valid for analysis at trace concentrations of determinand.

The operation of ion-selective electrodes in their non-Nernstian ranges is sufficiently well established in the laboratory[4,7,9,13] and inside industrial plant[5,6] to warrant a more rigorous definition of limit of detection than the IUPAC approach can provide, although the latter can be used as a convenient rule of thumb when it is desired to compare the performance limits of electrodes without collecting large amounts of data.

This work was carried out at the Central Electricity Research Laboratories and is published by permission of the Central Electricity Generating Board.

References

1. International Union of Pure and Applied Chemistry, *Pure Appl. Chem.*, 1976, **48**, 127.
2. International Union of Pure and Applied Chemistry, "Recommendations for Nomenclature of Ion-selective Electrodes (Recommendations, 1975)," Pergamon Press, Oxford, 1976.
3. Wilson, A. L., *Talanta*, 1973, **20**, 725.

4. Torrance, K., *Analyst*, 1974, **99**, 203.
5. Tomlinson, K., and Torrance, K., *Analyst*, 1977, **102**, 1.
6. Goodfellow, G. I., "Proceedings of the International Conference on Water Chemistry of Nuclear Reactor Systems, Bournemouth, 24–27 October," British Nuclear Energy Society, London, 1977, p. 127.
7. Bardin, V. V., Shartukov, O. F., and Tolstousov, V. N., *Zh. Analit. Khim.*, 1971, **27**, 25.
8. Roos, J. B., *Analyst*, 1962, **87**, 832.
9. Marshall, G. B., and Midgley, D., *Analyst*, 1979, **104**, 55.
10. Hawthorn, D., and Ray, N. J., *Analyst*, 1968, **93**, 158.
11. Goodfellow, G. I., and Webber, H. M., *Analyst*, 1972, **97**, 95.
12. Louw, C. W., and Richards, J. F., *Analyst*, 1972, **97**, 334.
13. Baumann, E. W., *Analyt. Chem.*, 1974, **46**, 1345.
14. Midgley, D., and Torrance, K., "Potentiometric Water Analysis," Wiley, Chichester and New York, 1978, p. 71.
15. Lilliefors, H. W., *J. Am. Statist. Ass.*, 1967, **62**, 399.
16. Ames, A. E., and Szonyi, G., *in* Kowalski, B. R., *Editor*, "Chemometrics: Theory and Practice," ACS Symposium Series 52, American Chemical Society, Washington, D.C., 1977, p. 219.
17. Conover, W. J., "Practical Nonparametric Statistics," Wiley, New York, London, Sydney and Toronto, 1971, p. 302.
18. Marshall, G. B., and Midgley, D., *Analyst*, 1978, **103**, 438.
19. Midgley, D., *Analytica Chim. Acta*, 1976, **87**, 7.
20. Midgley, D., *Analyt. Chem.*, 1977, **49**, 1211.
21. Midgley, D., *Analytica Chim. Acta*, 1976, **87**, 19.
22. Liteanu, C., Popescu, I. C., and Hopîrtean, E., *Analyt. Chem.*, 1976, **48**, 2010.
23. Veselý, J., Jensen, O. J., and Nicolaisen, B., *Analytica Chim. Acta*, 1972, **62**, 1.
24. Baumann, E. W., *Analytica Chim. Acta*, 1971, **54**, 189.

Received *September 20th*, 1978
Accepted *October 24th*, 1978

SHORT PAPERS

Spectrophotometric Method for the Determination of Paraquat

M. Ganesan, S. Natesan and V. Ranganathan

Department of Chemistry, United Planters' Association of Southern India, Tea Research Station, Cinchona 642 106, India

Keywords: Paraquat determination; spectrophotometry

The divalent 1,1'-dimethyl-4,4'-bipyridylium ion (paraquat) gives an orange-yellow precipitate of composition paraquat.HgI_4 with neutral potassium tetraiodomercurate(II) (K_2HgI_4) solution. At low concentrations of paraquat, a yellow colloidal solution is formed. A spectrophotometric method, after stabilisation of the colloidal solution with acetone, ethanol or starch solution, has been developed for the determination of paraquat.

The dichloride and dimethylsulphate salts of the divalent 1,1'-dimethyl-4,4'-bipyridylium ion are used extensively as herbicides.[1] Extensive work has been carried out on the determination of paraquat and diquat by Calderbank and co-workers,[2–4] and a spectrophotometric method described by Yuen *et al.*[5] has been adopted by both CIPAC[6] and AOAC.[7] Their method is based principally on reduction with alkaline sodium dithionite solution to a blue free radical, which is not very stable and requires immediate determination of the absorbance. A liquid-chromatographic method with an ultraviolet detector has also been reported for determining paraquat dichloride.[8] The present investigation was concerned with the development of a spectrophotometric method for the routine determination of paraquat in formulations and in mixtures with other herbicides. The colour developed is stable for up to 60 min and hence lends itself for adoption in routine work, requiring less attention than the dithionite method.

Experimental

Reagents

A neutral solution of potassium tetraiodomercurate(II) is prepared by mixing 22.8 g of mercury(II) iodide with 17.5 g of potassium iodide, dissolving them in distilled water and diluting to 1 l with water. The solution is allowed to stand for 1–2 d before the supernatant liquid is withdrawn for use.

Pure ethanol, acetone or 1% *m/V* starch solution is required as a stabiliser of the colloidal solution.

Procedure

To a 25-ml calibrated flask is added a suitable aliquot of solution of the formulation, containing up to 70 μg of paraquat, in the form of its dichloride or dimethylsulphate salt, and then 5 ml of ethanol, 1.5 ml of acetone or 1 ml of 1% *m/V* starch solution are added. The solution is mixed well, diluted to about 20 ml, 1 ml of neutral potassium tetraiodomercurate(II) solution is added and the solution is mixed well and made up to the mark with water. The absorbance of the yellow solution is measured at 400–420 nm after 15 min, but within 60 min after the colour development. Pure paraquat dichloride is used as a standard to analyse samples within an unknown paraquat content. The reaction is rapid and the optimum time for taking readings, after colour development, is between 15 and 60 min (see Table I).

The determination of mercury and iodine (in the reaction product) was carried out using the standard procedures described by Vogel.[9]

TABLE I

VARIATION OF ABSORBANCE WITH TIME

Average of a number of determinations by two different workers on both paraquat salts. Values given are for absorbance in Klett units, with the pH of the final solution between 7 and 8.

Stabiliser	Time/h 0	0.25	0.50	0.75	1.00	2.00	4.00
None	118	127	130	128	134	90	80
Starch	110	112	114	113	115	85	60
Acetone	146	113	113	115	114	87	66
Ethanol	109	110	112	111	110	68	60

Results and Discussion

The absorbance is linearly related to paraquat concentration up to 3 μg ml^{-1}. Pure paraquat dichloride is used only for standards. All interference tests and reliability tests are carried out with solutions of paraquat dichloride and paraquat dimethylsulphate. When the concentration of starch in the final solution is between 0.016 and 0.060% *m/V*, ethanol between 15 and 23% *V/V* or acetone between 2 and 10% *V/V*, there is little variation in the colour intensity with the variation in concentration of the stabiliser (see Table II). The

TABLE II

OPTIMUM STABILISER CONCENTRATION

Average of 5–10 determinations by two different workers on both paraquat salts.

Stabiliser: Starch		Ethanol		Acetone	
Concentration, % *m/V*	Absorbance, Klett units	Concentration, % *V/V*	Absorbance, Klett units	Concentration, % *V/V*	Absorbance, Klett units
0	68	0	96	0	106
0.008	50	12	111	1	110
0.016–0.060	53	15–23	143	2–10	113
0.080	57	24	128	12	87
0.100	60	40	24	18	14

colour diminishes rapidly at higher concentrations, beyond the upper optimum limit of ethanol or acetone, and almost disappears beyond 40% *V/V* of ethanol or 18% *V/V* of acetone. No interferences are observed with Na^+, K^+, NH_4^+, H^+, Cl^-, NO_3^-, SO_4^{2-} or $CH_3SO_4^-$, with common herbicides such as sodium 2,2-dichloropropionate, sodium 2,4-dichlorophenoxyacetate and monosodium methanearsonate when added to the solutions of the two paraquat salts (see Table III). Hydroxyl ions interfere when the pH is above

TABLE III

INTERFERENCE TESTS

All concentrations given are in the final solution. Results are the average of 4–6 determinations, carried out by three different workers, on both paraquat salts. The results given are paraquat concentration in milligrams per litre.

Species	Concentration of species/mmol l^{-1} 0	2	5
Na^+	1.596	1.583	1.596
K^+	1.596	1.586	1.596
NH_4^+	1.596	1.609	—
Cl^-	1.596	1.596	1.596
NO_3^-	1.596	1.583	1.583
SO_4^{2-}	1.596	1.583	1.610
Ansar	1.596	1.596	—
2,4-D	1.596	1.596	—
Dalapon	1.596	1.596	—

8. This is overcome by maintaining the pH between 6 and 8 by neutralising with dilute hydrochloric acid and by using neutral potassium tetraiodomercurate(II). The effects of pH and time on the absorbance are shown in Table IV.

TABLE IV

EFFECT OF pH OF THE FINAL SOLUTION AND TIME ON ABSORBANCE

All results are the average of 4 determinations, and the values given are absorbances in Klett units.

	Time/h						
pH range	0	0.25	0.50	0.75	1	2	4
3–5	78	88	85	76	65	62	44
6–8	69	80	80	80	80	77	53
9–11	97	115	117	120	120	121	117

Diquat (1,1′-ethylene-2,2′-bipyridylium ion) interferes with the paraquat determination; it also gives a yellow colloidal solution with absorption in the range 420–440 nm. The presence of diquat can be detected by the formation of a red colour with sodium hydroxide solution. Diquat is hydrolysed completely in dilute alkaline solution in the pH range 12.5–13.0 (2 ml of 0.2 N sodium hydroxide solution is sufficient for a 1-ml aliquot containing up to 50 μg ml^{-1} of diquat) within 5–6 h. Diquat interference can be overcome completely when determining paraquat (containing diquat) by keeping it in alkaline solution at pH 12.5–13.0 for 5–6 h and developing the colour in the same manner as described earlier, after neutralising with acid using phenolphthalein as an indicator. Table V shows the results of paraquat determinations in the presence of diquat.

TABLE V

ELIMINATION OF DIQUAT INTERFERENCE

Each result is the average of 3 or 4 determinations by three workers on both paraquat salts.

Paraquat, % *m/m*	Paraquat* taken/ mg l^{-1}	Diquat* added/ mg l^{-1}	Paraquat, after diquat elimination, % *m/m*†
21.14	1.713	2	21.41
20.95	1.676	3	21.00
21.00	1.680	2	21.00
21.00	1.680	3	21.13

* Concentration in the final solution.
† By the procedure described in the text.

At high concentrations, paraquat gives an orange - yellow precipitate with neutral potassium tetraiodomercurate(II) solution. Theoretical considerations suggest paraquat.HgI_4 as the probable product of any reaction between the two ionic substances, paraquat.Cl_2 and K_2HgI_4. On analysis, the precipitated substance was found to contain 20.5 $\pm$ 0.3% of paraquat, 22.3 $\pm$ 0.3% of mercury and 56.6 $\pm$ 0.2% of iodine, compared with the theoretical values of 20.8% of paraquat, 22.5% of mercury and 56.7% of iodine, confirming the formula paraquat.HgI_4. This is unlike the instance of ammonia, when a compound $NH_2Hg_2I_3$ is formed.[10] The precipitation is quantitative and there is a distinct possibility of developing this method further for the gravimetric determination of paraquat for quality control purposes.

The spectrophotometric method described is accurate, with coefficients of variation of 0.33, 0.41 and 1.41% with ethanol, acetone and starch, respectively, as stabilisers. The method is comparable to the CIPAC method[6] within $\pm$1% of the paraquat content, with the added advantage that the colour is stable for up to 60 min, unlike the standard methods that require colour development just before measurement of the absorbance (see Table VI).

TABLE VI

COMPARISON OF METHODS

Method	Coefficient of variation, %
CIPAC method	0.45
Present method without stabiliser	2.47
Present method with starch as stabiliser ..	1.41
Present method with acetone as stabiliser ..	0.41
Present method with ethanol as stabiliser ..	0.33

The authors thank Dr. C. S. Venkata Ram, Director of Research, for his keen interest in the work and Alkali and Chemical Corporation of India Ltd. for providing technical-grade paraquat dichloride for the investigation.

References

1. Martin, H., *Editor*, "Pesticide Manual," Third Edition, British Crop Protection Council, London, 1972.
2. Calderbank, A., Morgan, C. B., and Yuen, S. H., *Analyst*, 1961, **86**, 569.
3. Calderbank, A., and Yuen, S. H., *Analyst*, 1965 **90**, 99.
4. Calderbank, A., and Yuen, S. H., *Analyst*, 1966, **91**, 625.
5. Yuen, S. H., Bagness J. E., and Myles, D., *Analyst*, 1967, **92**, 375.
6. Raw, G. R., *Editor*, "CIPAC Handbook. Volume I. Analysis of Technical and Formulated Pesticides," W. Heffer and Sons, Cambridge, for Collaborative International Pesticides Analytical Council, 1970, p. 547.
7. Carlstrom, A. A., *J. Ass. Off. Analyt. Chem.*, 1968, **51**, 1306.
8. Kawano, Y., Audino, J., and Edlund, M., *J. Chromat.*, 1975, **115**, 289.
9. Vogel, A. I., "A Text Book of Quantitative Inorganic Analysis," Third Edition, Longmans Green, Harlow, 1962.
10. Partington, J. R., "Inorganic Chemistry," Macmillan, London, 1965.

Received *May 25th*, 1978
Accepted *September 27th*, 1978

Titrimetric Determination of Reducing Sugars with Copper(II) Sulphate

T. H. Khan

Department of Industries (Chemical Directorate), 58, Dilkusha Commercial Area, Dacca-2, Bangladesh

Keywords: *Reducing sugar determination*; *copper(II) sulphate reduction*; *titrimetry*

Of the copper reduction methods for the determination of reducing sugars, that of Lane and Eynon[1] is still considered to be a simple and rapid method and is often the most accurate.[2–5] Much work[5–12] has also been carried out on the automatic determination of reducing sugars but little use has been made of these methods. The use of a constant volume modification of the Lane and Eynon method has been reported,[4,13] but it does not seem to be based on any systematic investigation such as we have carried out in order to obtain information lacking in the literature on the determination of reducing sugars. During the work on the determination of reducing sugars by using the Lane and Eynon method, the following observations were made and necessary modifications were made to the method.

Modifications to Lane and Eynon Method

Time to reach boiling-point. The total boiling time has been fixed at 3 min (2 + 1 min) in the Lane and Eynon method but the time required to reach boiling has not been fixed. As the reaction of the reducing sugar with the Fehling's solution is non-stoicheiometric and the method is empirical, it is necessary to maintain this time constant in order to minimise errors.

Total boiling time. After boiling the mixture of sugar and Fehling's solution for 2 min before addition of the indicator, it was found to be red or orange - red owing to the presence of coagulated copper(I) oxide. When the reaction mixture of sugar and Fehling's solution was boiled for 5 min before addition of the indicator, the copper(I) oxide settled at the bottom of the flask, leaving a clear solution.

Colour of end-point. The end-point in the published method was given by the appearance of a bright red or orange colour, but when a clear solution was produced after boiling for 5 min, it was found possible to see the last trace of the blue colour of the indicator and a colourless end-point was obtained.

Effect of indicator concentration. When a clear reaction mixture was produced only 1 drop of 0.1% methylene blue solution was required in order to give a distinct blue colour, thus giving a sharp colour change at the end-point. This also eliminates any errors resulting from the use of a high concentration (3–5 drops of a 1% solution of methylene blue) as methylene blue itself oxidises some sugar or those errors caused by the back-oxidation of methylene white to methylene blue.

Reaction time. During the addition of the sugar solution to the boiling reaction mixture it has been found useful to allow some time for completion of the reaction and observation of the colour after the addition of each drop, and increasing this time from 1 to 3 min avoids errors caused by the addition of excess of the sugar solution.

Advantages of the use of a 200-ml flask. The use of a 200-ml Erlenmeyer flask in place of a 300- or 400-ml flask improves the detection of the end-point as the height of the liquid layer is greater in the smaller flask.

Fehling's solution. Fehling's solution was allowed to stand overnight and was then used without filtration through treated asbestos.[14] The tedious process of filtering the solutions through treated asbestos has been found to be unnecessary, as shown in Table I.

A series of experiments was performed with standard solutions of invert sugar, glucose, fructose and lactose of different concentrations using 5 or 10 ml each of Fehling's solutions A and B as in the procedure described below.

Experimental

Reagents

Copper(II) sulphate ($CuSO_4.5H_2O$). AnalaR grade.
Potassium sodium tartrate ($KNaC_4H_4O_6.4H_2O$). AnalaR grade.
Sodium hydroxide. AnalaR grade.
Methylene blue.
Sucrose, glucose and lactose ($C_{12}H_{22}O_{11}.H_2O$). AnalaR grade.
Maltose ($C_{12}H_{22}O_{11}.H_2O$). Laboratory-reagent grade.
Fructose. Laboratory-reagent grade, dried under vacuum.
Fehling's solutions. Prepared by Soxhlet's modified method.[14]
Invert sugar. A standard solution of invert sugar was prepared by hydrolysing sucrose with hydrochloric acid at room temperature.
Distilled water was used in all the experimental work.

Method

First determination

Fehling's solutions A and B (5 or 10 ml of each) were pipetted into a 200-ml Erlenmeyer flask, mixed well by shaking and approximately 25 ml of water were added. The flask, with its contents, was placed on an asbestos wire gauze on a hot-plate and allowed to boil. A sugar solution was added to this boiling mixture while observing the colour of the mixture. When the colour became a very light blue, 1 drop of 0.1% methylene blue solution was added and drops of the sugar solution were added slowly until the colour of the methylene blue disappeared, leaving a colourless solution.

Second determination

A second determination was then made by adding to the cold mixture of Fehling's solution about 98% of the total volume of sugar solution required in the first determination. A

measured amount of water was then added to make the total volume (sugar solution plus water) up to 50 ml and the flask put on the hot-plate, which had previously been adjusted so that boiling started in exactly 3 min, and was continued for 5 min. One drop of 0.1% methylene blue solution was then added and dropwise addition of the sugar solution was continued until the methylene blue colour disappeared. The final addition of sugar solution after the addition of the indicator was completed within 3 min.

Final determination

A final determination was then made in the same way as in the second determination except that 98% of the total volume of sugar solution required in the second determination was added initially and, after adding 1 drop of the indicator, addition of the sugar solution was continued until the end-point was nearly reached. A calculated amount of water was then added so that the volume of sugar solution or sugar solution plus water added at the final stage remained approximately constant at 1 ml. The determination was then completed by the addition of further amounts of the sugar solution.

Results and Discussion

By carrying out the determination using the above procedure, it was found that the factor, *i.e.*, the amount of any particular sugar required for the reduction of a fixed volume of Fehling's solution (either 10 or 20 ml), was always virtually constant, irrespective of the concentration of the sugar solution (Table I). In the Lane and Eynon method, this factor was found to vary with the variation in the concentration of any particular sugar solution being examined. By following this procedure the reducing sugar in an unknown sample can be determined without the use of Lane and Eynon sugar tables. A volume of sugar solution less than 15 ml can also be used, and in these studies volumes as low as 5 ml have been used. By the addition of 98% of the volume of the sugar solution in the cold during the final determination, it was possible to maintain the concentration of any particular reducing sugar, including the concentration of the reaction mixture in the flask, virtually constant, irrespective of the concentration of the sugar solution used.

TABLE I

FACTORS FOR THE DETERMINATION OF DIFFERENT SUGARS

Equal volumes, either 5 or 10 ml, of Fehling's solution A and B were used.

Sugar	Concentration range (mg per 100 ml) covered by 10 ml of solution (a)	Volume of each Fehling's solution/ml (b)	Factor ($a \times b/100$)		
			Maximum	Minimum	Mean
Invert sugar ..	210–1 800	10	102.30	102.24	102.27
	104–700	5	52.74	52.68	52.71
Glucose	200–2 000	10	99.10	99.00	99.06
	104–1 000	5	51.13	51.06	51.09
Fructose	210–1 800	10	105.48	105.40	105.42
	108–736	5	54.41	54.36	54.38
Maltose	320–4 000	10	160.03	159.94	160.00
	160–2 000	5	80.01	79.92	79.96
Lactose	270–3 000	10	134.49	134.40	134.43
	140–1 400	5	67.38	67.30	67.34

In the determination of invert sugar in the presence of sucrose, it has been found that the factor, *i.e.*, the amount of invert sugar required to reduce a fixed volume of Fehling's solution, decreases with the increase in the amount of sucrose in the flask (Tables II and III). Experiments were performed with different concentrations of invert sugar and with different amounts of sucrose added to the flask, and it was found that the variation of the amount of invert sugar required was due to the variation in the amount of sucrose present (Table III) but independent of the concentration of the invert sugar itself (Table II).

For the determination of the invert sugar content of any sample containing sucrose, correction factors for 1–4 g of sucrose present in the flask are given in Table III. These correction factors were calculated from the observed factor of invert sugar in the presence of sucrose (Table III) and the true factor for invert sugar determined with pure invert sugar (Table I). In the determination of invert sugar, the virtual result obtained is to be multiplied by the corresponding correction factor to obtain the correct results.

Table II

Effect of the presence of sucrose on the determination of invert sugar

Concentration range of invert sugar used/mg per 100 ml	Number of test solutions	Volume of each Fehling's solution used/ml	Amount of sucrose added/g	Factor		
				Maximum	Minimum	Mean
200–900	5	10	2	96.12	96.05	96.09
120–400	5	5	1	49.20	49.08	49.14

Table III

Correction factor for the determination of invert sugar in the presence of sucrose

Amount of sucrose present/g	Volume of Fehling's solution, A + B/ml	Observed factor	Correction factor
1	10 + 10	98.52	0.963
2		96.09	0.939
3		93.60	0.915
4		91.20	0.892
1	5 + 5	49.14	0.932
2		47.40	0.899
3		45.77	0.868
4		44.10	0.837

A comparative study of this method with the Lane and Eynon method was made with standard invert sugar solutions of different concentrations and the results are given in Table IV. It can be seen that the precision of the present method is always above 99.90% and is greater than that of the Lane and Eynon method.

Table IV

Comparative study of the Lane and Eynon method with this method

Concentration of the invert sugar solution used/ mg per 100 ml	Invert sugar content			
	By Lane and Eynon method/mg per 100 ml	Error, %	By present method/ mg per 100 ml	Error, %
120	119.30	−0.58	119.91	−0.075
140	137.66	−1.67	140.01	+0.007
160	159.30	−0.44	159.94	−0.038
200	200.98	+0.49	200.05	+0.025
240	235.48	−1.88	240.20	+0.083
320	314.34	−1.76	320.31	+0.097

This work was completed at the Food Science and Technology Unit, National Council for Scientific Research, Lusaka, Zambia. The author thanks Dr. S. Nkunika, Secretary General of the National Council for Scientific Research, Lusaka, for the facilities made available for these studies and Mr. R. T. Shantina for skilful technical assistance. The author also thanks Mr. Sirajul Karim, Assistant Professor of Analytical Chemistry, Bangladesh Agricultural University, for his kind co-operation and technical help.

References

1. Lane, J. H., and Eynon, L., *J. Soc. Chem. Ind., Lond.*, **1923**, **42**, 32T.
2. Jeslyn, M. A., "Methods in Food Analysis," Academic Press, New York, 1970, p. 486.
3. Jacobs, M. B., "The Chemical Analysis of Food and Food Products," Van Nostrand Reinhold, New York, 1958, p. 437.
4. Pearson, D., "The Chemical Analysis of Food," Churchill, London, 1970, pp. 129, 130.
5. Porter, D. G., and Sawyer, R., *Analyst*, 1972, **97**, 569.
6. Folin, O., *J. Biol. Chem.*, 1928, **77**, 421.
7. Hoffman, W. S., *J. Biol. Chem.*, 1937, **120**, 51.
8. Baum, E. H., *Ann. N.Y. Acad. Sci.*, 1960, **87**, 894.
9. Fingerhut, B., Ferzola, R., and Marsh, W. H., *Clinica Chim. Acta*, 1963, **8**, 953.
10. Fuller, K. W., *in* "Automation in Analytical Chemistry," Technicon Symposia, 1965, Mediad Inc., White Plains, N.Y., 1966, p. 78.
11. Fuller, K. W., *in* "Automation in Analytical Chemistry," Technicon Symposia, 1966, Volume II, Mediad Inc., White Plains, N.Y., 1967, p. 57.
12. Sawyer, R., *in* "Automation in Analytical Chemistry," Technicon Symposia, 1967, Volume I, Mediad Inc., White Plains, N.Y., 1968, p. 227.
13. J. R. Nickolls, "Aids to Analysis of Food and Drugs," Seventh Edition, Ballière, Tindall and Cox, London, 1952, p. 45.
14. Horwitz, W., *Editor*, "Official Methods of Analysis of the Association of Official Agricultural Chemists," Ninth Edition, Association of Official Agricultural Chemists, Washington, D.C., 1960, pp. 426 and 427.

Received *June 2nd*, 1975
Amended *December 9th*, 1977
Further amended *July 24th*, 1978
Accepted *October 5th*, 1978

Determination of Dimetridazole in Pig and Poultry Feeds by High-performance Liquid Chromatography

A. D. Jones, I. W. Burns and S. G. Sellings

Unilever Research Laboratory, Colworth House, Sharnbrook, Bedfordshire MK44 1LQ

Keywords: *Dimetridazole determination*; *animal feeds*; *high-performance liquid chromatography*

Dimetridazole (1,2-dimethyl-5-nitroimidazole) is an ingredient used in pig and poultry feeds for the control of swine dysentery, and blackhead in turkeys, chickens and game birds. It is also a growth promoter for both pigs and poultry. The usual content in feedstuffs is 50–300 mg kg^{-1}. Available analytical methods include polarography,[1] spectrophotometry[2,3] and thin-layer chromatography.[4] One high-performance liquid chromatographic (HPLC) method has been developed by Buizer and Severijnen,[5] which, although specific, requires a lengthy analysis time. The aim of this work was to develop an HPLC method that is both specific and rapid as an alternative to the presently available procedures.

Experimental

Reagents

All reagents were of analytical-reagent grade.
Dimetridazole.
Acetonitrile.
Dichloromethane.
Pyridine.
Hexane. Dried over sodium.
Xylene. Dried over sodium.
Chloroform.
Hexamethyldisilazane.
Dococylmethyldichlorosilane.

Apparatus

The liquid chromatograph consisted of a Model 6000 reciprocating pump (Waters Associates Inc., Milford, Mass., USA) and a Cecil Instruments, Model 212, ultraviolet - visible monitor set at 309 nm. Sample injection was achieved using a Rheodyne injection valve (Magnus Scientific, Stoke-on-Trent, Staffordshire) fitted with a 10-μl loop. The column was made from seamless stainless-steel tubing (HSCP, Bourne End, Bucks.) of dimensions 15 $\times$ 0.49 cm i.d. and was packed with dococylmethyldichlorosilane (Magnus Scientific) bonded to Partisil 10 (Whatman). Other equipment used included a rotary evaporator, a grinder and a mechanical shaker.

Procedure

Column preparation

Reflux 10 g of dry Partisil 10 silica (dried in an oven overnight at 110 °C), 12.7 g of dococylmethyldichlorosilane and 1 ml of pyridine in 50 ml of dry xylene. After 30 min add 2 ml of hexamethyldisilazane (HMDS) and reflux for a further 10 min. Filter the phase through a sintered-glass funnel under vacuum and wash with dry xylene (2 $\times$ 50 ml) and dry hexane (2 $\times$ 50 ml). Dry the phase in an oven at 60 °C for 30 min and then pass it through a 50-μm mesh sieve. Pack the column using the previously described slurry packing procedure.[6] Slurry 2.7 g of phase in 30 ml of chloroform and compress the slurry to a compact bed using acetonitrile at a pressure of 3000 lb in^{-2} for 20 min.

Method

Grind the sample in a grinder such that all material will pass through a 1-mm mesh. Weigh 5 g of sample containing between 50 and 300 mg kg^{-1} of dimetridazole into a 100-ml conical flask and extract with 50 ml of acetonitrile - water (2 + 3) by shaking on a mechanical shaker for 15 min. If the dimetridazole content is outside these limits the amount of sample should be adjusted accordingly. Filter and inject an aliquot of the filtrate on to the column using a mobile phase of acetonitrile - water (3 + 7) at a flow-rate of 2 ml min^{-1}. Determine the dimetridazole concentration of the extract by reference to a calibration graph.

Calibration graph. Make up solutions containing 5, 10, 20 and 40 μg ml^{-1} of dimetridazole in acetonitrile - water (2 + 3). Inject these solutions on to the column and plot a calibration graph (which should be linear) with the absorbance values on the ordinate and the corresponding amounts of dimetridazole in micrograms on the abscissa.

Calculation. The dimetridazole content of the feed is given by FY/M mg kg^{-1}, where F μg ml^{-1} is the concentration of dimetridazole in the extract, Y ml is the volume of extraction solvent and M g is the mass of sample taken.

Results and Discussion

Interferences

A variety of drugs and other ingredients are present in pig and poultry feeds, depending on the type of animal for which they are intended, the age and the possible diseases it may carry. It is possible that one or more of these constituents may elute with the same elution volume as dimetridazole during chromatography, thus preventing quantitation. Ingredients that commonly occur in these types of feed were therefore dissolved in acetonitrile - water (2 + 3) and their retention volumes determined on the column in order to see if they constituted a source of interference.

Both furazolidone and 3,5-dinitro-*o*-toluamide were found to interfere chromatographically with dimetridazole. A feed containing 100 mg kg^{-1} of furazolidone was found to give an "apparent" dimetridazole level of 4 mg kg^{-1} while 100 mg kg^{-1} of 3,5-dinitro-*o*-toluamide gave 9 mg kg^{-1}. Fortunately, these two drugs are very rarely found in combination with dimetridazole in a pig or poultry feed. No interference was found from the following ingredients: amprolium, ethopabate, sulphaquinoxaline, decoquinate, robenidine, monensin, halquinol, nitrovin, zinc bacitracin, vitamin A, vitamin D_3, vitamin E and copper sulphate.

None of the feeds studied contained bentonite (a hardening ingredient), which has been cited in earlier work[1] as a probable cause of low recovery figures.

Recovery of Dimetridazole from Feeds and Pre-mixes

Dimetridazole was incorporated into pig feed 1 at levels between 45 and 450 mg kg^{-1} by adding the drug to the feed base in dichloromethane, shaking for 30 min and then removing the solvent under reduced pressure. The range of feeds were then extracted and analysed by HPLC.

In a similar manner the recovery of dimetridazole from a range of different pig and poultry feeds and pre-mixes was determined. Dimetridazole was incorporated into the feeds at the level of 45 mg kg^{-1} and at 50 g kg^{-1} for the pre-mixes. (A pre-mix is generally added to a feed base at the level of approximately 4 kg $tonne^{-1}$.) Pre-mixes were extracted in a manner identical with that of a feed but the extracts were diluted by a factor of 1000 with acetonitrile - water (2 + 3) just prior to chromatography.

Recoveries of between 96 and 109% were obtained for dimetridazole in pig feed 1 (Table I). The blank value for the feed was found to be less than 1 mg kg^{-1} and was subtracted before quoting the recovery figures.

TABLE I

RECOVERY OF DIMETRIDAZOLE FROM PIG FEED

Level of dimetridazole addition/mg kg^{-1}	Recovery, %	Average recovery, %
45	109, 109	109
110	105, 109	107
220	99, 96	98
340	103, 108	106
450	98, 94	96

A similar range of recoveries was obtained for the different pig and poultry feeds and pre-mixes. The results of this study are presented in Table II.

TABLE II

RECOVERY OF DIMETRIDAZOLE FROM PIG AND POULTRY FEEDS AND PRE-MIXES

Pre-mix or feed type	Recovery, %	Average recovery, %
Poultry feed 1	101, 106	104
Poultry feed 2	99, 99	99
Poultry feed 3	94, 99	97
Poultry feed 4	96, 96	96
Pig feed 1	102, 102	102
Pig feed 2	97, 97	97
Pig feed 3	92, 92	92
Poultry pre-mix 1	110, 102	106
Poultry pre-mix 2	103, 101	102
Poultry pre-mix 3	100, 103	102
Poultry pre-mix 4	97, 99	98
Pig pre-mix 1	97, 97	97

Comparison of Methods

The results obtained by the HPLC method were compared with those obtained by a spectrophotometric procedure developed by Stone and Hobson.[3] For this study a range of commercially available feeds were used that had theoretical dimetridazole levels of 200 mg kg^{-1}.

The HPLC results on finished feeds were found to be consistently lower than those obtained by spectrophotometry although the agreement in general was good (Table III). As occasional changes occur in the composition of feeding stuffs, it is possible that the higher results obtained by using the spectrophotometric procedure are a result of interference from a co-extractive.

TABLE III

DETERMINATION OF DIMETRIDAZOLE IN COMMERCIAL FEEDS BY HPLC AND BY A SPECTROPHOTOMETRIC METHOD

	Dimetridazole content/mg kg^{-1}			
	HPLC method		Spectrophotometric method	
Feed	Individual results	Average	Individual results	Average
1	158, 158	158	173, 173	173
2	283, 291	287	300, 300	300
3	190, 190	190	203, 215	209
4	125, 121	123	139, 135	137
5	174, 174	174	201, 194	197

A typical chromatogram of a feed extract is shown in Fig. 1. The elution time for dimetridazole is approximately 2 min, which permits the analysis of approximately 30 samples (in duplicate) in one day by one experienced technical assistant.

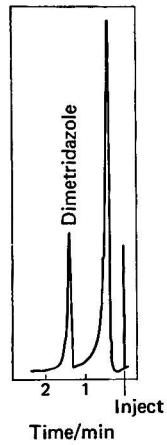

Fig. 1. Determination of dimetridazole in a commercial pig feed. Solvent, acetonitrile - water (3 + 7); flow-rate, 2 ml min^{-1}; detector, ultraviolet at 309 nm; sensitivity, 0.05 a.u.f.s.; injection volume, 10 μl (loop).

References

1. Analytical Methods Committee, *Analyst*, 1971, **96**, 746.
2. Analytical Methods Committee, *Analyst*, 1969, **94**, 925.
3. Stone, L. R., and Hobson, D. L., *J. Ass. Off. Analyt. Chem.*, 1974, **57**, 343.
4. Hammond, P. W., and Weston, R. E., *Analyst*, 1969, **94**, 921.
5. Buizer, F. G., and Severijnen, M., *Analyst*, 1975, **100**, 854.
6. Jones, A. D., Burns, I. W., Sellings, S. G., and Cox, J. A., *J. Chromat.*, 1977, **144**, 169.

Received *September 11th*, 1978
Accepted *October 17th*, 1978

Book Reviews

TOPICS IN ENZYME AND FERMENTATION BIOTECHNOLOGY. Volume 2. Edited by ALAN WISEMAN. Pp. 308. Chichester: Ellis Horwood. Distributed by John Wiley, Chichester. 1978. Price £15.

This volume contains reviews of unequal length contributed, with one exception, by authors who have already appeared in the first volume and in its precursor, the "Handbook of Enzyme Biotechnology."

The exception is a very comprehensive review by Kent, Rosevear and Thompson of "Enzymes Immobilised on Inorganic Supports." The important features of the physical form of the matrix and the preparation and properties of the immobilised enzymes are clearly described and illustrated by numerous examples. The engineering aspects of batch and continuous enzyme reactors using such catalysts are discussed including a section on reactor modelling and the review concludes with a useful summary of recent work on the industrial, medical and analytical applications of such catalysts. This introduction should be of great help to anyone wishing to utilise immobilised enzyme technology efficiently.

A short article on "Stabilisation of Enzymes" by Wiseman should be read in conjunction with this review and collects a great deal of scattered information on the use of additives, the effects of immobilisation and of crosslinking.

Enzyme electrodes have now come of age and are effectively reviewed by Barker and Somers and many examples are given based on electrochemical sensors. However, possibly the most significant non-electroactive sensor has resulted from the development of the enzyme thermistor in which the heat of the reaction can be registered and this is only briefly mentioned.

Antibiotic resistance is an ever present problem and the study of the mechanism of resistance has led to the discovery and design of more effective antibacterial agents. Apart from permeability changes the production of antibiotic inactivating enzymes is an important mechanism and three therapeutically important types of enzymes, those that inactivate the β-lactams, the amino-glycosides and chloramphenicol, are reviewed by Melling.

The second longest review is that by Winkler and Thomas on the "Biological Treatment of Aqueous Wastes." The problems of oxygen transfer and desludging are discussed and the theoretical and practical design and operation of biological film systems for waste treatment and the activated sludge process are illustrated and described. The anaerobic treatment of waste and the removal of nitrogen, a major pollutant of water, are more briefly but admirably covered. This one review justifies the purchase of the book.

If one accepts the proposition that editors of books bringing together reviews have a responsibility to select articles that summarise existing knowledge but also look to the future to provide the reader with the vital pointers and stimulus for future research then I found the present volume lacking the latter. The summaries of existing knowledge have been done conscientiously and well and will be valuable to those looking for a general introduction to a topic, or the general reader.

I. D. FLEMING

FUNDAMENTAL RESEARCH IN HOMOGENEOUS CATALYSIS. Edited by MINOURU TSUTSUI and RENATO UGO. *Proceedings of the First International Workshop on Fundamental Research in Homogeneous Catalysis held at Santa Flavia, Italy, December,* 1976. Pp. x + 242. New York and London: Plenum Press. 1977. Price $33.

The nature of the workshop or conference described in the title was unusual and the consequent presentation in this volume is also unusual. However, it provides an illuminating insight into the use of inorganic compounds as catalysts in homogeneous organic reactions connected with developments in the use of energy resources. It must be stressed that the book has no contact with analytical chemistry or analysis. Part I contains the texts of eight invited lectures, all of which review important areas of homogeneous catalysis such as the activation of oxygen and nitrogen, the use of metal clusters and the application of catalysts supported on the surface of polymers or silica based materials. In the second part of the conference, delegates divided into five working groups to discuss current developments on different topics and to define areas in which further research would produce beneficial results. In each instance, a report was produced

by the chairman, discussed further by the complete conference and subsequently published with relevant recommendations. As someone with only a peripheral interest in the subject, I found these reports exciting in both style and content. The working groups covered hydrocarbon conversion, homogeneous selective oxidation, carbon monoxide reactions, frontier areas between homogeneous and heterogeneous catalysis and catalytic processes. To anyone with an interest in the theory or industrial applications of homogeneous catalysts this book can be highly recommended.

J. M. OTTAWAY

HANDBUCH DER ANALYTISCHEN CHEMIE. DRITTER TEIL. QUANTITATIVE BESTIMMUNGS- UND TRENNUNGSMETHODEN. Band 6bγ. ELEMENTS DER SECHSTEN NEBENGRUPPE. WOLFRAM. By G. WÜNSCH. Pp. xiv + 286. Berlin, Heidelberg and New York: Springer-Verlag. 1978. Price DM146; $73.

Tungsten is an element that most analysts do not encounter often, so that detailed methods of determination, when they *are* required, are often not to hand. The present text is particularly valuable in this respect, in that it provides a comprehensive selection of complete analytical procedures, applicable to numerous matrices, and using all of the commonly encountered classical and instrumental techniques. The book also describes methods of dissolution of tungsten and its compounds, a wide variety of separation procedures and some special topics such as heteropolytungstic acids, tungsten bronzes, interactions with periodate ions, cluster compounds and cyanotungstate ions. The book continues the high standard of previous volumes in this series and should be available in all non-routine analytical laboratories.

A. TOWNSHEND

HANDBUCH DER ANALYTISCHEN CHEMIE. DRITTER TEIL. QUANTITATIVE ANALYSE. Band 4aγ. ELEMENTE DER VIERTEN HAUPTGRUPPE. ZINN. (In English.) By J. W. PRICE and R. SMITH. Pp. xv + 262. Berlin, Heidelberg and New York: Springer-Verlag. 1978. Price DM146; $73.

It is reasonable to assume that at some time or other most analysts have been involved in the determination of tin, especially at "low" levels, and most would agree that each type of sample has its own, often unpredictable, analytical problems. Even when the metal is present as a major constituent, its determination is by no means straightforward, and a consensus of opinion is likely to reveal that of all the metals that are regularly determined at "high" levels, up to 100%, the determination of tin is the most difficult; that has certainly been my experience.

Titrimetric determination of the metal is applicable over a very wide range, from the high levels just indicated, down to about 0.1%, and the method is usually, though not always, based on the formation of Sn(II) followed by iodimetric re-oxidation. Other titrimetric procedures that do not involve this preliminary reduction tend to be less reliable, for a variety of reasons.

Essentially, therefore, only two apparently simple basic stages are involved in this titrimetric method, yet I cannot cite any other analytical procedure that is more liable to give such erroneous (often reproducible) results than this one.

So much for the more important aspects of the unusual analytical proclivities of tin that are so admirably dealt with in appropriate chapters of this excellent, up-to-date and timely publication.

Throughout the book, sampling, a very important precursor to most analytical procedures, receives due attention, especially in, for example, such chapters as "Analysis of Tin Ores and Concentrates" and "Analysis of Secondary Materials and Intermediates."

Other chapter headings include "Gravimetric Methods," "Photometric Methods," "Electrochemical Methods," "Solvent Extraction," "Atomic-Absorption Spectroscopy," "Emission Spectroscopy," "X-ray Fluorescence," "Radiochemical and Mössbauer Methods," "Analysis of Ingot Tin," "Tinplate," "Organotin Compounds" and "Tin and Tin-Alloy Electroplating Solutions"; the final chapter (21) deals with "Tin Chemicals."

Apart from its fly-cover, the book is presented entirely in English—a new departure in the series?

The authors make no claim to have catalogued all of the work published on the related subject matter; their objective has been to present a reliable account of currently accepted practice in various associated fields, influenced, and rightly so, by their personal preferences in the light of their combined long and wide experience.

The book has all the attributes of an authoritative publication and can almost be guaranteed a prominent place at the right hand of anyone who has an occasional or regular need to determine tin.

W. T. ELWELL

PRACTICE OF THIN LAYER CHROMATOGRAPHY. By JOSEPH C. TOUCHSTONE and MURRELL F. DOBBINS. Pp. xxiv + 383. New York, Chichester, Brisbane and Toronto: John Wiley. 1978. Price £14.05; $27.30.

The main difference between this book and the many other published volumes on the practice of thin-layer chromatography is that here the authors aim to provide details of all the basic techniques needed to apply this form of chromatography as it is used currently in biochemical and pharmaceutical research and quality control.

There is no doubt that the language used is very easy to understand and to follow and, on the assumption, presumably, that the reader will wish to read the book from beginning to end before commencing practical work (as recommended by the authors), there is a glossary of terms at the beginning rather than at the end of the book.

The volume has 14 chapters and over 400 references. It deals with the basic description and uses of the technique, the preparation of the plates (including a chapter on commercial pre-coated plates), preparation and application of the sample, the mobile phase, development techniques, detection procedures, documentation, quantitation and reproducibility. Each of these subjects is dealt with thoroughly. In addition, there are chapters covering radioactive procedures, preparative thin-layer chromatography and the combination of this with the other analytical techniques of column and gas chromatography, mass spectrometry and infrared spectroscopy.

The special techniques of vapour-programmed development, radial chromatography, hot-plate and programmed multiple development are mentioned, as also are pyrolysis TLC, bioautography and enzyme inhibition techniques. Brief mention is also made of autotransfer chromatography and the combination of differential thermal analysis and of photoacoustic spectrometry.

While there is not a separate section on applications, these are referred to throughout the book, including amino acids, alkaloids, steroids, pesticides and antibiotics. Possibly more applications would have been advantageous, but for ease of following the instructions this method scores highly.

If the reviewer had to recommend three books to a student about to work in this field, this would be one of them.

D. SIMPSON

DIOXIN: TOXICOLOGICAL AND CHEMICAL ASPECTS. Edited by FLAMINIO CATTABENI, ALDO CAVALLARO and GIOVANNI GALLI. *Monographs of the Giovanni Lorenzini Foundation, Volume* 1. Pp. xiv + 222. New York and London: SP Medical and Scientific Books. Distributed by Halsted Press, New York. 1978. Price £14.50; $26.50.

This book represents a collection of 21 papers presented at a 2-day workshop on dioxin held in Milan, Italy, in October, 1976. It has been organised into three broad sections, *viz.*, Chemistry and Analysis; Toxicology; and Decontamination. There are original contributions from many eminent scientists in each of these areas.

The book starts with an introductory review of the events that occurred at Seveso in July, 1976. Facts are presented on the geographic extent of the pollution and on numbers of persons living in the most contaminated zones. This section also deals with some of the chemistry involved in the formation of dioxin and tabulates previous industrial accidents.

There are several excellent chapters on the analysis of 2,3,7,8-tetrachlorodibenzo-*p*-dioxin (TCDD) using gas chromatography - mass spectrometry (GC - MS). The approaches range from packed-column gas chromatography with low-resolution mass spectrometry through to high-efficiency capillary column gas chromatography combined with high-resolution mass spectrometry. In this section I found the chapter by Hans-Rudolf Buser, illustrating the use of capillary GC - MS, particularly impressive. The need for maximum sensitivity and specificity in TCDD analysis is a clear message from this section of the book. For those unfamiliar with GC - MS there are a number of simple introductory treatments with definitions of important terms such as mass fragmentography. Isolation and clean-up procedures are covered in this section and also the analysis of closely related and highly toxic chlorinated dibenzofurans, which are shown to be present in many commercial polychlorinated biphenyl formulations.

The toxicology section brings home the disturbing fact that although many penetrating studies have been carried out on TCDD, the reason for its incredible toxicity remains somewhat of a mystery. Liver enzyme induction measurements are used by several authors as an index of potency and are used to illustrate the vast differences in toxicity between the various halogenated dibenzodioxin isomers. A useful review chapter lists and summarises the findings of many of the animal studies on TCDD that have appeared in the literature.

The final section deals with the problem of decontamination, with particular reference to the Seveso incident. The encouraging results of the field trials described offer a ray of hope for the future.

In general, I found this an interesting and worthwhile book, which contains many examples of elegant analytical work. However, it suffers from a significant amount of repetition. This is undoubtedly the consequence of independently prepared papers, but I believe that the Editors should have been able to remove some of this overlap. The book also might have benefitted from the inclusion of some of the discussion that presumably took place at the workshop.

G. T. STEEL

EMISSION SPECTROCHEMICAL ANALYSIS. By TIBOR TOROK, JOZSEF MIKA and ERNO GEGUS. Pp. 692. Bristol: Adam Hilger. Budapest: Akadémiai Kiadó. 1978. Price £31.50.

The authors of this text have made very considerable efforts to include between its covers information relating to all aspects of the practice of emission spectrochemical analysis. They must be congratulated on their systematic treatment of the basic principles of sampling and sample preparation, sources, conditions affecting line intensities, semi-quantitative and quantitative spectrographic analysis, equipment installation, safety and economics and evaluation of spectrographic data. The book is augmented with tables containing physico-chemical data for spectrochemical analysis, instructions and descriptions of procedures for qualitative, semi-quantitative and quantitative analysis, conversion tables and numerical examples. The authors indicate in the introduction that they were aware of the difficulties involved in attempting to produce a comprehensive treatise devoted to a subject that is undergoing rapid development; nevertheless, the book contains a wealth of useful information and data that will remain relevant to practising spectroscopists well into the future.

This volume can be recommended as a companion text to the earlier book by the same authors ("Analytical Emission Spectroscopy—Fundamentals," Akadémiai Kiadó, Budapest, and Butterworths, London, 1973). It should take its place with other volumes concerned with practical emission spectrochemical analysis on the shelves of libraries of reference. The book is well written and translated; unfortunately, however, the binding and production quality of the copy in the hands of the present reviewer left much to be desired in such a high-priced text.

G. F. KIRKBRIGHT

Determination of Selenium in Soil Digests by Non-dispersive Atomic-fluorescence Spectrometry Using an Argon - Hydrogen Flame and the Hydride Generation Technique

The determination of selenium at submicrogram levels by atomic-fluorescence spectrometry, based on the evolution of hydrogen selenide into an argon - hydrogen air-entrained flame, is described. Using a simple purpose-built non-dispersive atomic-fluorescence spectrometer a detection limit of 10 ng cm^{-3} of selenium is obtained. The technique has been applied to the determination of selenium in soil digests and experiments have been carried out in order to study the interference of other elements on the determination. Procedures for the elimination of interferences from copper are recommended.

Keywords: *Selenium determination*; *atomic-fluorescence spectrometry*; *hydride generation*; *soil digests*

J. AZAD, G. F. KIRKBRIGHT and R. D. SNOOK
Department of Chemistry, Imperial College, London, SW7 2BP.

Analyst, 1979, **104**, 232–240.

Investigations on Reaction Mechanisms in the Determination of Non-ionic Surfactants in Waters as Potassium Picrate Active Substances

The two-phase extraction and spectrophotometric determination of polyoxyethylene non-ionic surfactants in water at trace levels is examined in detail by considering both monodisperse and polydisperse surfactants of the type $RO(CH_2CH_2O)_nH$, where R = *p-tert*-nonylphenyl and *n* is the degree of polymerisation. Potassium picrate is used as a reagent for the polyoxyethylene chain and 1,2-dichloroethane as an extracting phase.

Monodisperse surfactants with *n* from 4 to 15 were isolated by liquid - solid absorption chromatography. Their purity was checked by temperature-programmed gas - liquid chromatography. Their reactivity to the reagent is explained qualitatively by considering the equilibria involved in the extraction.

Polydisperse surfactants with *n* (number-average degree of polymerisation) ranging from 3.3 to 21.5 are also considered and compared with other polydisperse surfactants in which R = dodecyl. The concentration of these non-ionics in waters is conveniently expressed as potassium picrate active substances (PPAS). It can be referred to the standard synthetic monodisperse surfactant $RO(CH_2CH_2O)_6H$, where R = dodecyl, which gives a spectrophotometric response acceptably near to that of the examined series of commercial surfactants.

Keywords: *Polyoxyethylene alkylphenyl ether non-ionic surfactant trace determination*; *water analysis*; *spectrophotometry*; *potassium picrate*; *reaction mechanism*

L. FAVRETTO, B. STANCHER and F. TUNIS
Istituto di Merceologia, Università di Trieste, 34100 Trieste, Italy.

Analyst, 1979, **104**, 241–247.

Limit of Detection in Analysis with Ion-selective Electrodes

The limit of detection in analysis with ion-selective electrodes is discussed and definitions that are based only on the deviation of an electrode's calibration from the theoretical, and take no account of the random errors of measurement, are shown to be inadequate. Equations are derived that express the limit of detection in terms of the random error of measurement and the factors determining the deviation of the electrode response from the Nernstian value, *i.e.*, reagent blanks, solubility products and interferences. The equations enable one to predict (*a*) the degree of precision with which the e.m.f. has to be measured if an electrode is to attain a desired limit of detection in specified conditions or (*b*) whether changing the conditions might bring the desired limit of detection within reach of a given precision of measurement. Practical examples with ion-selective electrodes justify the proposed statistical treatment of limit of detection and demonstrate that the errors for electrodes operating in the non-Nernstian region are normally distributed.

Keywords: *Ion-selective electrodes*; *potentiometry*; *limit of detection*

DEREK MIDGLEY

Central Electricity Research Laboratories, Kelvin Avenue, Leatherhead, Surrey, KT22 7SE.

Analyst, 1979, **104**, 248–257.

Spectrophotometric Method for the Determination of Paraquat

Short Paper

Keywords: *Paraquat determination*; *spectrophotometry*

M. GANESAN, S. NATESAN and V. RANGANATHAN

Department of Chemistry, United Planters' Association of Southern India, Tea Research Station, Cinchona 642 106, India.

Analyst, 1979, **104**, 258–261.

Titrimetric Determination of Reducing Sugars with Copper(II) Sulphate

Short Paper

Keywords: *Reducing sugar determination*; *copper(II) sulphate reduction*; *titrimetry*

T. H. KHAN

Department of Industries (Chemical Directorate), 58, Dilkusha Commercial Area, Dacca-2, Bangladesh.

Analyst, 1979, **104**, 261–265.

Determination of Dimetridazole in Pig and Poultry Feeds by High-performance Liquid Chromatography

Short Paper

Keywords: *Dimetridazole determination*; *animal feeds*; *high-performance liquid chromatography*

A. D. JONES, I. W. BURNS and S. G. SELLINGS

Unilever Research Laboratory, Colworth House, Sharnbrook, Bedfordshire, MK44 1LQ.

Analyst, 1979, **104**, 265–268.

APPOINTMENT VACANT

Lancashire County Council
County Laboratory — Assistant Analyst
(Salary £4,461 – £4,761 per annum + £312 per annum supplement)

Applicants should have B.Sc. Honours (Chemistry) or M.R.I.C. Experience of Food Chemistry preferable.

Application forms from Chief Executive/Clerk (Ref: 41/PAT), County Hall, Preston, PR1 8XJ (Preston 54868, Ext. 566) to be returned by 22nd March 1979.

BRITISH PATENT NO. 1 407 298

Filtering Element

Owner desires commercial exploitation on reasonable terms by license or sale. Inquiries Fitzpatricks, Chartered Patent Agents, 14-18 Cadogan Street, Glasgow, G2 6QW and Warwick House, Warwick Court, London, WC1R 5DJ.

FOR SALE

The Analyst 1952–70; Journal of the Association of Public Analysts 1965–71 and Reports on the Progress of Applied Chemistry 1963–99.

Telephone 01-204 6871 (evenings).

ANALAO 104 (1236) 177–272 (1979) March 1979
ISSN 0003–2654

THE ANALYST

THE ANALYTICAL JOURNAL OF THE CHEMICAL SOCIETY

CONTENTS

Printed by Heffers Printers Ltd Cambridge England
Entered as Second Class at New York, USA, Post Office